



Calhoun: The NPS Institutional Archive

Theses and Dissertations

Thesis Collection

1984

Infrared detection of surface vehicle, calculation using atmospheric model LOWTRAN 6.

Egolfopoulos, Ioannis

Monterey, California. Naval Postgraduate School

<http://hdl.handle.net/10945/19383>



Calhoun is a project of the Dudley Knox Library at NPS, furthering the precepts and goals of open government and government transparency. All information contained herein has been approved for release by the NPS Public Affairs Officer.

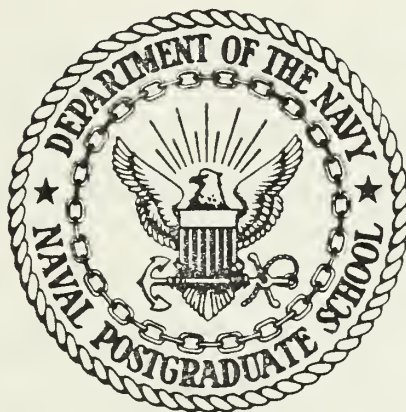
Dudley Knox Library / Naval Postgraduate School
411 Dyer Road / 1 University Circle
Monterey, California USA 93943

<http://www.nps.edu/library>

DUDLEY KNOX LIBRARY
NAVAL POSTGRADUATE SCHOOL
MONTEREY, CALIFORNIA 93943

NAVAL POSTGRADUATE SCHOOL

Monterey, California



THESIS

INFRARED DETECTION OF SURFACE VEHICLE,
CALCULATION USING ATMOSPHERIC MODEL LOWTRAN 6

by

Ioannis Egolfopoulos

December 1984

Thesis Advisor:

A. W. Cooper

Approved for public release; distribution is unlimited.

T220199

REPORT DOCUMENTATION PAGE

READ INSTRUCTIONS
BEFORE COMPLETING FORM

1. REPORT NUMBER		2. GOVT ACCESSION NO.	3. RECIPIENT'S CATALOG NUMBER
4. TITLE (and Subtitle) Infrared Detection of Surface Vehicle, Calculation Using Atmospheric Model LOWTRAN 6		5. TYPE OF REPORT & PERIOD COVERED Master's Thesis; December 1984	
		6. PERFORMING ORG. REPORT NUMBER	
7. AUTHOR(s) Ioannis Egolfopoulos		8. CONTRACT OR GRANT NUMBER(s)	
9. PERFORMING ORGANIZATION NAME AND ADDRESS Naval Postgraduate School Monterey, California 93943		10. PROGRAM ELEMENT, PROJECT, TASK AREA & WORK UNIT NUMBERS	
11. CONTROLLING OFFICE NAME AND ADDRESS Naval Postgraduate School Monterey, California 93943		12. REPORT DATE December 1984	
		13. NUMBER OF PAGES 158	
14. MONITORING AGENCY NAME & ADDRESS (if different from Controlling Office)		15. SECURITY CLASS. (of this report)	
		15a. DECLASSIFICATION/DOWNGRADING SCHEDULE	
16. DISTRIBUTION STATEMENT (of this Report) Approved for public release; distribution is unlimited			
17. DISTRIBUTION STATEMENT (of the abstract entered in Block 20, if different from Report)			
18. SUPPLEMENTARY NOTES			
19. KEY WORDS (Continue on reverse side if necessary and identify by block number) DRIVER9 SHIP1 SHIP			
20. ABSTRACT (Continue on reverse side if necessary and identify by block number) The thermal signature of a surface vehicle, "SPRUANCE" type destroyer, quantified by the signal to noise ratio of a thermal seeking missile head is parametrically investigated. The effects of the ship internal temperature, ship body paint emissivity, sky condition, sun elevation angle above the horizon, atmospheric profile, missile optics and flight altitude are examined in detail. Results show that both the ship body temperature and signal to noise ratio increase as the incident solar energy and the ship			

Block 20 Contd.

body paint emissivity increase and that the signal to noise ratio appears a pick for sun elevation angle in the range of 40° to 60° . Moreover the signal to noise ratio increases as the missile flight altitude decreases and keeping the other parameters constant higher values are found the for Midlatitude Summer atmospheric profile than for the Tropical atmosphere.

Approved for public release; distribution is unlimited.

Infrared Detection of Surface Vehicle,
Calculation Using Atmospheric Model LOWTRAN 6

by

Ioannis Egolfopoulos
Lieutenant, Hellenic Navy
B.S., Hellenic Naval Academy, 1975

Submitted in partial fulfillment of the
requirements for the degree of

MASTER OF SCIENCE IN ENGINEERING SCIENCE

from the

NAVAL POSTGRADUATE SCHOOL
December 1984

44-512
72-73
2.1
DUDLEY KNOX LIBRARY
NAVAL POSTGRADUATE SCHOOL
MONTEREY, CALIFORNIA 93943

ABSTRACT

The thermal signature of a surface vehicle, "SPRUANCE" type destroyer, quantified by the signal to noise ratio of a thermal seeking missile head is parametrically investigated. The effects of the ship internal temperature, ship body paint emissivity, sky condition, sun elevation angle above the horizon, atmospheric profile, missile optics and flight altitude are examined in detail. Results show that both the ship body temperature and signal to noise ratio increase as the incident solar energy and the ship body paint emissivity increase and that the signal to noise ratio appears a peak for sun elevation angle in the range of 40° to 60° . Moreover the signal to noise ratio increases as the missile flight altitude decreases and keeping the other parameters constant higher values are found for the Midlatitude Summer atmospheric profile than for the Tropical atmosphere.

TABLE OF CONTENTS

I.	INTRODUCTION	13
II.	SHIP MODELING	16
	A. ASSUMPTIONS	16
	B. GEOMETRY AND MATERIAL OF THE SHIP	17
	C. SOLAR HEAT FLUX IN THE SEA LEVEL SURFACE	18
	D. CALCULATION OF SHIP BODY TEMPERATURE	25
	E. DETERMINATION OF THE SHIP "HOTTEST" AREA	27
	F. DETERMINATION OF THE DETECTOR INSTANTANEOUS FIELD OF VIEW	28
	G. DETERMINATION OF THE DIMENSIONS OF THE TRACKED SHIP AREA	31
III.	ATMOSPHERIC TRANSMITTANCE USING LOWTRAN 6	35
	A. DESCRIPTION OF LOWTRAN 6	35
	B. DATA USED	35
	C. RESULTS	36
IV.	CALCULATION OF SHIP AND BACKGROUND RADIANCE	39
	A. NORMAL COMPONENT OF SHIP RADIANCE DUE TO THERMAL RADIATION	39
	B. NORMAL COMPONENT OF SHIP RADIANCE DUE TO REFLECTED SOLAR ENERGY	40
	C. NORMAL COMPONENT OF STACK EXIT PLANE RADIANCE	40
	D. TOTAL SHIP RADIANT INTENSITY IN THE DIRECTION FROM SHIP TO MISSILE	41
	E. BACKGROUND RADIANT INTENSITY	43
V.	DETECTOR MODELING AND CALCULATION OF S/N RATIO	47

A.	DETECTOR SYNTHESIS	47
B.	SIGNAL VOLTAGE	51
C.	NOISE VOLTAGE	53
VI.	RESULTS AND DISCUSSION	74
A.	SHIP BODY TEMPERATURE	74
B.	DETECTOR S/N RATIO	75
C.	RECOMMENDATIONS	76
APPENDIX A:	TABLES FOR SHIP BODY TEMPERATURE	78
APPENDIX B:	TABLES FOR DETERMINATION OF I.F.V.	103
APPENDIX C:	TABLES WITH DATA USED FOR LOWTRAN 6	116
APPENDIX D:	PLOTS OF S/N RATIO	141
APPENDIX E:	COMPUTER PROGRAMS	150
LIST OF REFERENCES	157
INITIAL DISTRIBUTION LIST	158

LIST OF TABLES

1.	Normal Component of Solar Heat Flux on a Surface at Sea Level	22
2.	Final Choice for the Dimensions of I.F.V.	33
3.	Geometrical Parameters for Observed Sea Area	45
4.	Dimensions of the Detector Element	52
5.	Ship Body Temperature for Midlatitude Summer T_{in} =293.15K and $\epsilon_o=0.80$	79
6.	Ship Body Temperature for Midlatitude Summer T_{in} =303.15K and $\epsilon_o=0.80$	82
7.	Ship Body Temperature for Midlatitude Summer T_{in} =293.15K and $\epsilon_o=0.55$	85
8.	Ship Body Temperature for Midlatitude Summer T_{in} =303.15K and $\epsilon_o=0.55$	88
9.	Ship Body Temperature for Tropical $T_{in}=293.15K$ and $\epsilon_o=0.80$	91
10.	Ship Body Temperature for Tropical $T_{in}=303.15K$ and $\epsilon_o=0.80$	94
11.	Ship Body Temperature for Tropical $T_{in}=293.15K$ and $\epsilon_o=0.55$	97
12.	Ship Body Temperature for Tropical $T_{in}=303.15K$ and $\epsilon_o=0.55$	100
13.	Side of Instantaneous Field of View in Meters for Flight Altitude= 50 m	104
14.	Path in Meters for Flight Altitude= 50 m	105
15.	Side of Instantaneous Field of View in Meters for Flight Altitude= 60 m	106
16.	Path in Meters for Flight Altitude= 60 m	107
17.	Side of Instantaneous Field of View in Meters for Flight Altitude= 70 m	108

18.	Path in Meters for Flight Altitude=70 m	109
19.	Side of Instantaneous Field of View in Meters for Flight Altitude= 80 m	110
20.	Path in Meters for Flight Altitude= 80 m	111
21.	Side of Instantaneous Field of View in Meters for Flight Altitude= 90 m	112
22.	Path in Meters for Flight Altitude=90 m	113
23.	Side of Instantaneous Field of View in Meters for Flight Altitude=100 m	114
24.	Path in Meters for Flight Altitude=100 m	115
25.	Data Used for Month October	117
26.	Average Transmittances for Month October	118
27.	Data Used for Month November	119
28.	Average Transmittances for Month November	120
29.	Data Used for Month December	121
30.	Average Transmittances for Month December	122
31.	Data Used for Month January	123
32.	Average Transmittances for Month January	124
33.	Data Used for Month February	125
34.	Average Transmittances for Month February	126
35.	Data Used for Month March	127
36.	Average Transmittances for Month March	128
37.	Data Used for Month April	129
38.	Average Transmittances for Month April	130
39.	Data Used for Month May	131
40.	Average Transmittances for Month May	132
41.	Data Used for Month June	133
42.	Average Transmittances for Month June	134
43.	Data Used for Month July	135
44.	Average Transmittances for Month July	136
45.	Data Used for Month August	137
46.	Average Transmittances for Month August	138
47.	Data Used for Month September	139

48.	Average Transmittances for Month September . . .	140
-----	--	-----

LIST OF FIGURES

2.1	Ship Side View	19
2.2	Ship Top View	20
2.3	Illuminance Level on the Surface of the Earth [Ref. 5]	21
2.4	Control Volume for Determination of Ship Body Temperature	25
2.5	Determination of Instantaneous Field of View . . .	30
2.6	Three-Dimensional Sketch of the "Hottest" Area . .	32
3.1	Spectral Transmittance in the Window 4.435 μ m-5.00 μ m Through LOWTRAN 6	38
4.1	The 4.4 μ m Emission Band of CO [Ref. 12]	41
4.2	Relative Position Between Surface- Missile	42
4.3	Geometry for Determination of Background Radiant Intensity	44
5.1	The D* of the Detectors in Each Atmospheric Window at the Most Common Operation Temperature [Ref. 10]	48
5.2	Data Sheet for Photovoltaic Indium Antimonide Receiver [Ref. 12]	49
5.3	System of Two Mirrors in the Detector	50
5.4	Total Detector Search Field	54
5.5	Influence of Missile Flight Altitude for Unobscured Sun, $\epsilon_0=0.80$, Midlatitude Summer	56
5.6	Influence of Missile Flight Altitude for Sun with Light Clouds, $\epsilon_0=0.80$, Midlatitude Summer . . .	57
5.7	Influence of Missile Flight Altitude for Sun with Heavy Storm Clouds, $\epsilon_0=0.80$, Midlatitude Summer	58

5.8	Influence of Missile Flight Altitude for Unobscured Sun, $\epsilon_0=0.55$, Midlatitude Summer	59
5.9	Influence of Missile Flight Altitude for Sun with Light Clouds, $\epsilon_0=0.55$, Midlatitude Summer	60
5.10	Influence of Missile Flight Altitude for Sun with Heavy Storm Clouds, $\epsilon_0=0.55$, Midlatitude Summer	61
5.11	Influence of Missile Flight Altitude for Unobscured Sun, $\epsilon_0=0.80$, Tropical Atmosphere	62
5.12	Influence of Missile Flight Altitude for Sun with Light Clouds, $\epsilon_0=0.80$, Tropical Atmosphere . . .	63
5.13	Influence of Missile Flight Altitude for Sun with Heavy Storm Clouds, $\epsilon_0=0.80$, Tropical Atmosphere	64
5.14	Influence of Missile Flight Altitude for Unobscured Sun, $\epsilon_0=0.55$, Tropical Atmosphere	65
5.15	Influence of Missile Flight Altitude for Sun with Light Clouds, $\epsilon_0=0.55$, Tropical Atmosphere . . .	66
5.16	Influence of Missile Flight Altitude for Sun with Heavy Storm Clouds, $\epsilon_0=0.55$, Tropical Atmosphere	67
5.17	Influence of Emissivity and Atmospheric Profile for Flight Altitude 50m and Unobscured Sun	68
5.18	Influence of Emissivity and Atmospheric Profile for Flight Altitude 50m and Sun with Light Clouds	69
5.19	Influence of Emissivity and Atmospheric Profile for Flight Altitude 50m and Sun with Heavy Storm Clouds	70
5.20	Influence of Emissivity and Atmospheric Profile for Flight Altitude 100m and Unobscured Sun	71
5.21	Influence of Emissivity and Atmospheric Profile for Flight Altitude 100m and Sun with Light Clouds	72

5.22	Influence of Emissivity and Atmospheric Profile for Flight Altitude 100m and Sun with Heavy Storm Clouds	73
D.1	S/N Ratio for Midlatitude Summer, $\epsilon_0=0.80$ and Flight Altitude 50m	142
D.2	S/N Ratio for Midlatitude Summer, $\epsilon_0=0.80$ and Flight Altitude 100m	143
D.3	S/N Ratio for Midlatitude Summer, $\epsilon_0=0.55$ and Flight Altitude 50m	144
D.4	S/N Ratio for Midlatitude Summer, $\epsilon_0=0.55$ and Flight Altitude 100m	145
D.5	S/N Ratio for Tropical, $\epsilon_0=0.80$ and Flight Altitude 50m	146
D.6	S/N Ratio for Tropical, $\epsilon_0=0.80$ and Flight Altitude 100m	147
D.7	S/N Ratio for Tropical, $\epsilon_0=0.55$ and Flight Altitude 50m	148
D.8	S/N Ratio for Tropical, $\epsilon_0=0.55$ and Flight Altitude 100m	149

I. INTRODUCTION

The basic function of a thermal-seeking-head missile is to track on a surface vehicle using the vehicle's radiant intensity. This operation is based on the fact that a moving vehicle shows a generally higher surface temperature than the environment. Reasons for this are the existence of operating engines, resulting in both increased engine room temperature and "hot" combustion products exiting into the atmosphere from the stack, the operation of a number of devices which result in heat generation, the requirement for certain compartment temperatures comfortable to the crew, and the incident solar energy on the painted metallic vehicle surfaces.

Exact information about the heat seeking missile characteristics is not available because of their classification. Hence our study will be a parametric one in order to examine the relative influence of a number of parameters on the vehicle thermal signature which is quantified by the signal to noise ratio of the thermal detector head. The range of the parameter values will be chosen using both experience and unclassified information.

Exceptional cases such as operation of the vehicle close to the coast or other vehicles, which could have similar or higher temperatures, will not be considered. At this point we must realize that the thermal interaction of the vehicle with the environment is a very complicated phenomenon, and its exact determination for the different parts of the ship body is outside of the scope of the present work. Instead we will consider a simplified case of uniform interaction for all the ship parts with the environment (convection, radiation, solar absorption energy) and will limit the source for

the thermal head detector enviromental noise only to that of the sea water.

The main procedure steps of the present study will be :

To create a simplified model for the calculation of the vehicle body temperature and to show what parameters affect it and in what direction.

To determine the "hottest" vehicle area and combining with the operating characteristics of the missile to calculate the dimensions of the tracked area of the vehicle.

To calculate the total radiant intensity of the tracked area of the vehicle in a certain wavelength range, where the thermal detector head is operating.

To calculate the atmospheric transmittance, using LOWTRAN 6, for each given combination of the parameters of our interest in the given detector wavelength range and consequently the radiant heat flux detected by the thermal head.

To create an appropriate detector model that could show optimum operation for the conditions of our problem, and finally to calculate the creating signal-to-noise ratio which quantifies the vehicle thermal signature and describes the detector operational quality.

To discuss the relative influence of all the pertinent parameters and to propose certain considerations about both the vehicle and the missile.

Without expecting significant quantitative importance for our results, due to the simplifications that have been made, their qualitative importance must be more remarkable.

Parameters that will play significant roles in our study will be :

- vehicle internal temperature,
- vehicle body paint emissivity,
- sky condition,
- sun elevation angle above the horizon,

atmospheric profile,
missile flight altitude,
instantaneous Field of View (I.F.V.) created by the
detector's optic system,
detector material,

The present work consists of five Chapters. In the first Chapter we state the assumptions of the problem, we calculate the vehicle body temperature, and we determine its "hottest" area which is tracked by the detector. In the second Chapter we use the LOWTRAN 6 program in order to determine the atmospheric transmittance and in the third Chapter we calculate the total vehicle and background radiant intensity incident on the tracker aperture. In the fourth Chapter we calculate the detector signal-to-noise ratio for all the possible combinations of the parameters, and finally in the fifth Chapter we discuss the relative importance of each parameter and we suggest ways that could improve both the vehicle thermal signature and the detector operation.

II. SHIP MODELING

In order to create an exact ship model, it is necessary to acquire a significant amount of empirical data. For the present study, and for several reasons, the available data are limited, and are based only on the unclassified literature given in the first six references, with relatively reasonable assumptions.

A. ASSUMPTIONS

All compartments of the ship have a uniform temperature of $20^{\circ}\text{C}=293.15\text{K}$ except the main engine rooms 1 and 2, which have a temperature of $30^{\circ}\text{C}=303.15\text{K}$.

The stack exit temperature is uniform and we study the heat radiation from the exit plane neglecting the plume radiation. Reasons for doing this are the non-uniformity of the plume geometry and temperature distribution, and the fact that it is cooled significantly in a relatively short distance from the exit plane [Ref. 3]. We choose as stack exit temperature $306^{\circ}\text{F}=152.2^{\circ}\text{C}=425.4\text{K}$

In order to account for the heat convection from the ship to the air we will use the relative wind-speed of 30 Knots. For this case we will have forced convection with a heat transfer coefficient in the range of 5 to 10 ($\text{BTU}/\text{H FT}^2\text{R}$) or equivalently 28.4 to 56.8 ($\text{W}/\text{M}^2\text{K}$). We will not account for the heat leakage from the ship body to the sea water or for the heat loss due to the vaporization effect on the wet surfaces above sea level. For this reason and in order to be closer to reality we choose for our heat convection losses calculation the value of 10 ($\text{BTU}/\text{H FT}^2\text{R}$) or 56.8 ($\text{W}/\text{M}^2\text{K}$) as representative for the convection heat transfer coefficient.

The present study will be in Mediterranean atmospheric conditions and more specifically for the area of the Aegean Sea. We will use two atmospheric profiles i.e. Midlatitude Summer for months October through April and Tropical for months May through September. The corresponding ambient temperatures are $21^{\circ}\text{C}=294.2\text{K}$ and $26.6^{\circ}\text{C}=299.7\text{K}$ respectively [Ref. 6].

B. GEOMETRY AND MATERIAL OF THE SHIP

In Figures 2.1 and 2.2 you will find the ship side and top view respectively with the appropriate dimensions.

The material of the ship lower body construction is constructional carbon steel with thickness 13.5mm and thermal conductivity 54 (W/M K) [Ref. 9].

The material of ship body superstructure is duraluminum with thickness 3mm and thermal conductivity 164 (W/M K).

These small values of the thickness and the high values of the thermal conductivities for both materials result in negligible temperature gradients inside the materials. Hence it is reasonable to assume a uniform temperature throughout the thickness of both materials.

Both structures are painted with gray paint i.e. the emissivity and absorptivity will be spectrally independent and equal between them. A typical value for oil paint emissivity - absorptivity is 0.94 [Ref. 10:p.07] and for TiO_2 gray paint is 0.87 [Ref. 4:p.278] both for temperatures 300K. From these values we observe that the available data give us paint emissivity - absorptivity values in the range of 0.90. Based on the facts that these values play a significant role in the determination of the ship body temperature and that intensive research resulted in the production of new paints with half the values of the already existing ones [Ref. 7] we will use two (2) different values i.e. 0.80,

0.55. Therefore we cover the useful range of the existing and the newly developed paints. At this point we must note that we don't have any available information about selectively absorbing paints that could exist and give the minimum possible thermal signature and our assumption about the equality between emissivity and absorptivity is inevitable as a first approximation. Moreover the solution of the problem for two (2) different emissivities constitutes a good research point for the relative influence of this factor.

The emissivity of the interior surface of the ship body will be approximated as that of stainless steel which is 0.44 [Ref. 4:p.278].

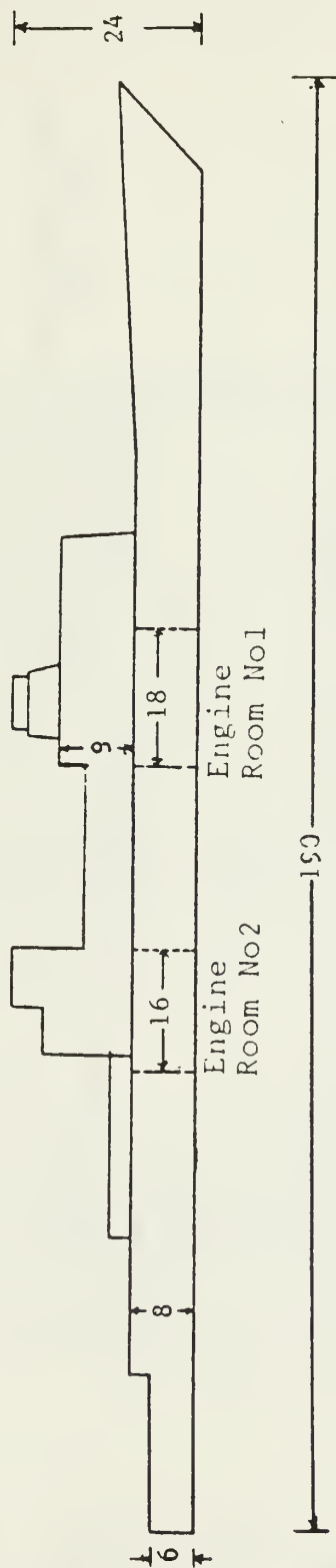
C. SOLAR HEAT FLUX IN THE SEA LEVEL SURFACE

In Figure 2.3 you will find the illuminance levels on the surface of the earth due to the sun for three different sky conditions i.e. Unobscured Sun, Sun with Light Clouds and Sun with Heavy Storm Clouds as a function of the elevation angle above the horizon. These three sky conditions and the elevation angle above the horizon will be two more parameters in the solution of our problem.

Since the given values in Figure 2.3 are in photometric units (Lux) and we want to convert into useful radiometric units (W/M^2) we have to determine a conversion factor.

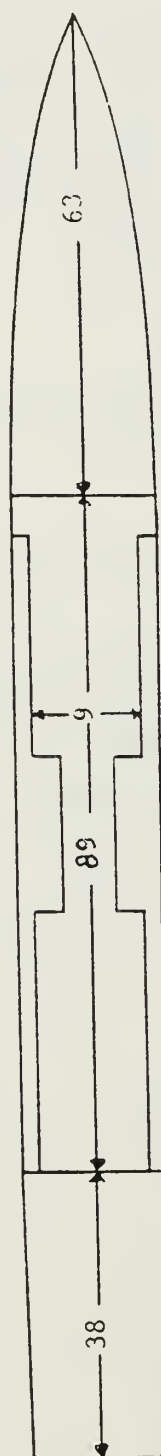
We know that the maximum incident solar flux on the earth surface is approximately 900 (W/M^2) [Ref. 10:p.11]. This value corresponds to $1.15 \cdot 10^5$ (Lux) and therefore the conversion factor will be:

$$CF = 900 / 1.15 \cdot 10^5 = 5.826 \cdot 10^{-3} \quad (W/M^2Lux)$$



SCALE 1:900
DIMENSIONS IN (mm)

Figure 2.1 Ship Side View



SCALE 1:900
DIMENSIONS IN (mm.)

Figure 2.2 Ship Top View

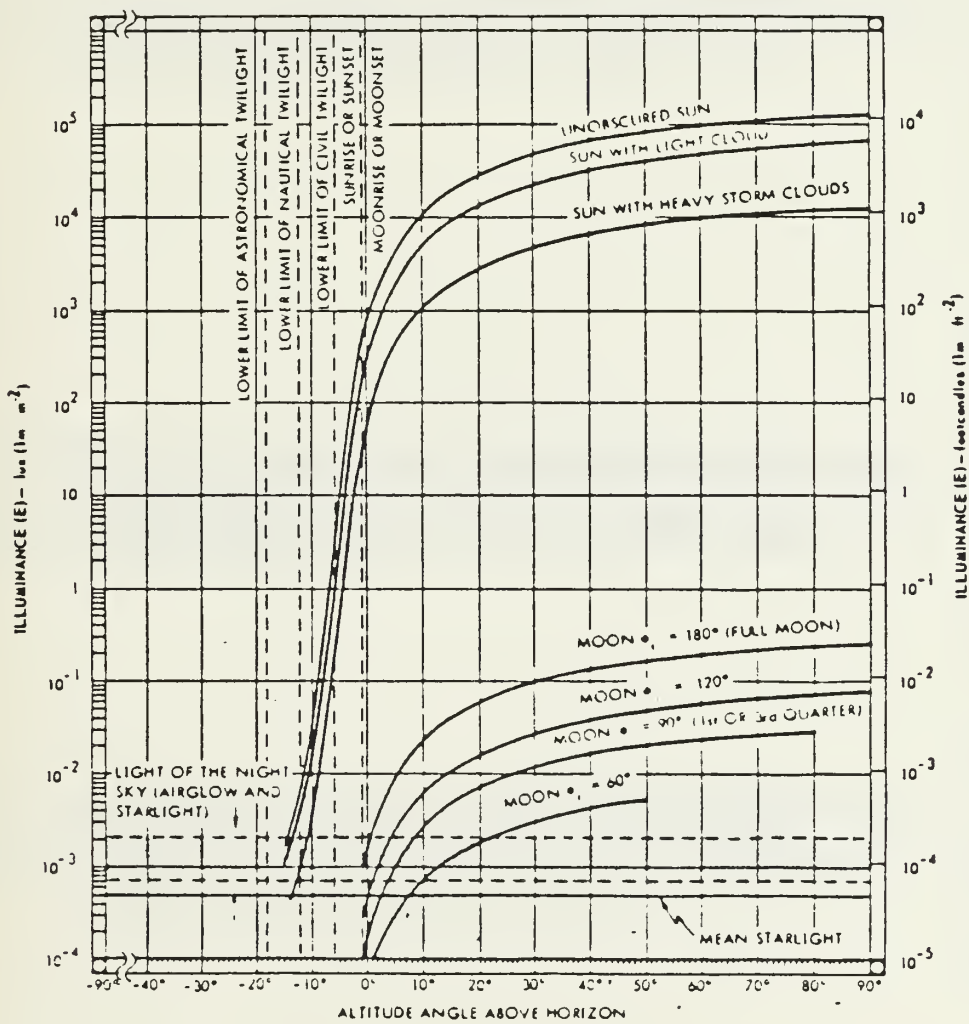


Figure 2.3 Illuminance Level on the Surface of the Earth [Ref. 5]

TABLE 1

Normal Component of Solar Heat Flux on a Surface at Sea Level

ELEV. ANGLE	UNOBSCURED SUN	SUN WITH LIGHT CLOUDS	SUN WITH HEAVY STORM CLOUDS
0.	6.70	70	0.50
1.	15.06	2.10	1.26
2.	23.42	6.50	2.02
3.	31.78	9.90	2.78
4.	40.14	12.30	3.54
5.	48.50	16.70	4.30
6.	57.90	19.58	5.24
7.	67.30	23.46	6.18
8.	76.70	27.34	7.12
9.	86.10	31.22	8.06
10.	95.50	35.10	9.00
11.	105.96	44.16	9.88
12.	116.88	49.28	10.82
13.	127.38	54.40	11.76
14.	137.80	59.40	12.70
15.	147.38	64.86	13.88
16.	157.96	69.32	14.06
17.	166.54	75.78	16.24
18.	176.12	80.24	17.42
19.	186.70	86.70	18.60
20.	195.90	91.84	19.76
21.	207.10	96.98	20.92
22.	220.30	101.12	21.08
23.	232.50	107.26	23.24
24.	244.70	112.40	24.40
25.	256.90	117.62	25.90
26.	268.10	123.84	26.40
27.	281.30	129.06	28.90
28.	294.50	136.28	29.40
29.	307.70	142.50	31.90
30.	319.90	148.14	32.92
31.	334.18	155.78	34.94
32.	348.46	161.42	36.96
33.	362.74	168.42	38.96

ELEV. ANGLE	UNOBSURED SUN	SUN WITH LIGHT CLOUDS	SUN WITH HEAVY CLOUDS	STORM
34.	377.02	175.06	40.98	
35.	391.02	181.18	43.00	
36.	409.74	189.66	45.04	
37.	426.74	196.66	47.08	
38.	444.46	204.14	49.12	
39.	462.18	211.62	51.16	
40.	479.90	219.10	53.20	
41.	496.72	226.24	54.76	
42.	513.54	233.38	56.32	
43.	530.36	240.52	57.88	
44.	547.18	247.66	59.44	
45.	564.00	254.80	61.00	
46.	578.54	264.02	62.34	
47.	593.08	273.24	63.68	
48.	607.62	282.46	65.02	
49.	622.16	291.68	66.36	
50.	636.70	300.90	67.70	
51.	649.98	309.16	69.02	
52.	663.26	317.42	70.34	
53.	676.54	325.68	71.66	
54.	689.82	333.94	72.98	
55.	703.10	342.20	74.30	
56.	716.14	349.62	75.42	
57.	726.16	357.04	76.54	
58.	737.18	364.46	77.66	
59.	749.18	371.88	78.78	
60.	760.28	379.30	79.90	
61.	771.44	386.70	80.94	
62.	781.86	392.52	81.02	
63.	792.02	399.26	83.06	
64.	803.60	406.00	84.10	
65.	813.68	413.22	85.04	
66.	821.76	419.44	86.08	
67.	829.92	425.66	86.92	
68.	837.92	431.88	87.92	
69.	845.00	437.10	88.80	
70.	854.00	444.10	89.80	

ELEV. ANGLE	UNOBSCURED SUN	SUN WITH LIGHT CLOUDS	SUN WITH HEAVY CLOUDS	STORM
71.	859.18	449.20		
72.	864.36	454.30		90.64
73.	869.54	459.40		91.48
74.	874.72	464.50		92.32
75.	879.90	469.60		93.16
76.	882.54	474.36		94.00
77.	885.18	479.12		94.86
78.	887.82	483.88		95.72
79.	890.46	488.64		96.58
80.	893.10	493.40		97.44
81.	894.10	497.36		98.30
82.	895.10	501.32		99.06
83.	896.10	505.28		99.82
84.	897.10	509.24		100.58
85.	898.10	513.20		101.34
86.	898.48	517.00		102.10
87.	898.86	520.80		102.82
88.	899.24	524.60		103.54
89.	899.62	528.40		104.26
90.	900.00	532.20		104.98
				105.70

Using this conversion factor and the values of Figure 2.3 we obtain the normal component of the solar heat flux in (W/M^2) on a surface at sea level. Table 1 demonstrates the above values.

In order to calculate the values of the solar heat flux falling obliquely on a surface we must introduce the incident angle θ and multiply the values of Table 1 by $\cos\theta$.

For a vertical face the angle θ is identical with the elevation angle above the horizon. For a horizontal face i.e. the deck in our case, the angle θ is the complement of elevation angle above the horizon.

D. CALCULATION OF SHIP BODY TEMPERATURE

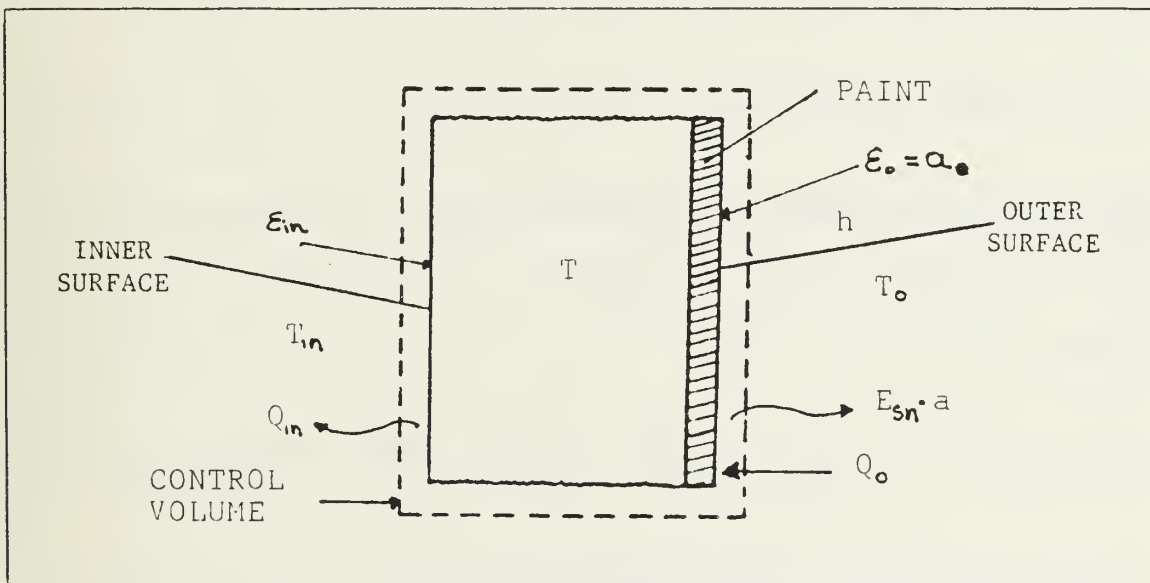


Figure 2.4 Control Volume for Determination of Ship Body Temperature

In Figure 2.4 you will find the appropriate control volume of the ship body and the pertinent energy flows that are related with it. For simplicity the control volume has

unit area exposed to both the environment and the ship interior. More specifically:

ϵ_o : paint emissivity

a_o : paint absorptivity ($\epsilon_o = a_o$)

ϵ_{in} : emissivity of the interior surface. ($\epsilon_{in} = 0.44$)

T_o : ambient temperature

T_{in} : ship compartment temperature

E_{sh} : normal component given by Table 2

Q_o : net heat exchange of control volume with the environment

Q_{in} : net heat exchange of control volume with the interior of the ship

h : convection heat transfer coefficient with the air

The absorbed solar heat flux is $E_{sh} \cdot a_o$. The net heat exchange with the environment is due to heat radiation and heat convection i.e.

$$Q_o = \epsilon_o \sigma (T^4 - T_o^4) + h(T - T_o) \quad (2.1)$$

The net heat exchange with the interior is due only to heat radiation i.e.

$$Q_{in} = \epsilon_{in} \sigma (T^4 - T_{in}^4) \quad (2.2)$$

Energy balance of the control volume under thermal equilibrium gives:

$$E_{sh} \cdot a_o = \epsilon_o \sigma (T^4 - T_o^4) + h(T - T_o) + \epsilon_{in} \sigma (T^4 - T_{in}^4) \quad (2.3)$$

or

$$F(T) = (\epsilon_o + \epsilon_{in}) \sigma T^4 + hT - \sigma (\epsilon_o T_o^4 + \epsilon_{in} T_{in}^4) - hT_o - E_{sh} \cdot a_o = 0 \quad (2.4)$$

Equation 2.4 must be solved numerically. We will use the Steffensen Recursive Method [Ref. 11]. The idea of this method is that starting with an x close enough to the exact solution S of the equation $F(x)=0$ then the sequence:

$$x_{k+1} = x_k - [f^2(x_k) / (f(x_k + f(x_k)) - f(x_k))] \quad (2.5)$$

will converge very fast to the exact solution S .

In our case the equation is $F(T)=0$ and we are looking for the value of T that satisfies it.

In order to obtain an initial value so that our sequence will converge we use the value:

$$T_{1n} = [(E_{sn} \cdot a_o + \epsilon_o \sigma T_o^4 + \epsilon_n \sigma T_{1n}^4) / (\epsilon_o + \epsilon_n) \sigma]^{1/4} \quad (2.6)$$

The above initial value of T does not account for the heat convection and for our purpose gives acceptable initial values. Finally we stop the recursive formula when $|T_{k+1} - T_k|$ is less than or equal to 10^{-6} .

In Appendix A, Tables 5 through 18 demonstrates the ship body temperature for both horizontal and vertical faces, for all the combinations of two (2) atmospheric profiles, three (3) different sky conditions, two (2) internal (T_{in}) temperatures and two (2) paint emissivities.

E. DETERMINATION OF THE SHIP "HOTTEST" AREA

From the calculations in section D, we observe that the higher ship body temperatures happen to be in the region of the two engine rooms (higher internal temperature).

From the ship geometry, it is obvious that the dimensions of the engine room No 1 are greater than those of engine room No 2. Therefore the total radiant intensity (W/Sr) of engine room No 1 will be greater since for both regions we

have the same normal components of radiance (W/cm^2Sr). In addition to that to each engine room there corresponds the same stack geometry also going a 'hot' region too.

Under this simplified assumption we conclude that for a heat seeking missile head the area of engine room No 1 from the stack exit all the way down to sea level is the most significant region.

At this point it is necessary to couple the ship with some characteristics of the missile detector operation.

Without getting involved in details of the detector operation, which will be studied in later sections, we will determine the detector Instantaneous Field of View (I.F.V.), so that we will know exactly the dimensions of the 'hottest' area which will be tracked by the detector and therefore we will be able to calculate the amount of radiant energy that will be transmitted to the missile.

F. DETERMINATION OF THE DETECTOR INSTANTANEOUS FIELD OF VIEW

The following range of data is based on our experience and research, aiming to calculate a reasonable and useful I.F.V. In Figure 2.5 you will find the corresponding geometry.

The range of the missile flight altitude will be from 50m to 100m above sea level. Since we want to reduce as much as possible the background noise, the detector must have an inclination with respect to the horizontal. We choose the range for this inclination (angle ϕ) from 2° degrees to 5° degrees.

From general consideration for the detectors [Ref. 4] we know that I.F.V. is a function of the 'hottest' ship area that the detector has to track.

For the creation of I.F.V. it is necessary that the detector accepts radiation from inside an area which is related to an angle 2δ generated by the detector mirror system as in Figure 2.5 . From the same figure we conclude the following:

$$\begin{aligned}\theta &= 90^\circ - \phi - \delta \\ BC &= AB \cdot \tan\theta \\ AC &= (AB^2 + BC^2)^{1/2} \\ CF &= AC \cdot \sin\delta \\ CG &= 2CF = 2AC \cdot \sin\delta = \text{SIDE} \\ AF &= CG / 2 \tan\delta = \text{PATH}\end{aligned}$$

Where:

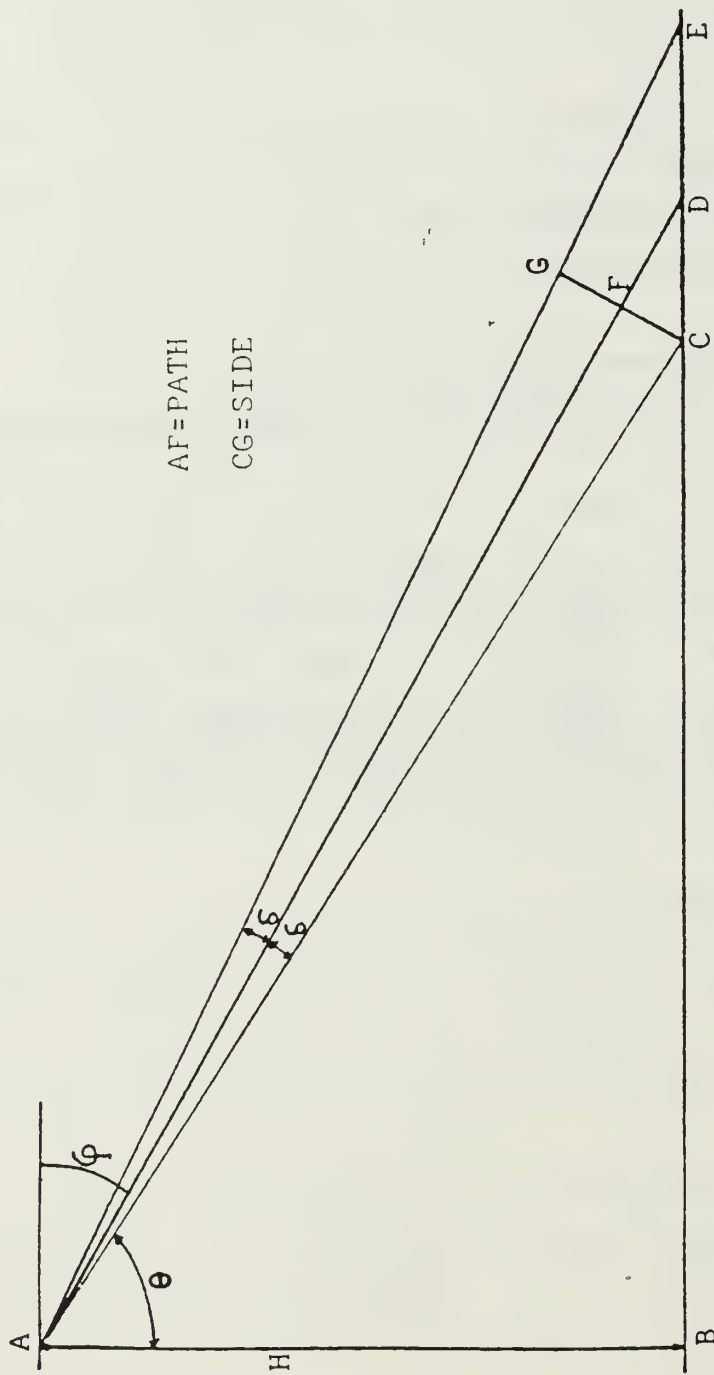
CG represents the side of the I.F.V.

AF represents the distance or path length between detector and the I.F.V.

AB = H : flight altitude

For simplicity we will consider that the shape of I.F.V. is square with side equal to CG of Figure 2.5

In Appendix B Tables 19 through 29 demonstrate the values of PATH and SIDE for all the possible combinations of ϕ , δ and H. Program SHIP 1, in Appendix E, has been used for the calculation of the above values.



$AF = \text{PATH}$

$CG = \text{SIDE}$

Figure 2.5 Determination of Instantaneous Field of View

G. DETERMINATION OF THE DIMENSIONS OF THE TRACKED SHIP AREA

In the previous section we have shown that the detector will track on the area of engine room No 1.

In Figure 2.6 you will find a three-dimensional sketch for the engine room No 1 area. Before we start the calculations of the different surfaces we will explain why the side of I.F.V. is greater than the width of the engine room No 1 which is $W_1=1,620\text{cm}$. We consider as useful that the I.F.V. will include the whole area between sea level and the stack exit plane. The total height of this dimension is:

$$H_1 + H_3 + H_4 + H_5 = 720 + 900 + 360 + 180 = 2,160\text{cm}$$

From the Tables 13 to 24, we choose for each flight altitude and for constant $\sigma=0.56^\circ$ the minimum SIDE that is greater than or equal to 2.160cm

Table 2 demonstrates the results of this choice

Based on Figure 2.6 we will now determine the characteristics of each individual surface.

$$A_1 = W_1 \cdot H_1$$

Vertical face

$$T_{1n} = 303.15\text{K}$$

$$A_{1L} = (\text{SIDE} - W_1) \cdot H_1$$

Vertical face

$$T_{1n} = 293.15\text{K}$$

$$A_2 = W_1 \cdot H_2$$

Horizontal face

$$T_{1n} = 303.15\text{K}$$

$$A_{2L} = (\text{SIDE} - W_1) \cdot H_2$$

Horizontal face

$$T_{1n} = 293.15\text{K}$$

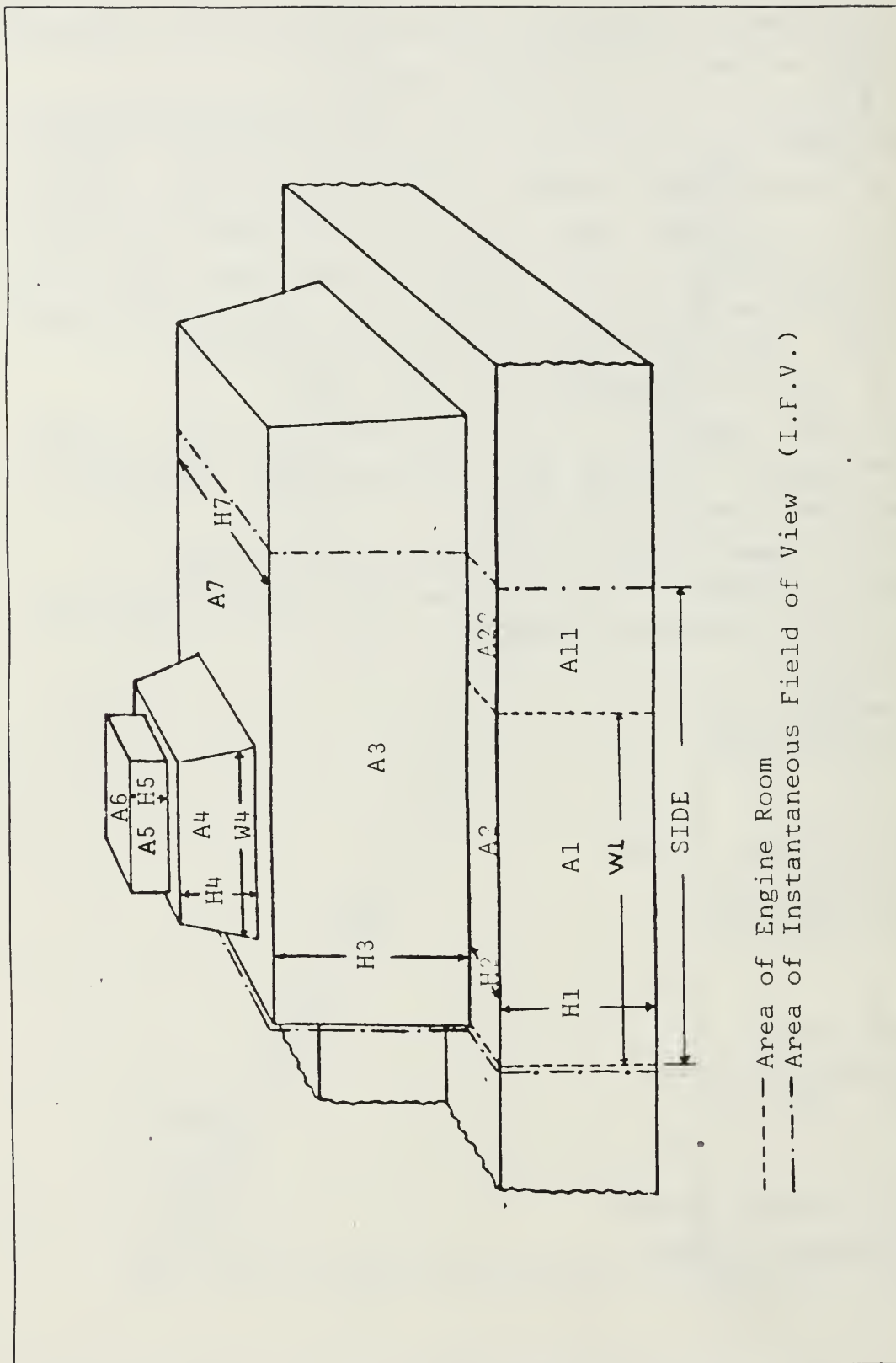


Figure 2.6 Three-Dimensional Sketch of the "Hottest" Area

TABLE 2
Final Choice for the Dimensions of I.F.V.

HEIGHT FLIGHT	SIDE (m)	PATH (m)	DELTA	PHI
50 (m)	21.88	1119.34	0.56°	2.0°
60 (m)	21.97	1123.89	0.56°	2.5°
70 (m)	22.04	1127.25	0.56°	3.0°
80 (m)	22.09	1129.84	0.56°	3.5°
90 (m)	22.13	1131.96	0.56°	4.0°
100 (m)	22.16	1133.72	0.56°	4.5°

$$A_3 = \text{SIDE} \cdot H_3$$

Vertical face

$$T_{\eta} = 293.15\text{K}$$

$$A_4 = W_4 \cdot H_4$$

Vertical face

$$T_{\eta} = 303.15\text{K}$$

At this point we must notice that surface A_5 corresponds to the stack and, since we don't have information about the insulation of this structure, we approximate its temperature with that of the surface with $T = 303.15^\circ\text{K}$

$$A_6 = 4.43 \cdot 10^4 \text{ cm}^2$$

Horizontal face

$$T_{\eta} = 425.4\text{K}$$

$$A_7 = \text{SIDE} \cdot H_7 - (\pi/4) \cdot W_4^2$$

Horizontal face

$$T_{\eta} = 293.15\text{K}$$

For the order of magnitude of PATH i.e. the distance between missile and ship we will approximate the thermal emission of each individual surface as point source emission. These "point sources" will be:

$(A_1 + A_{11}), (A_2 + A_{21}), A_3, A_4, A_5, A_6, A_7$.

with corresponding mean altitudes from sea level:

$$H_{m1} = H_{m11} = H_1 / 2$$

$$H_{m2} = H_{m21} = H_1$$

$$H_{m3} = H_1 + H_3 / 2$$

$$H_{m4} = H_1 + H_3 + H_4 / 2$$

$$H_{m5} = H_1 + H_3 + H_4 + H_5 / 2$$

$$H_{m6} = H_1 + H_3 + H_4 + H_5$$

$$H_{m7} = H_1 + H_3$$

The data for the above calculations are:

$$W_1 = 1,620 \text{ cm}$$

$$H_1 = 720 \text{ cm}$$

$$H_2 = 210 \text{ cm}$$

$$H_3 = 900 \text{ cm}$$

$$H_7 = 1,260 \text{ cm}$$

$$W_4 = 900 \text{ cm}$$

$$H_4 = 360 \text{ cm}$$

$$H_5 = 180 \text{ cm}$$

III. ATMOSPHERIC TRANSMITTANCE USING LOWTRAN 6

A. DESCRIPTION OF LOWTRAN 6

LOWTRAN 6 is the latest issue of LOWTRAN code that has been designed to calculate the transmittance of the atmosphere over spectral bands from $0.25\mu\text{m}$ to $28.5\mu\text{m}$ along paths of various inclinations and, of course, through different atmospheric profiles and parameters.

In order to use LOWTRAN 6 program we have to fill four (4) cards (groups) of input data.

Cards 1 and 2 require the significant meteorological parameters for the atmospheric profile. Card 3 requires the geometry of the problem i.e. initial and final altitude and the path length. Card 4 is related to the wavelength range and limits.

B. DATA USED

For card 1 we used data for the Mediterranean Sea and more specifically for the Aegean Sea area and the region from Crete to North Africa.

For this area we have two different atmospheric profiles, namely Midlatitude Summer for months October through April, and Tropical for months May through September [Ref. 6].

For card 2 we used again data from [Ref. 6] for each month individually and for card 3 we used all the possible combinations between final altitude and PATH from Table 2 and for the initial altitude the mean altitudes of each "point source" of the "hottest" ship area as given in Section G of Chapter II.

At this point we have to choose one more parameter that will be needed for our problem : the wavelength range of the detector operation. We decide that this range will be, in first approximation, in the 5um window (i.e. $\lambda_1=4.20\mu\text{m}$ - $\lambda_2=5.18\mu\text{m}$) [Ref. 4:ch 5, p.89].

Lowtran 6 has the advantage of giving us, besides the average transmittance between two limits, the spectral transmittance as well. From this spectral distribution we can reject certain values of very low spectral transmittance and therefore the wavelength range can be narrower. This peculiarity will have an influence on card 4.

C. RESULTS

Running LOWTRAN 6 for all the flight altitudes of the missile and for both Midlatitude and Tropical atmospheric profiles, we observed that, for wavelengths less than $4.435\mu\text{m}$ and greater than $5.0\mu\text{m}$, the spectral transmittance generally shows values less than about 0.10. Deciding to reject these low values we choose as the final spectral range of the detector operation to be from $4.435\mu\text{m}$ to $5.0\mu\text{m}$

In Figure 3.1 you will find the spectral transmittance in the above range for both atmospheric profiles.

Using the final wavelength range we calculated the average transmittance for all the possible combinations between atmospheric profile, missile flight altitude and individual "point sources" of the ship's tracked area. Tables 23 to 46 in Appendix C demonstrate both the data and total average transmittance for each month.

From the data of the above tables, it is obvious that the influences of both missile flight altitude (from 50m to 100m) and the relative differences between the individual "point source" altitudes (4m to 16m) are very weak on the

average transmittance. Averaging in both directions in this two dimensional table results in a unique representative value for each month. Checking these average values we observe again a relatively small difference between months belonging in the same atmospheric profile. Since a unique value of average transmittance of each atmospheric profile would be very convenient for the calculations to follow, we average over several months yielding the following final values:

Midlatitude summer : 0.4711

Tropical: 0.4259

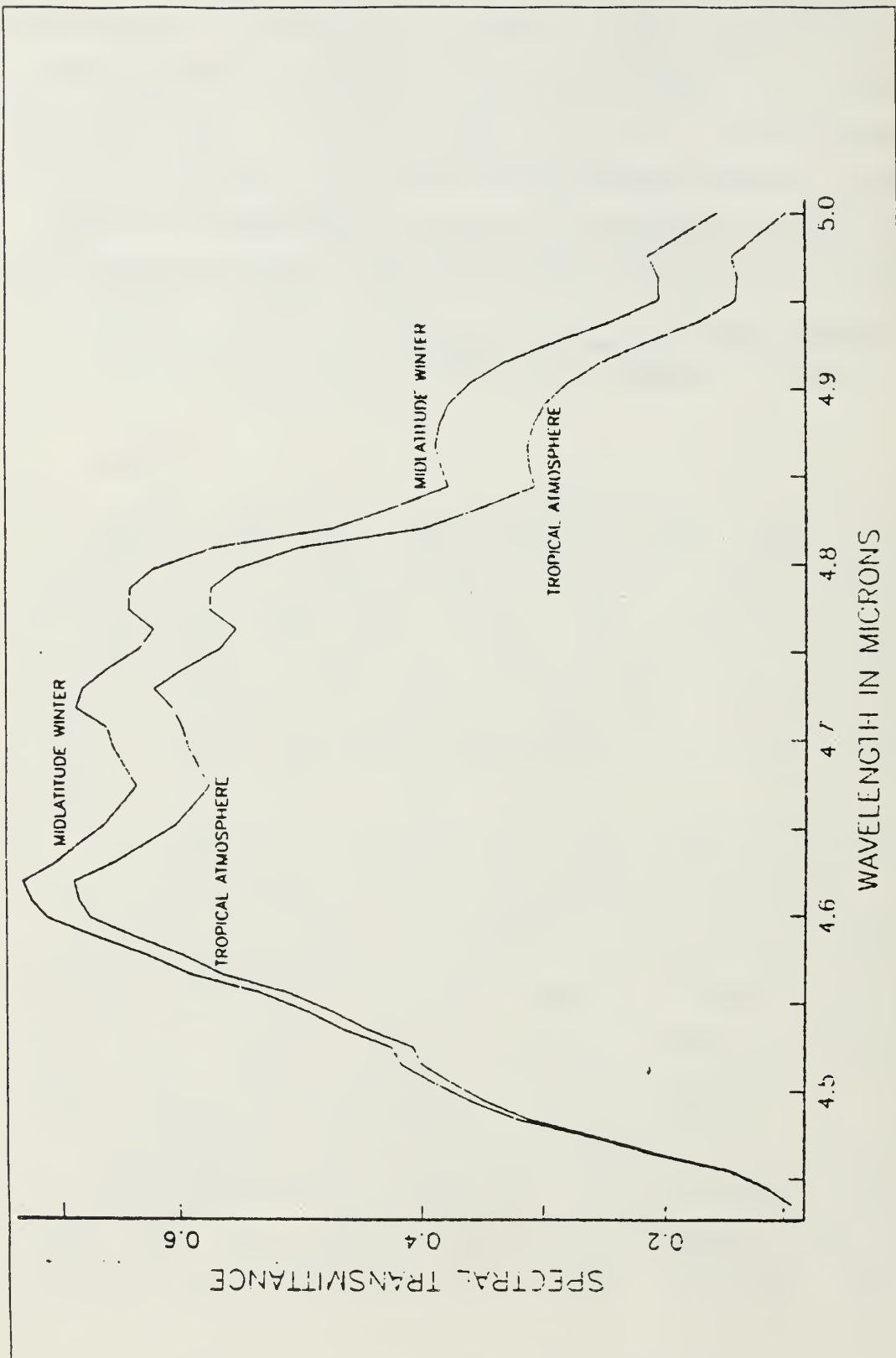


Figure 3.1 Spectral Transmittance in the Window of 4.435 μ m-5.00 μ m Through LOWTRAN 6

IV. CALCULATION OF SHIP AND BACKGROUND RADIANCE

A. NORMAL COMPONENT OF SHIP RADIANCE DUE TO THERMAL RADIATION

The purpose of this calculation is to find, by integrating the Plank's radiation law, the radiance in the given wavelength range.

From Plank's radiation law we know that:

$$M_{\lambda}(T) = [2\pi c^2 h / \lambda^5] \cdot [1 / (e^{\frac{hc}{\lambda T}} - 1)] \quad (\text{W/cm}^2 \text{ cm})$$

or

$$M(T) = C_1 \lambda^5 / (e^{\frac{C_2}{\lambda T}} - 1)$$

where:

$$C_1 = 2\pi c^2 h = 3.7415 \cdot 10^{12} \quad (\text{W} \cdot \text{cm}^2)$$

$$C_2 = hc/k = 1.4388 \quad (\text{cm} \cdot \text{K})$$

The above formula is in the form of:

$$M(T) = C \cdot x^m (e^x - 1)$$

Integrating this between the band limits λ_1 , λ_2 , we will find the in-band energy radiance [Ref. 4:p. 19].

Therefore:

$$L_{\Delta\lambda} = \epsilon_0 / \pi \int_{\lambda_1}^{\lambda_2} M_{\lambda}(T) d\lambda = [C_1 \epsilon_0 / \pi C_2^4] \cdot T^4 \cdot \sum_1 \quad (\text{W/cm}^2 \cdot \text{Sr})$$

Where:

$$\sum_1 = \left| \sum_{m=1}^{\infty} m^4 [(m \cdot x)^3 + 3(m \cdot x)^2 + 6(m \cdot x) + 6] e^{-mx} \right|_{x_1}^{x_2}$$

and $x = C_2 / \lambda T$

$$\sum_1 = \sum_{m=1}^{\infty} m^{m x_2} \cdot m^4 [(m \cdot x)^3 + 3(m \cdot x)^2 + 6m \cdot x + 6] - e^{-m x_1} m^4 [(m \cdot x)^3 + 3(m \cdot x)^2 + 6m \cdot x + 6]$$

In the above relations, the temperature T is taken from Tables 5, 18 in Appendix A.

B. NORMAL COMPONENT OF SHIP RADIANCE DUE TO REFLECTED SOLAR ENERGY

We have already calculated the normal component of solar irradiance E incident on each ship surface. In the energy balance calculation we considered that the solar energy absorbed by the surface is $E_{s\eta} a_o$. Obviously the amount $(1-a_o) \cdot E_{s\eta}$ is reflected.

Defining as $D(0-\lambda)$ the percentage of the solar constant associated with wavelengths shorter than λ we take [Ref. 4:p. 17].

$$D(0-4.435)=99.3075454\%$$

$$D(0-5.000)=99.511500\%$$

Therefore

$$\Delta D = D(0-5.000) - D(0-4.435) = 0.2039546\%$$

In conclusion we have that the normal reflected solar energy per m^2 from $\lambda_1=4.435\mu m$ to $\lambda_2=5.00\mu m$ is:

$$(1-a_o) \cdot \Delta D \cdot E_{s\eta} = (1-a_o) \cdot 2.04 \cdot 10^{-3} \cdot E_{s\eta} \quad (W/m^2)$$

In order to determine the normal component of radiance due to reflection we must divide the above value by π and in order to transform into cm^2 we must divide by 10^4 . Finally the normal component of radiance due to reflection in $(W/cm^2 \cdot Sr)$ from $\lambda_1=4.435\mu m$ to $\lambda_2=5.00\mu m$ will be:

$$L_{R\Delta\lambda} = (1-a_o) \cdot 2.04 \cdot 10^{-3} \cdot E_{s\eta} / \pi \cdot 10^4 = (1-a_o) \cdot 4.08 \cdot 10^{-8} \cdot E_{s\eta} \quad (W/cm^2 \cdot Sr)$$

C. NORMAL COMPONENT OF STACK EXIT PLANE RADIANCE

So far we know that the stack exit plane area is $4.43 \cdot 10^4 \text{ cm}^2$ and that the corresponding uniform temperature is $425.4K$.

For simplicity we consider that the greater part of the exhaust gas is CO_2 . Since CO_2 is a selective emitter we need to carry out the approximation shown in Figure 4.1 which partially accounts for atmospheric absorption and approximates the peak with a constant emissivity over a limited

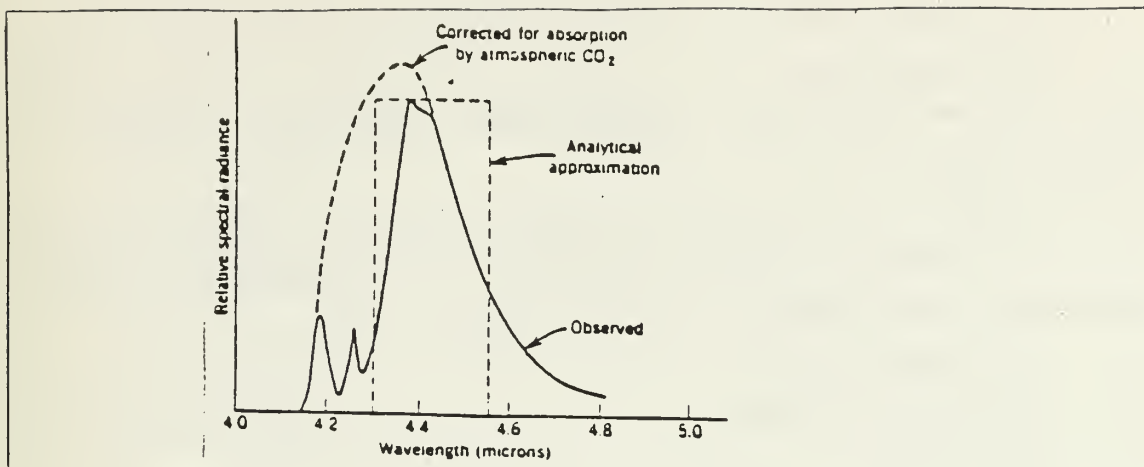


Figure 4.1 The 4.4um Emission Band of CO₂ [Ref. 12]

range. Taking the band to be from $\lambda_1=4.35\mu\text{m}$ to $\lambda_2=4.55\mu\text{m}$ and the emissivity 0.5 we find for the radiance:

$$\begin{aligned} L &= \epsilon_0 \int_{4.35}^{4.55} M_\lambda d\lambda = (\epsilon_0 \sigma T^4 / \pi) \int_{4.35}^{4.55} M_\lambda d\lambda / \int_0^\infty M_\lambda d\lambda = (\epsilon_0 \sigma T^4 / \pi) \cdot (0.05) \\ &= (0.5) \cdot (5.67 \cdot 10^{-12}) \cdot (425.4)^4 \cdot (0.05) / \pi \\ &= 1.478 \cdot 10^{-3} \quad (\text{W/cm}^2 \cdot \text{Sr}) \end{aligned}$$

Since our band of interest overlaps with half of the 4.4 μm emission band of CO₂ the above value must be divided by 2. Therefore:

$$L = 7.39 \cdot 10^{-4} \quad (\text{W/cm}^2 \cdot \text{Sr})$$

D. TOTAL SHIP RADIANT INTENSITY IN THE DIRECTION FROM SHIP TO MISSILE

As mentioned in Section G of Chapter II, we will consider the surfaces $(A_1 + A_{11})$, $(A_2 + A_{12})$, A_3 , A_4 , A_5 , A_6 , A_7 , as "point sources". For each source we know the corresponding radiance due to thermal radiation and reflection i.e.

$$L_{T1} = L_{\Delta\lambda_1} + L_{R\Delta\lambda_1}$$

$$L_{T11} = L_{\Delta\lambda_{11}} + L_{R\Delta\lambda_{11}}$$

$$L_{T2} = L_{\Delta\lambda_2} + L_{R\Delta\lambda_2}$$

$$L_{T12} = L_{\Delta\lambda_{12}} + L_{R\Delta\lambda_{12}}$$

$$L_{T3} = L_{\Delta\lambda_3} + L_{R\Delta\lambda_3}$$

$$L_{T4} = L_{\delta\lambda_4} + L_{R\delta\lambda_4}$$

$$L_{T5} = L_{\delta\lambda_5} + L_{R\delta\lambda_5}$$

$$L_{T7} = L_{\delta\lambda_7} + L_{R\delta\lambda_7}$$

For L_{T6} we have the unique value given in section C of chapter III

In order to obtain the normal radiant intensity (W/Sr) of each surface we must multiply the corresponding values of each area and radiance. Doing this we take:

$$I_{1N} = L_{T1} \cdot A_1 + L_{T11} \cdot A_{11}$$

$$I_{2N} = L_{T2} \cdot A_2 + L_{T22} \cdot A_{22}$$

$$I_{3N} = L_{T3} \cdot A_3$$

$$I_{4N} = L_{T4} \cdot A_4$$

$$I_{5N} = L_{T5} \cdot A_5$$

$$I_{6N} = L_{T6} \cdot A_6$$

$$I_{7N} = L_{T7} \cdot A_7$$

The important magnitude for us is the radiant intensity in the direction of source - missile.

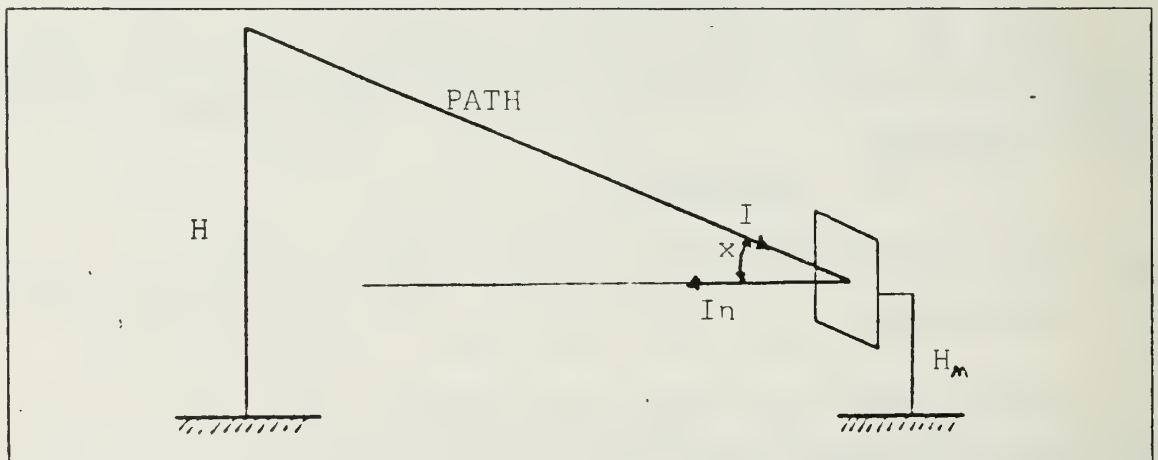


Figure 4.2 Relative Position Between Surface- Missile

In Figure 4.2 you will find a sketch representing the relative position between the surface and the missile. Based on that we conclude this the radiant intensity will be:

$$I = I_N \cdot \cos x \text{ for a vertical face}$$

$I = I_N \cdot \sin x$ for a horizontal face

where $x = \sin^{-1}(H - H_N / \text{PATH})$

The resulting relations will be:

$$I_1 = I_{1N} \cdot \cos x$$

$$I_2 = I_{2N} \cdot \sin x$$

$$I_3 = I_{3N} \cdot \cos x$$

$$I_4 = I_{4N} \cdot \cos x$$

$$I_5 = I_{5N} \cdot \cos x$$

$$I_6 = I_{6N} \cdot \sin x$$

$$I_7 = I_{7N} \cdot \sin x$$

E. BACKGROUND RADIANT INTENSITY

In the ideal case in which the detector tracks perfectly on the ships "hottest" area and the square I.F.V. will fit perfectly on that the detector will still see some areas outside of the ship. This is due to the fact that the upper construction of the ship has not a perfect rectangular shape. Therefore the detector will receive signal from an area of the sea that radiates behind the ship. Since this signal constitutes noise for the detector, it has important meaning.

In Figure 4.3 you will find the geometry from which we will determine the background radiant intensity. We must notice that the sketch in Figure 4.3 has been magnified for convenience in the ship region. In other words angle $(\theta + \delta)$ is very close to 90° and the side of I.F.V. AE is ASE is practically equal to the ship dimension ABC.

AB represents the height of surface A_s [Figure 2.6] from the sea level or $AB = H_1 + H_2$

BC then represents the path through which the detector will see the sea area FG past the stack.

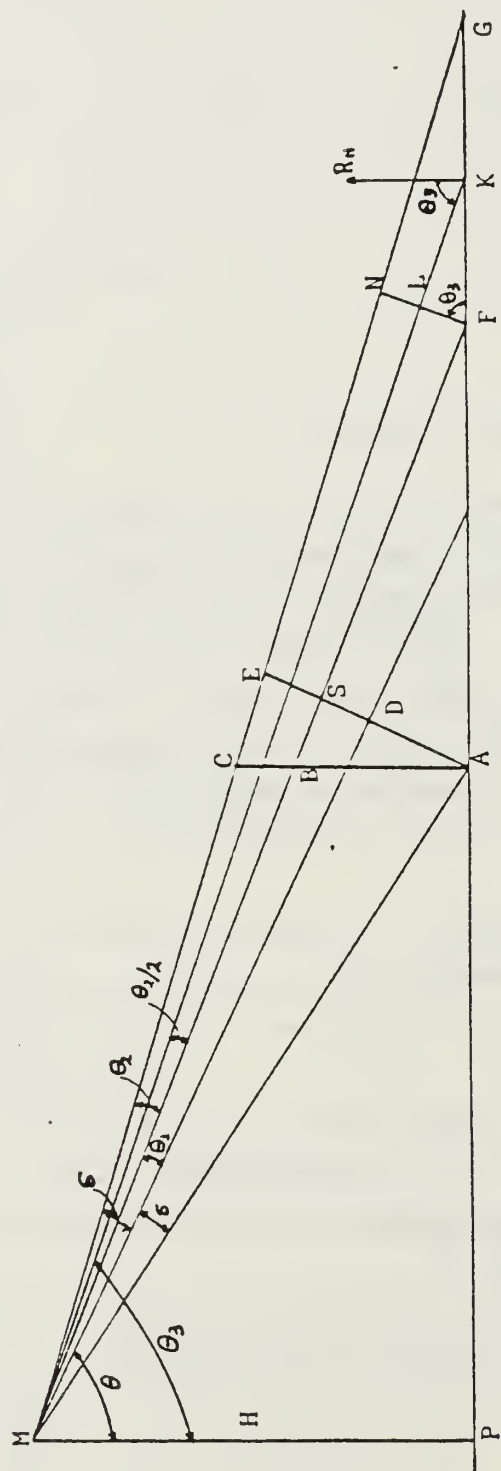


Figure 4.3 Geometry for Determination of Background Radiant Intensity

The width of this area is (SIDE- W_1) which represents the free horizontal dimension over the surface A_1 .

From the geometry of Figure 4.3 we have:

$$DS=AS-SIDE$$

$$\theta_1 = \tan^{-1} (DS/PATH)$$

$$\theta_2 = \delta - \theta_1$$

$$MA=PATH/\cos\delta$$

$$\theta = \cos^{-1} (H/MA)$$

$$PF=H \cdot \tan(\theta + \delta + \theta_1)$$

$$PG=H \cdot \tan(\theta + 2\delta)$$

$$FG=PG-PF$$

$$\theta_3 = \theta + \delta + \theta_1 + \theta_2 / 2$$

$$MK=H \cdot \tan\theta_3$$

$$AREA=FG \cdot [SIDE-W_6] \cdot \cos\theta_3$$

Table 3 demonstrates the result of the above calculations for six different flight altitudes.

TABLE 3
Geometrical Parameters for Observed Sea Area

H (m)	FG (m)	θ (deg)	MK (m)	AREA (m^2)
50	333.67	88.415	1806.98	144.90
60	230.54	87.915	1648.07	131.68
70	180.09	87.410	1547.47	127.76
80	144.50	86.91	1481.94	122.29
90	116.07	86.4	1430.50	114.42
100	99.42	85.9	1395.07	111.60

For the sea water we know that the average temperature in the geographical area of our interest is $13^\circ\text{C}=286.15\text{K}$ for Midlatitude Summer and $18^\circ\text{C}=291.15\text{K}$ for Tropical atmosphere [Ref. 6].

For the sea water emissivity we chose the value of 0.96 [Ref. 10:p.07].

For the calculation of the normal component of the sea radiance ($\text{W}/\text{cm}^2 \cdot \text{Sr}$) in the range $\lambda_1=4.435\mu\text{m}$ to $\lambda_2=5.00\mu\text{m}$ we will use again the formulas from section A of chapter IV. This value must be multiplied by the water emissivity =0.96. For convenience we consider the observed area of sea as a point source.

The normal component of the radiant intensity of this point source it will be:

$$I_{wn} = L_{wn} \cdot \text{AREA}$$

And in the direction leading to the missile will be:

$$I_w = I_{wn} \cdot \cos\theta$$

V. DETECTOR MODELING AND CALCULATION OF S/N RATIO

A. DETECTOR SYNTHESIS

We already studied the geometry of the detection problem which shows us what the detector is required to do, and of course from this side we are interested in the most realistic performance of the detector. Since we do not have available experimental data that could show us the performance of the detector element we have to choose this according to the literature.

From Figure 5.1 [Ref. 10] the possible choices for the detector include photovoltaic or photocontactive Indium Antimonide and Lead Selenide. The detailed data sheets for these detectors [Ref. 12:pp.365-368] show the relative advantages and disadvantages of each. When they are compared on the basis of D^* , photovoltaic Indium Antimonide is clearly the best detector. A possible difficulty with this conclusion arises when the responsivities are compared and it is noted that value of Lead Selenide is 10 times higher than it is for the other two types of detector. In an ideal operating environment, that is, in which there are no extraneous sources of noise, the designer is interested in the signal - to - noise ratio of the detector, as described by D^* and not the signal level, as described by responsivity. In advance we know that during the experimental trials photovoltaic Indium Antimonide had the better performance. Therefore we are led to the decision to use one element of photovoltaic Indium Antimonide, and we can see the detailed data for this material in Figure 5.2 [Ref. 12:p.368].

This one element will be placed in the middle of an assumed two mirror system as in Figure 5.3, with

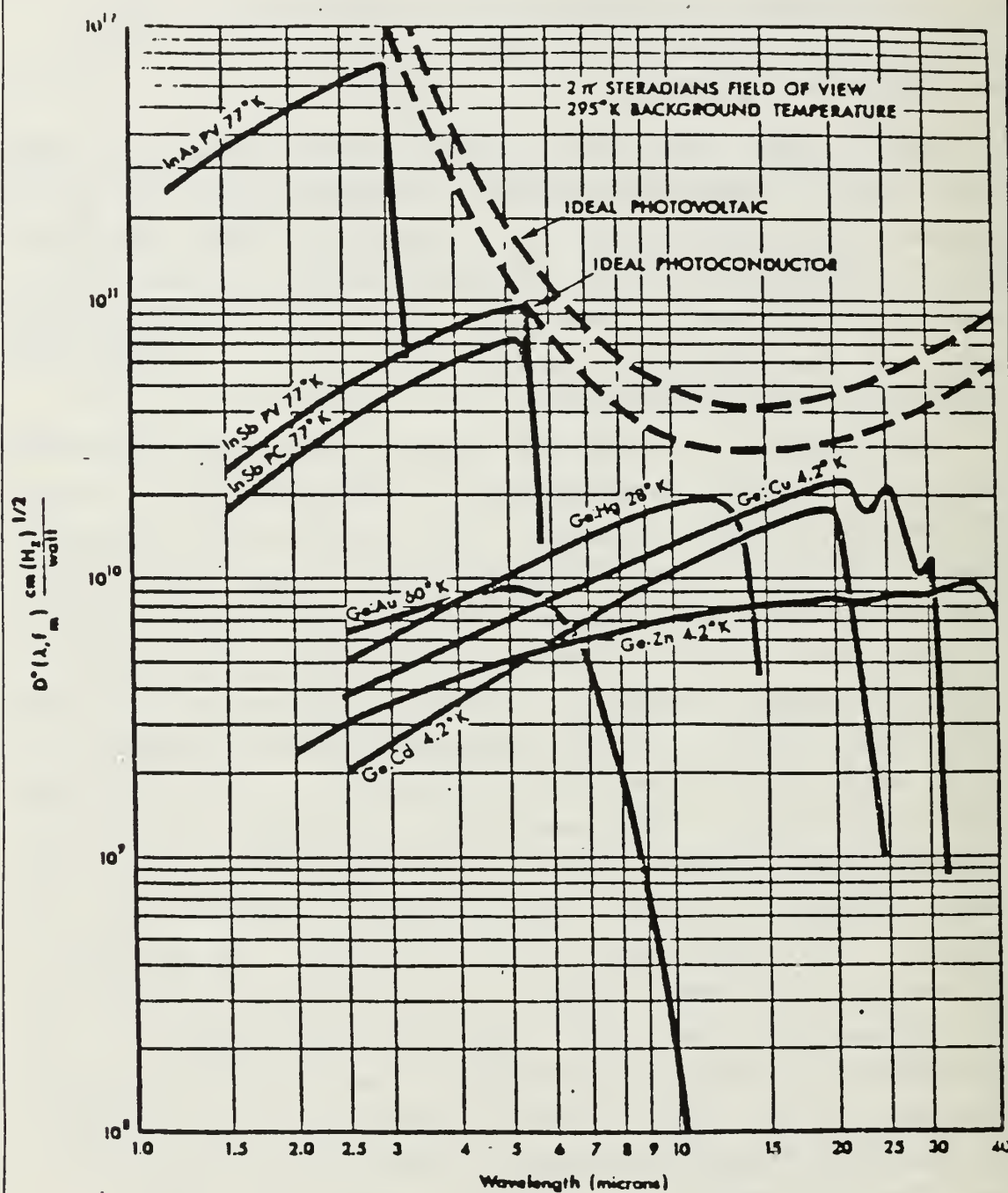


Figure 5.1 The D^* of the Detectors in Each Atmospheric Window at the Most Common Operation Temperature [Ref. 10]

Indium Antimonide (InSb)

Type: Photovoltaic.

Element sizes available: From 0.1×0.1 to 10×10 mm. Rectangular elements from 0.1 mm wide. Circular elements with diameters from 0.1 to 10 mm.

Time constant: Less than $1 \mu\text{sec}$.

Dynamic impedance: $2-5 \times 10^4 \text{ ohm}$.

Responsivity: $2 \times 10^4 \text{ VW}^{-1}$.

$$\frac{D^* (\text{peak})}{D^* (500^\circ\text{K})}: 6.2$$

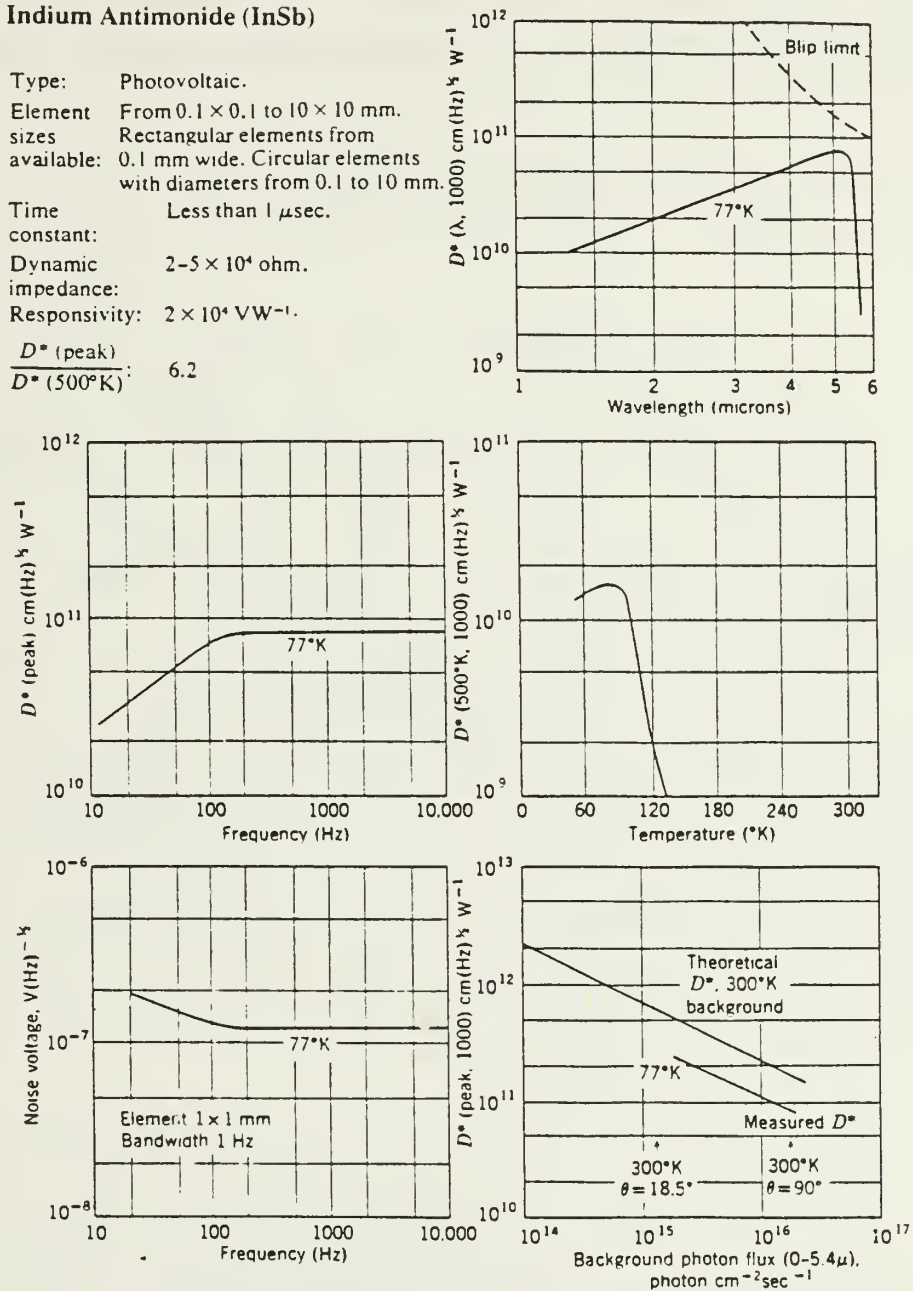


Figure 5.2 Data Sheet for Photovoltaic Indium Antimonide Detector [Ref. 12]

reflectivity 0.9 each mirror and total of two $r_t = 0.9 \cdot 0.9 = 0.81$. The detector will be considered to be used with a two-mirror system designed so that the detector element will subtend area equal to the I.F.V. at a distance of PATH. Thus we have to determine the size of the sensitive element (detector).

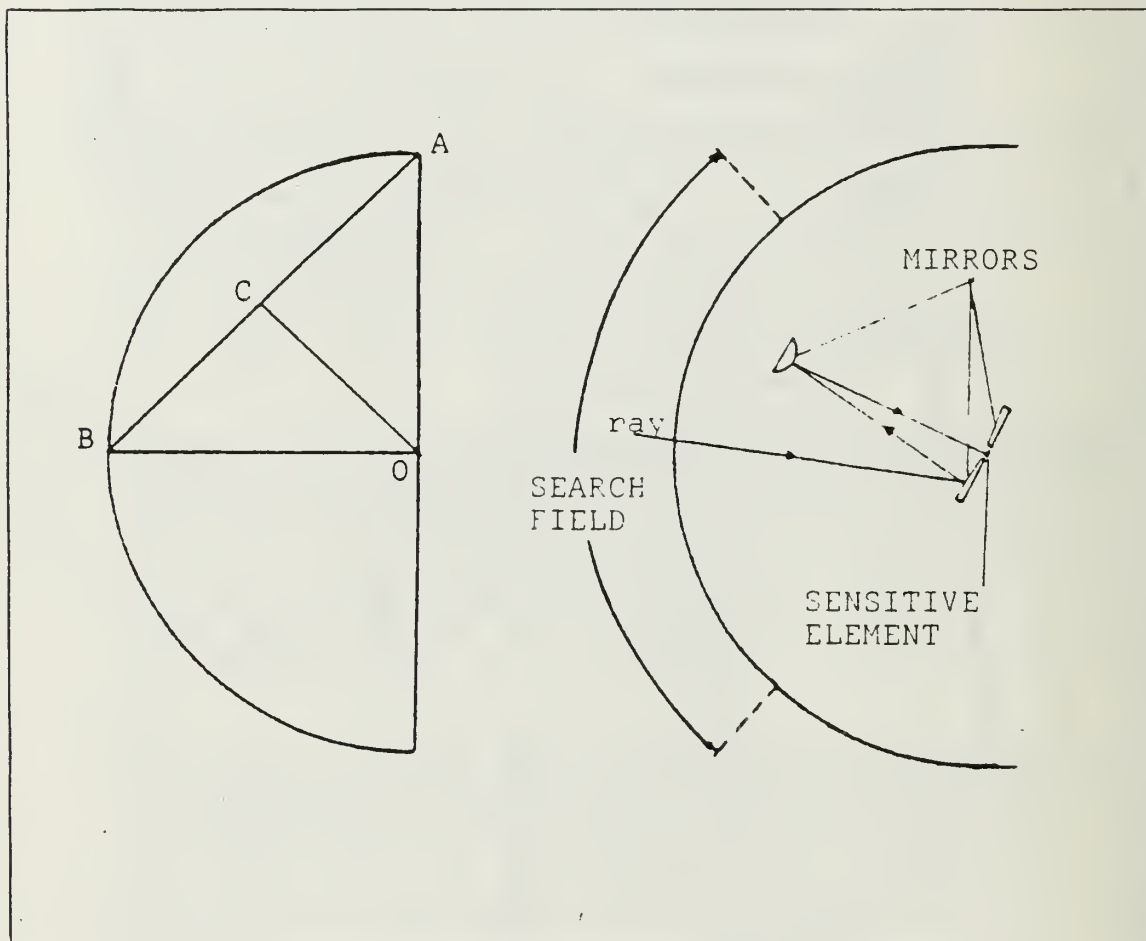


Figure 5.3 System of Two Mirrors in the Receiver

We know that the area of the detector A is given by:

$$A_d = w \cdot f^2$$

where

w = Instantaneous Field of View in (Sr)

$$w = (\text{SIDE} \cdot \text{SIDE}) / (\text{PATH})^2 = (2200 \cdot 2200) / (\text{PATH})^2 \text{ (Sr)}$$

f=equivalent focal length

and for PATH we have to use the values from Table 2 which is function of the flight altitude.

For the our purpose of work a very good and accurate approach to calculate the equivalent focal length of the system of two mirrors is the following.

First we have to choose the diameter of the entrance aperture $D_o=12\text{cm}$. This dimension is good enough to have an aerodynamic shape in the nose of the missile. Thus from the Figure 5.3 we have:

$$(AB)^2 = (AO)^2 + (OB)^2 = 72 \text{ and } AB = 8.4\text{cm}$$

$$(AO)^2 = (AC)^2 + (CO)^2 \text{ or}$$

$$(CO)^2 = (AO)^2 - (AC)^2 = (AO)^2 - (AB/2)^2 = \\ = (CO)^2 = 6^2 - (8.49/2)^2 = 17.98\text{cm}^2$$

and $CO = 4.24\text{cm}$

We can define the distance CO as the equivalent focal length $f = 4.24\text{cm}$

And

$$A_d = w \cdot f^2 = (2200)^2 \cdot (4.24)^2 / (\text{PATH})^2$$

Substituting the values of PATH for each flight altitude gives A and the square root of this gives us the side of the detector element. Table 4 demonstrates the dimensions of the detector element shows that with reasonable detector size the I.F.V. at about 1125 meters slant path range will include the hot region of the ship regardless of the flight altitude.

B. SIGNAL VOLTAGE

The general formula that gives the signal voltage is:

$$V_s = [A_o \cdot r_o \cdot R / (\text{PATH})^2] \cdot \left[\int_{\lambda_1}^{\lambda_2} I_\lambda \tau_a(\lambda) d\lambda \right]$$

Where

A_o : Area of entrance aperture

$$A_o = \pi D^2 / 4 = 113.1\text{cm}^2$$

r_o : Optics reflectance

TABLE 4
Dimensions of the Detector Element

FLIGHT ALTITUDE (m)	PATH (m)	DIMENSION OF DETECTOR ELEMENT (m:m)
50	1,120	0.83 x 0.83
60	1,124	0.83 x 0.83
70	1,127	0.83 x 0.83
80	1,130	0.83 x 0.83
90	1,132	0.83 x 0.83
100	1,134	0.83 x 0.83

R : responsivity = $2 \cdot 10^4$ (V/W)

I_λ : Spectral radiant intensity of the source

τ_a : Spectral atmospheric transmittance

The above relation can be further simplified using instead of the spectral transmittance an average one as we determined in Section C of Chapter III i.e. 0.4711 for Midlatitude summer and 0.4259 for Tropical atmosphere.

Taking $\tau_a(\lambda)$ outside of the integral then the quantity $\int_{\lambda_1}^{\lambda_2} I_\lambda d\lambda$ becomes simply the inband radiant intensity of the source which has been calculated in section D of chapter III. Hence the signal voltage formula becomes:

$$V_s = A \cdot r \cdot R \cdot \tau_a \cdot I_\lambda / (\text{PATH})^2$$

In order to determine the signal voltage due to all the available point sources inside the I.F.V. we use the superposition principle:

$$V_s = [A \cdot r \cdot R \cdot \tau_a / (\text{PATH})^2] \cdot [I_1 + I_2 + I_3 + I_4 + I_5 + I_6 + I_7]$$

C. NOISE VOLTAGE

The noise voltage is due to two main factors, namely the background noise that is created from the background radiant intensity and the noise from the optical system.

In Section E of Chapter III we determined the radiant intensity of the sea region that the detector observes and we named I_w (W/Sr). The noise voltage of this reason will be:

$$V_{NB} = A_d \cdot r_o \cdot R \cdot \tau_o \cdot I_w / (MK)^2$$

where MK is determined in Figure 4.3 and indicates the average path between the observed sea surface and the detector.

The noise signal due to the optical system is given by: [Ref. 12].

$$V_{NO} = R \cdot (A_d \cdot \Delta f)^{1/2} / D^*$$

where

D^* : Detectivity with average value $9 \cdot 10^{11}$ [cm(Hz)^{1/2}/W] in the wavelength range $\lambda_1 = 4.435 \mu\text{m}$ to $\lambda_2 = 5.00 \mu\text{m}$

A_d : Area of the detector as determined in previous section of the present chapter.

R : Responsivity

Δf : equivalent noise bandwidth

The equivalent noise bandwidth is given by

$$\Delta f = 1/2\tau_d$$

where

τ_d : dwell time (time required for the image of the target to pass across the detector).

and $\tau_d = w \cdot c / \dot{Q}$

where

c : number of detector elements (1 for our case)

\dot{Q} : Time rate of search.

and

$$\dot{Q} = Q / \tau_F$$

where

Q :size of search field in (Sr)

T_f :frame time (time required to scan the entire search field). For our case we chose 10msec.

Therefore

$$\Delta f = 1/2 T_f = Q/2 \cdot w \cdot c = Q/2 \cdot w \cdot c \cdot T_f$$

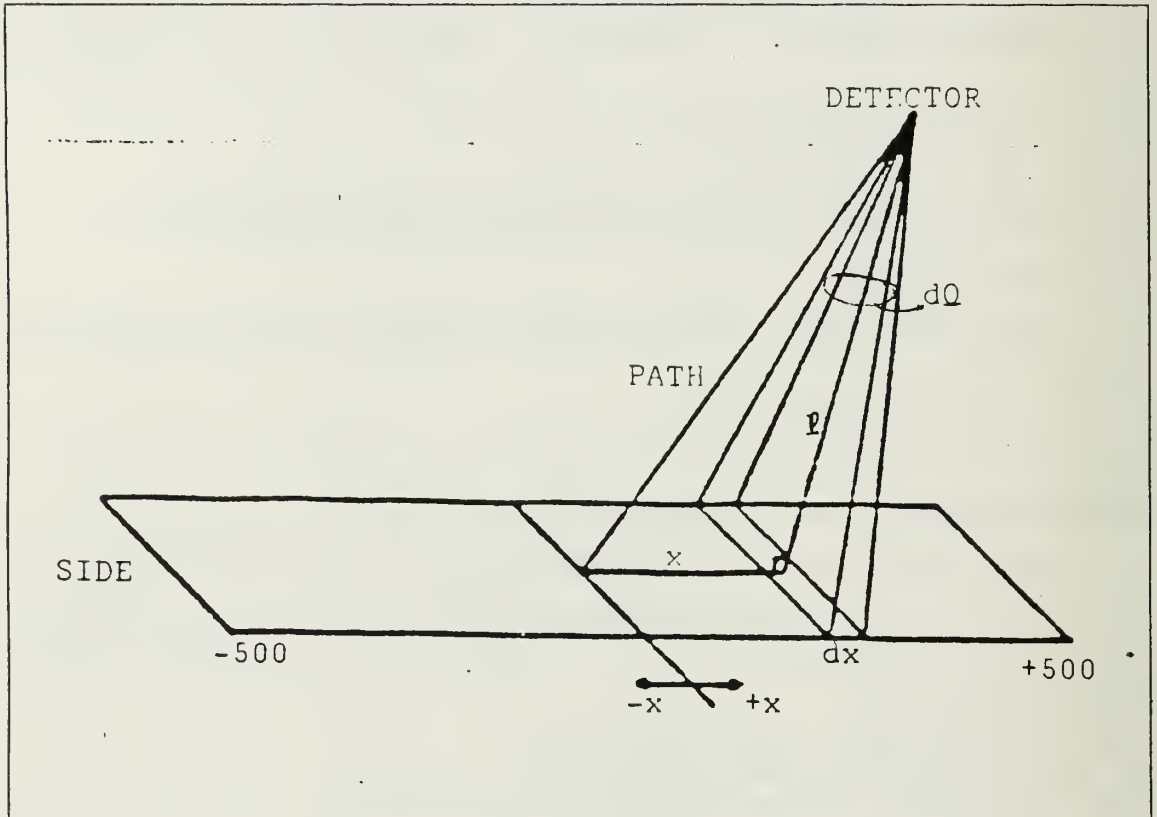


Figure 5.4 Total Detector Search Field

In Figure 5.4 you will find the geometrical representation of the total search field which will have total length of 1000m and is scanned by the detector in =10msec.

The total solid angle that the search field subtends at the detector is:

$$Q = dQ$$

$$dQ = dx \cdot SIDE / l^2$$

$$l^2 = (PATH)^2 - x^2$$

$$dQ = [SIDE / (PATH)^2 - x^2] \cdot dx$$

$$Q = (SIDE) \int dx / (PATH)^2 - x^2$$

Since $(PATH)^2 > 500^2$ always, from the tables we get:

$$\begin{aligned} Q &= (SIDE) / 2(PATH) [\ln((PATH+x)/(PATH-x))] \\ &= (SIDE) / 2(PATH) [\ln((PATH+500)/(PATH-500)) \\ &\quad - \ln((PATH-500)/(PATH+500))] \\ &= ((SIDE) / 2(PATH)) \cdot \ln[(PATH+500)/(PATH-500)]^2 \\ Q &= ((SIDE) / (PATH)) \cdot \ln[(PATH+500)/(PATH-500)] \end{aligned}$$

Therefore

$$\Delta f = (1/2(SIDE) \cdot c \cdot \tau_p) \cdot \ln[(PATH+500)/(PATH-500)]$$

The total noise voltage is

$$V_n = V_{NB} + V_{No}$$

And the signal to noise ratio is:

$$V_s / V_n = V_s / (V_{NB} + V_{No})$$

In figures 5.5 to 5.22 we can see the summary of the results of the above calculation for all the possible combinations of the relative parameters.

In Appendix D we can see the influence of sky condition to S/N ratio for the two extremes flight altitude i.e. 50 (m) - 100 (m) and for all the combinations between atmospheric profile and paint emissivity.

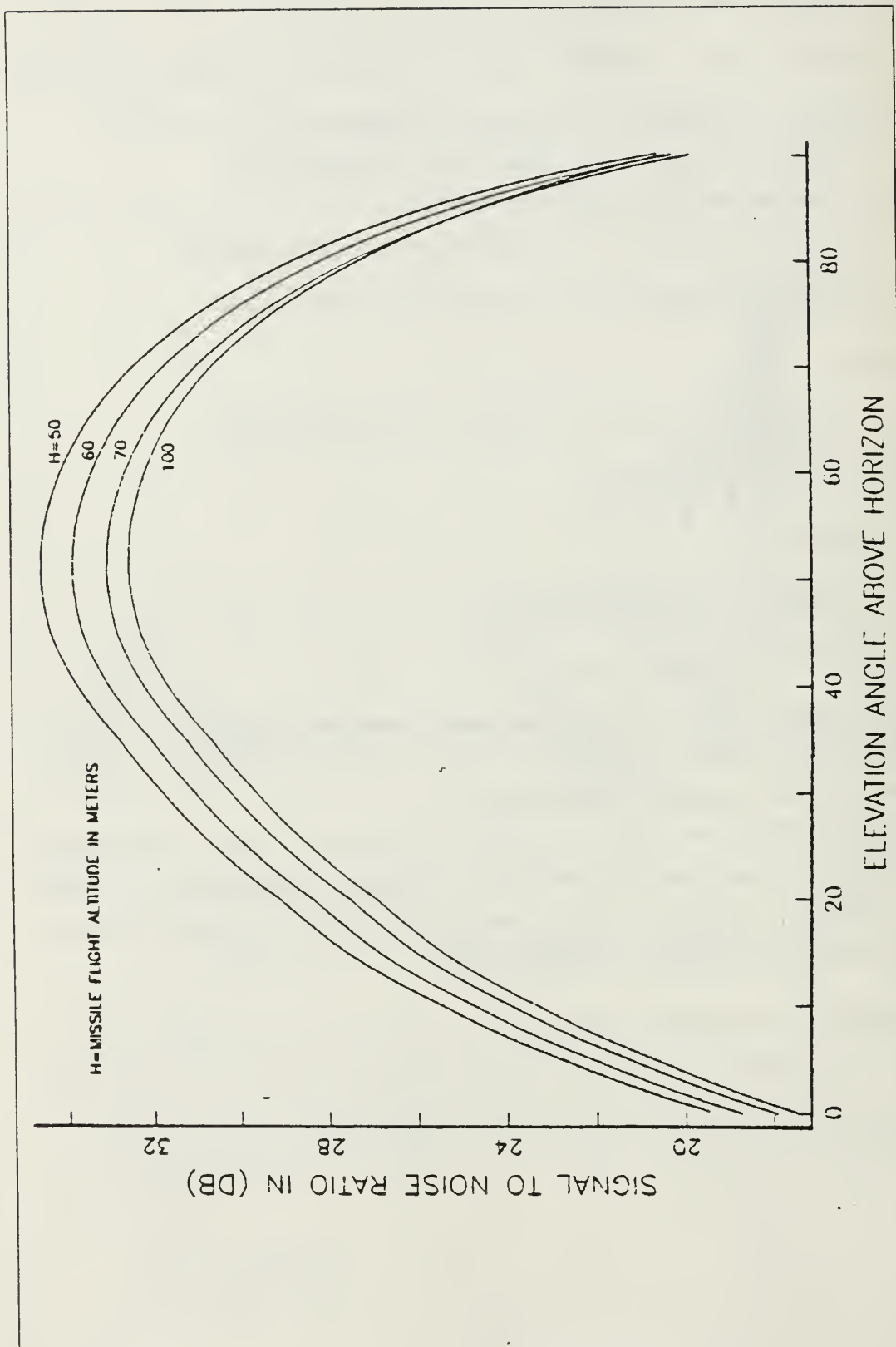


Figure 5.5 Influence of Missile Flight Altitude for Unobscured Sun, $\epsilon_0=0.80$, Midlatitude Summer

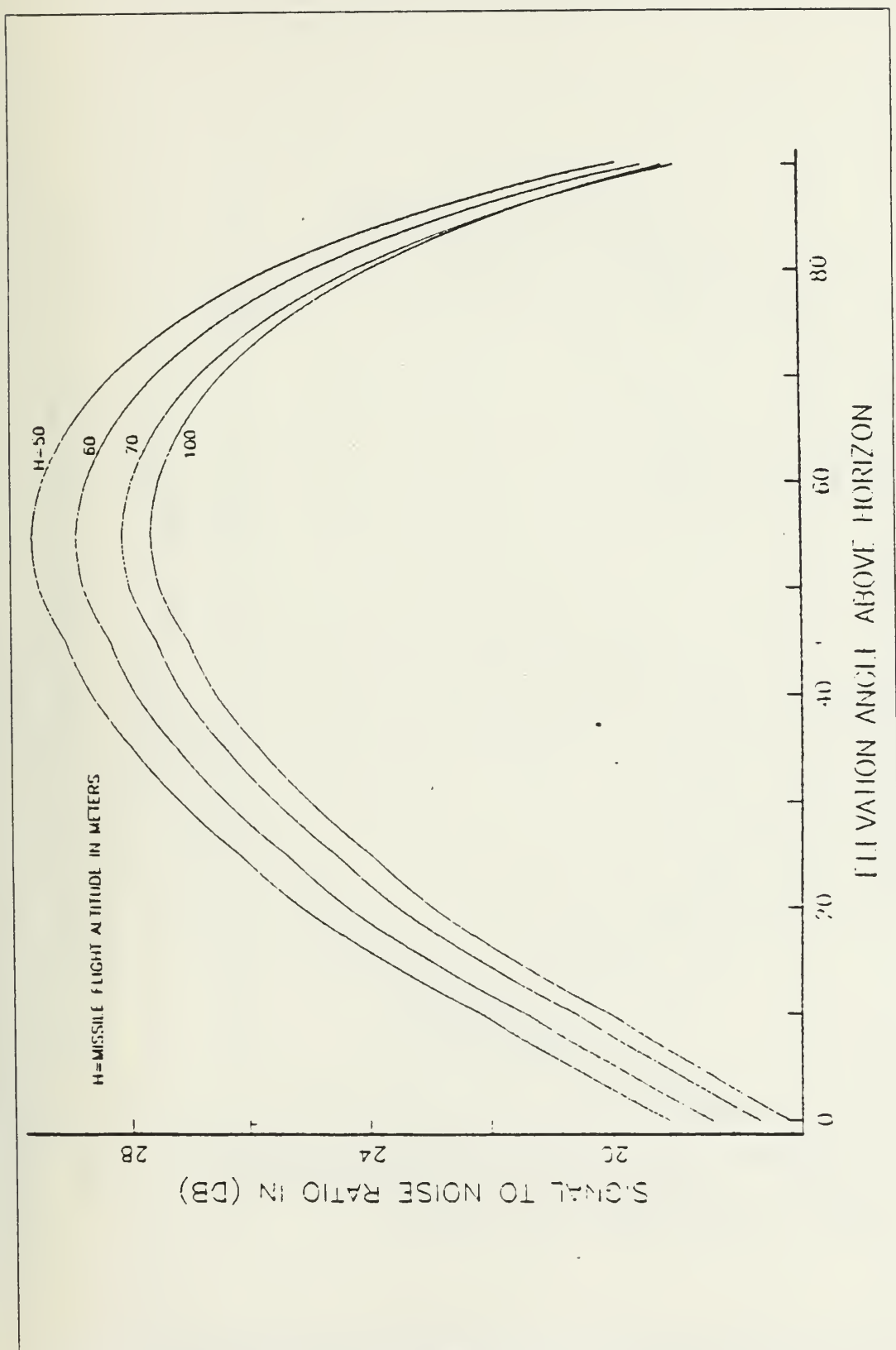


Figure 5.6 Influence of Missile Flight Altitude for Sun with Light Clouds, $\epsilon_{\infty}=0.80$, Midlatitude Summer

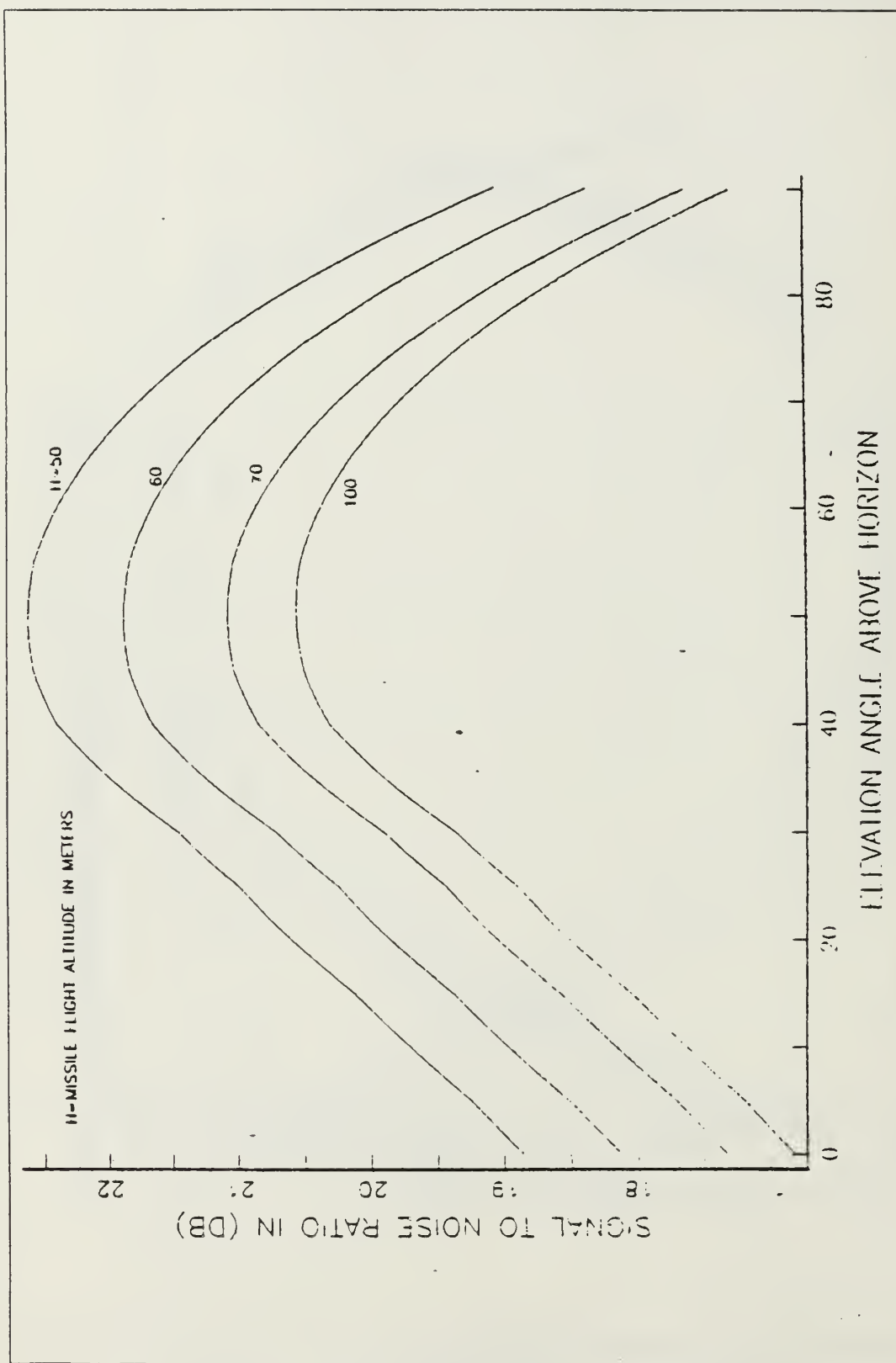


Figure 5.7 Influence of Missile Flight Altitude for Sun with Heavy Storm Clouds, $\epsilon_0=0.80$, Midlatitude Summer

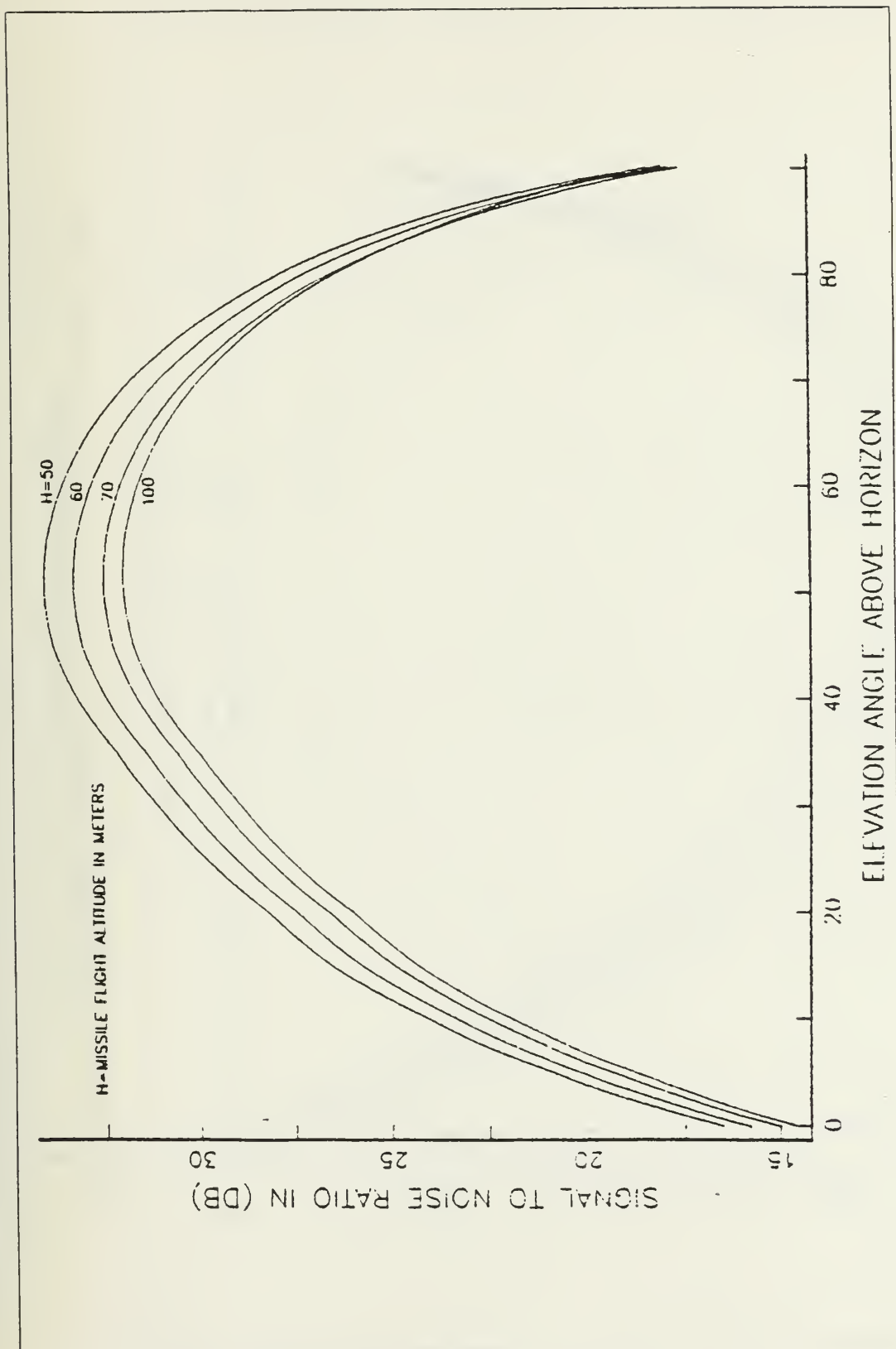


Figure 5.8 Influence of Missile Flight Altitude for Unobserved Sun, $\epsilon_0=0.55$, Midlatitude Summer

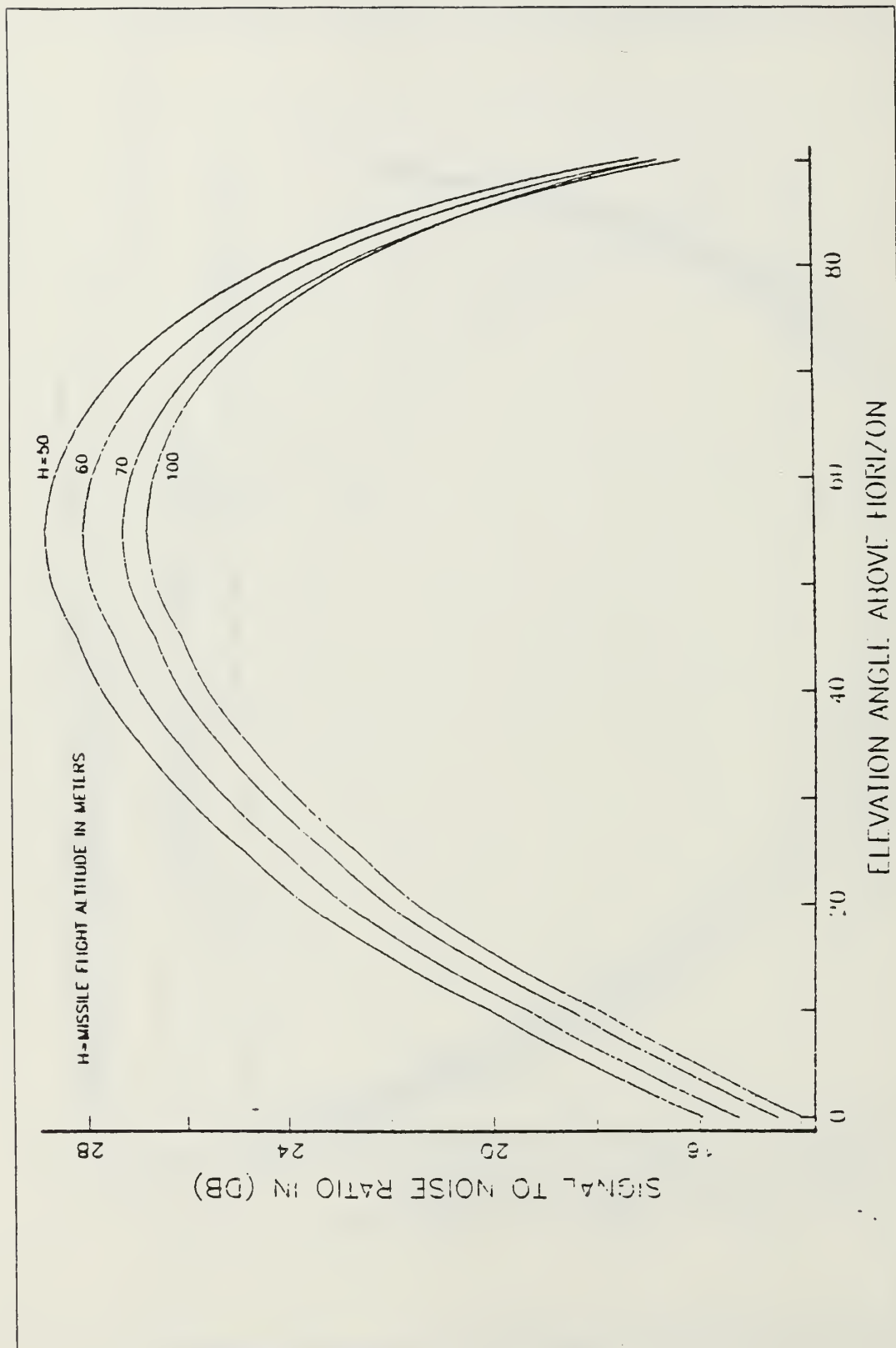


Figure 5.9 Influence of Missile Flight Altitude for Sun with Light Clouds, $\epsilon_0=0.55$, Midlatitude Summer

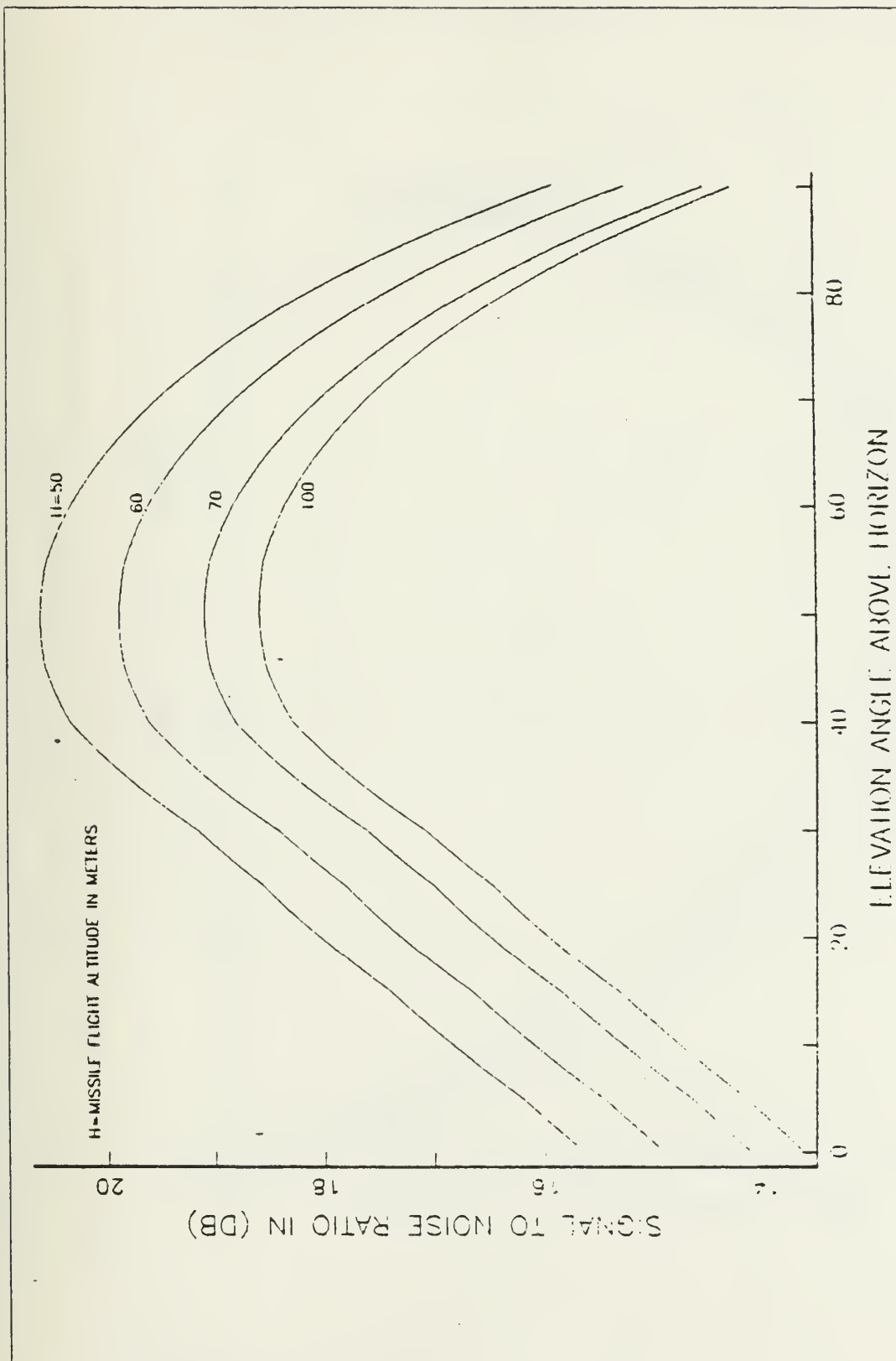


Figure 5.10 Influence of Missile Flight Altitude for Sun with Heavy Storm Clouds, $\epsilon_c=0.55$, Midlatitude Summer

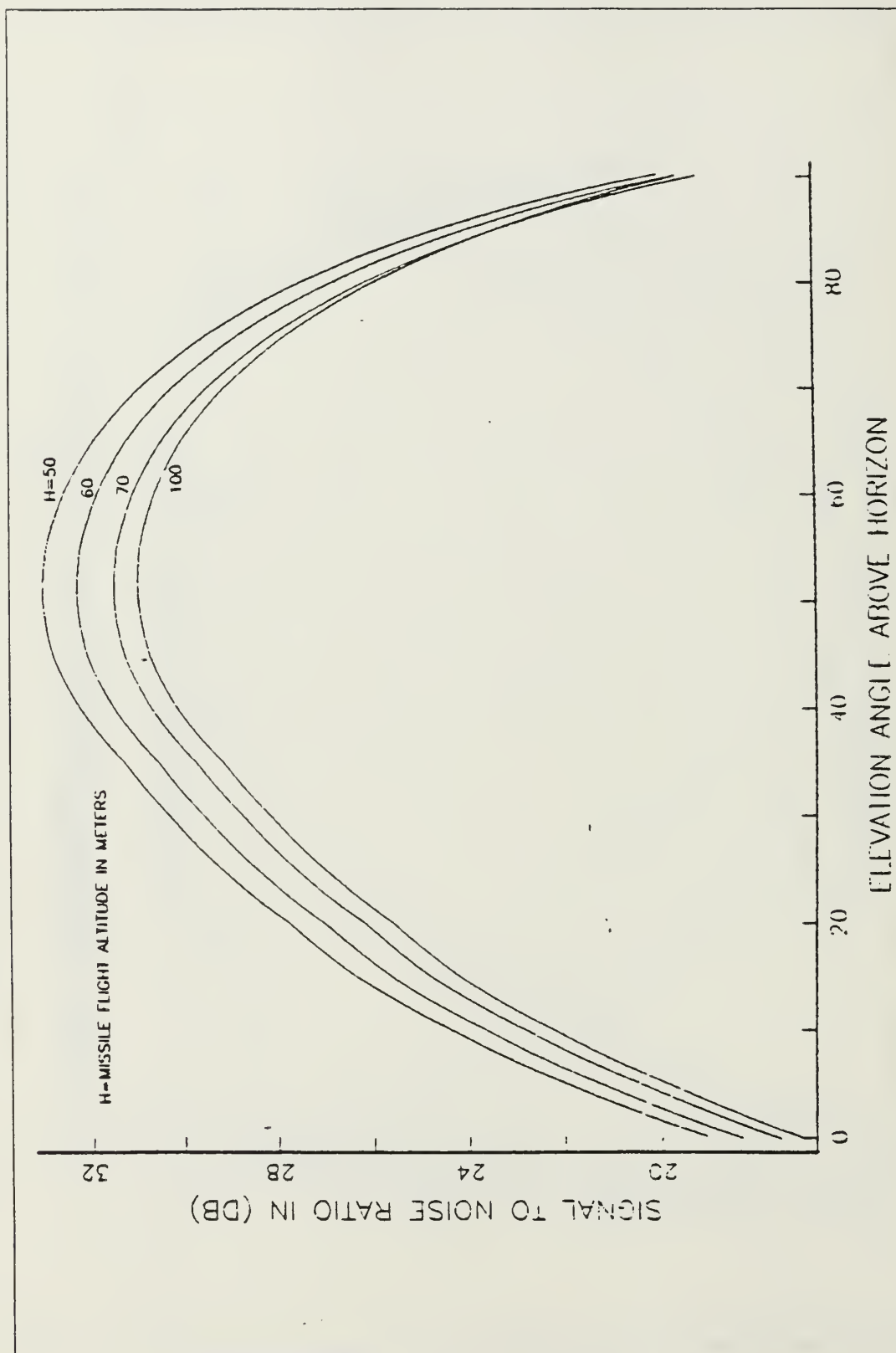


Figure 5.11 Influence of Missile Flight Altitude for Unobscured Sun, $\xi_0=0.80$, Tropical Atmosphere

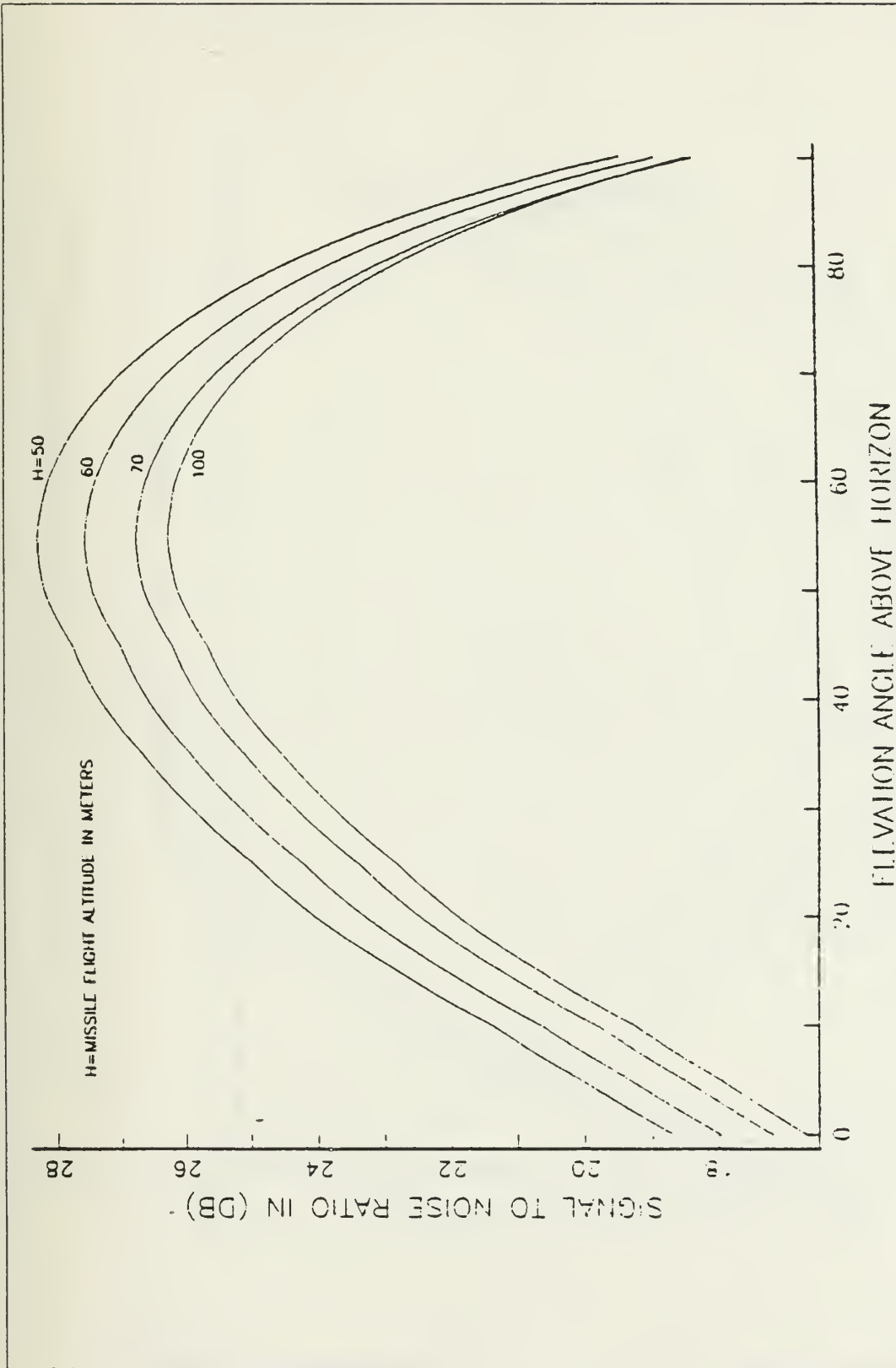


Figure 5.12 Influence of Missile Flight Altitude for Sun with Light Clouds, $\epsilon_s=0.80$, Tropical Atmosphere

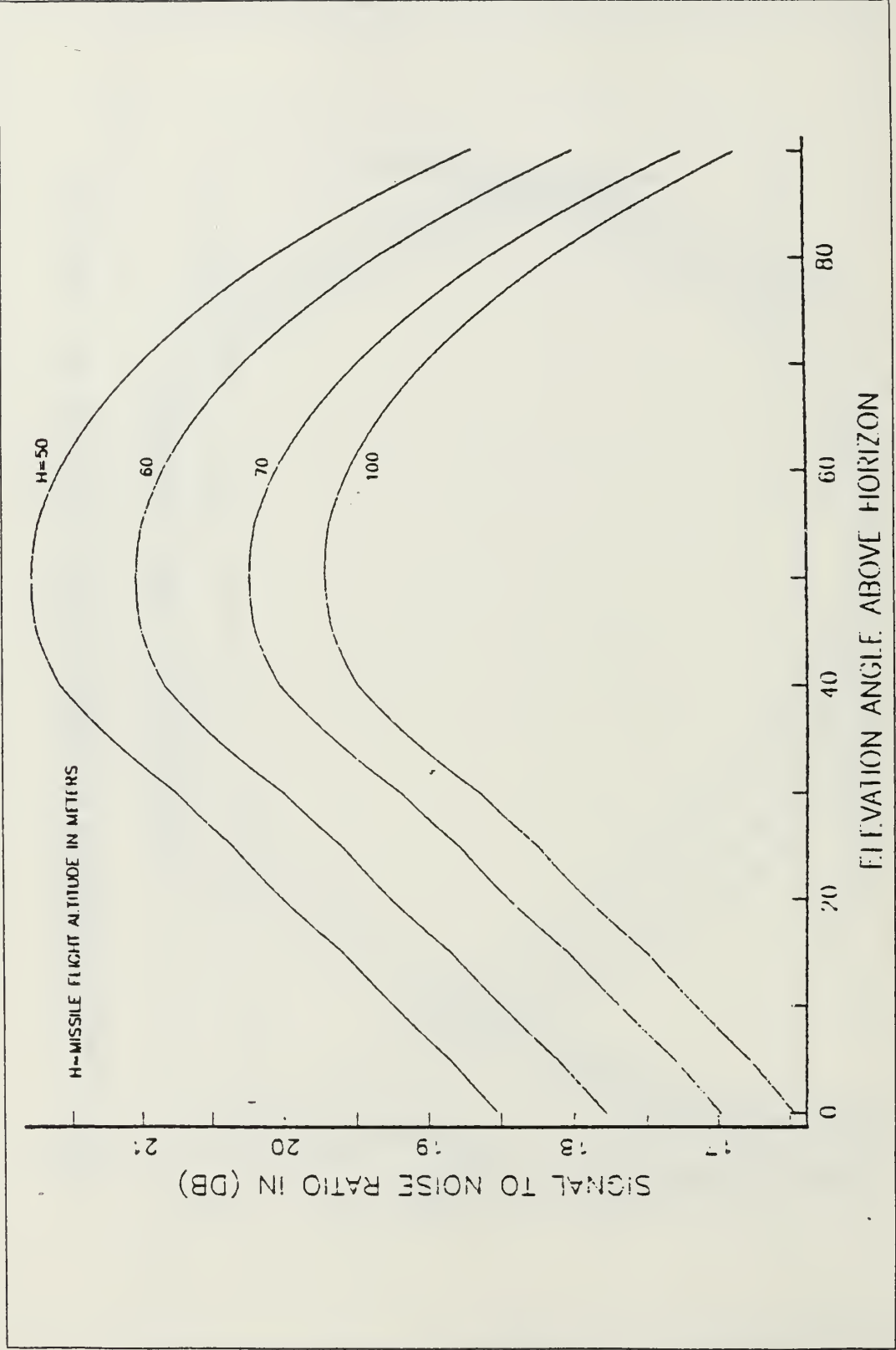


Figure 5.13 Influence of Missile Flight Altitude for Sun with Heavy Storm Clouds, $\epsilon_s=0.80$, Tropical Atmosphere

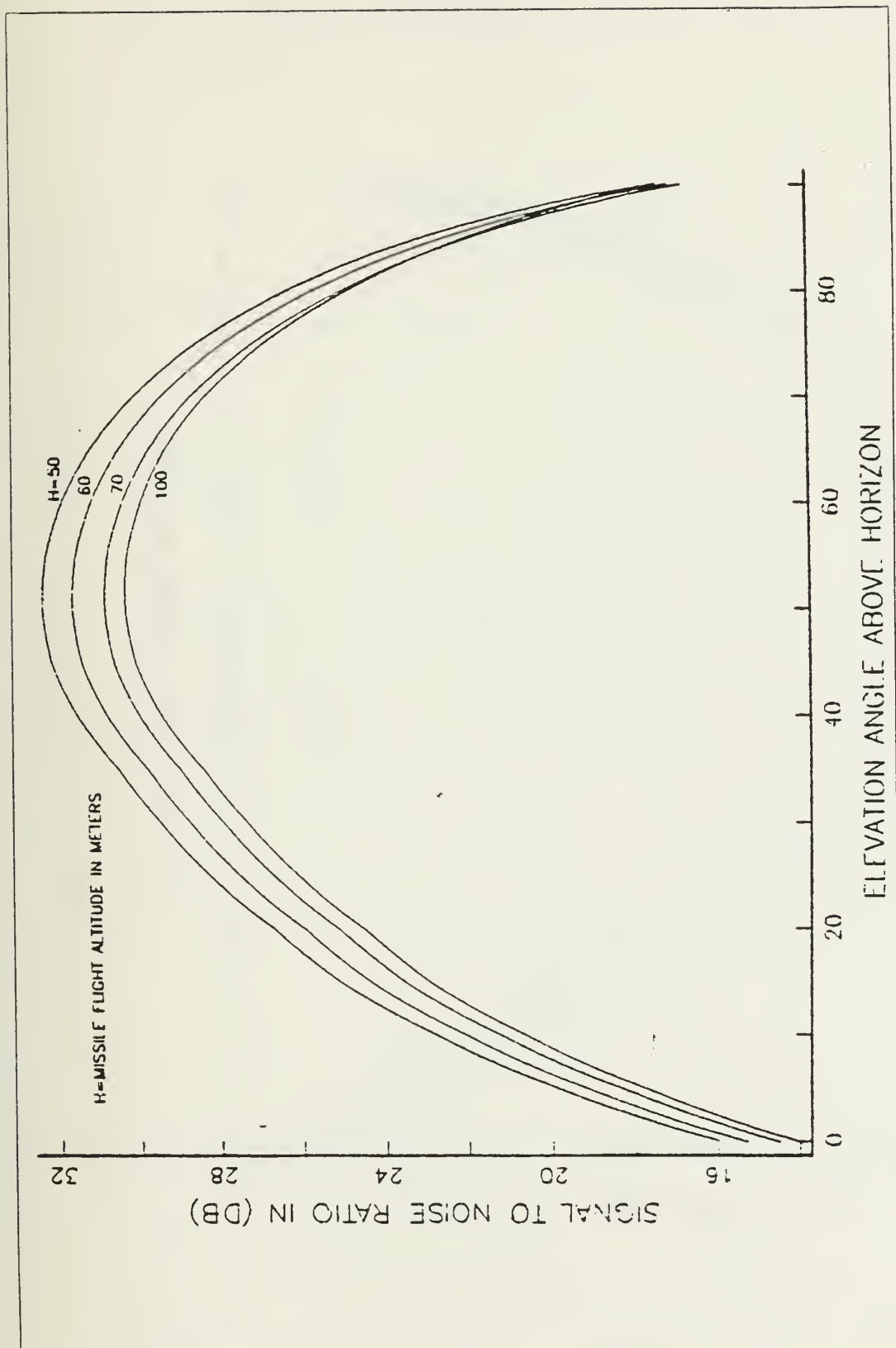


Figure 5.14 Influence of Missile Flight Altitude for Unobserved Sun, $\epsilon_s=0.55$, Tropical Atmosphere

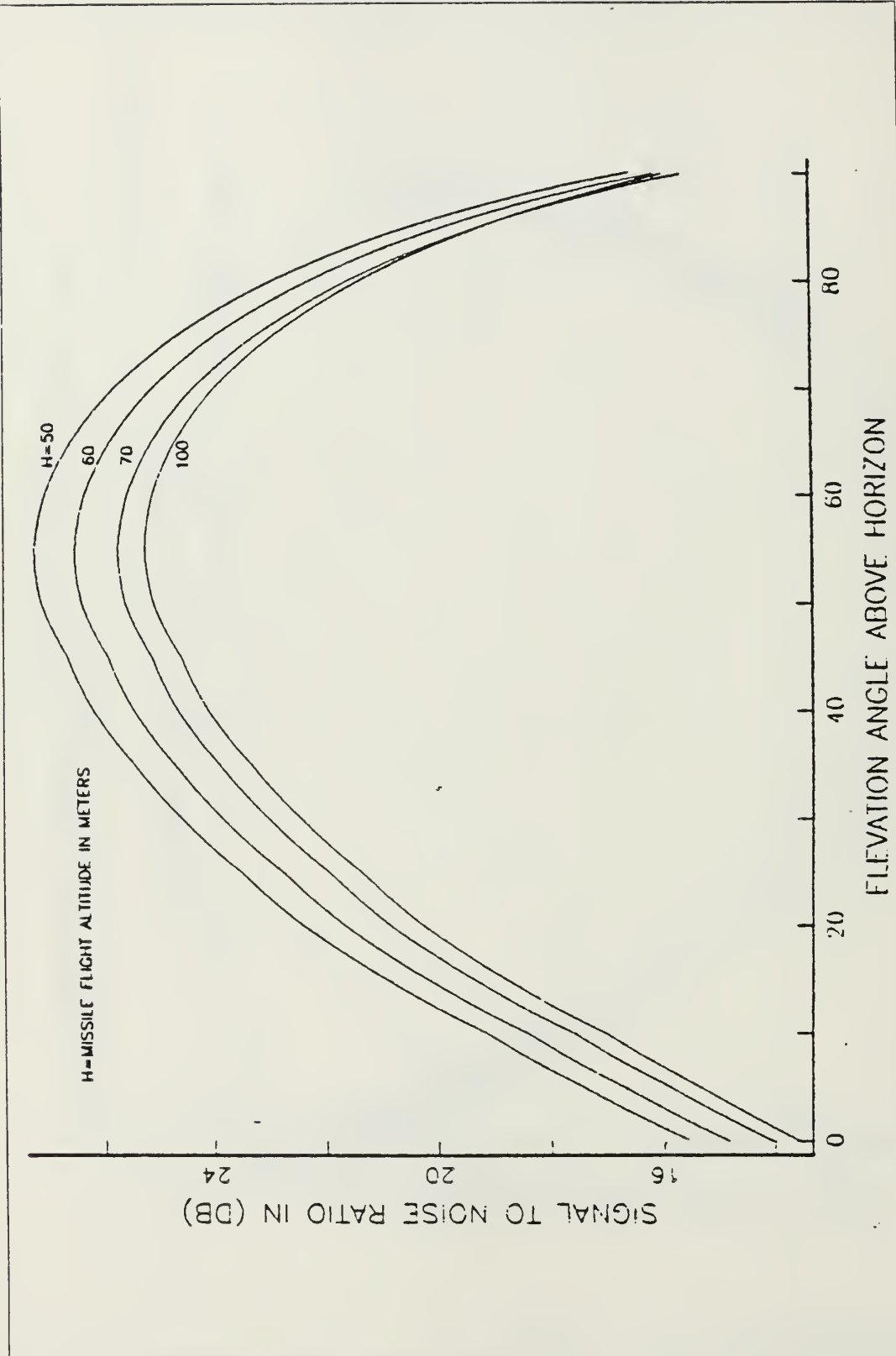


Figure 5.15 Influence of Missile Flight Altitude for Sun with Light Clouds, $\epsilon_s=0.55$, Tropical Atmosphere

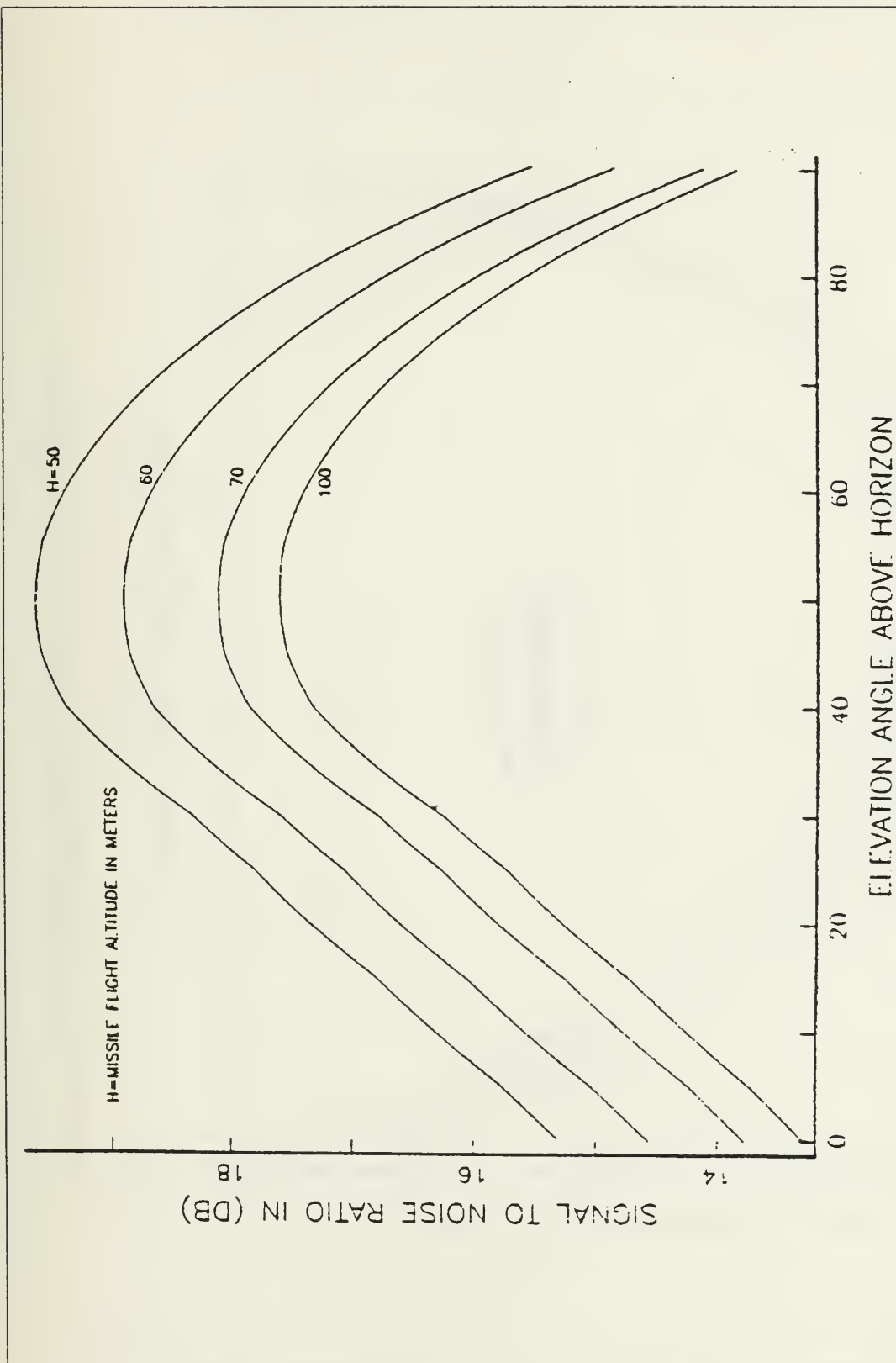


Figure 5.16 Influence of Missile Flight Altitude for Sun with Heavy Storm Clouds, $\epsilon_0=0.55$, Tropical Atmosphere

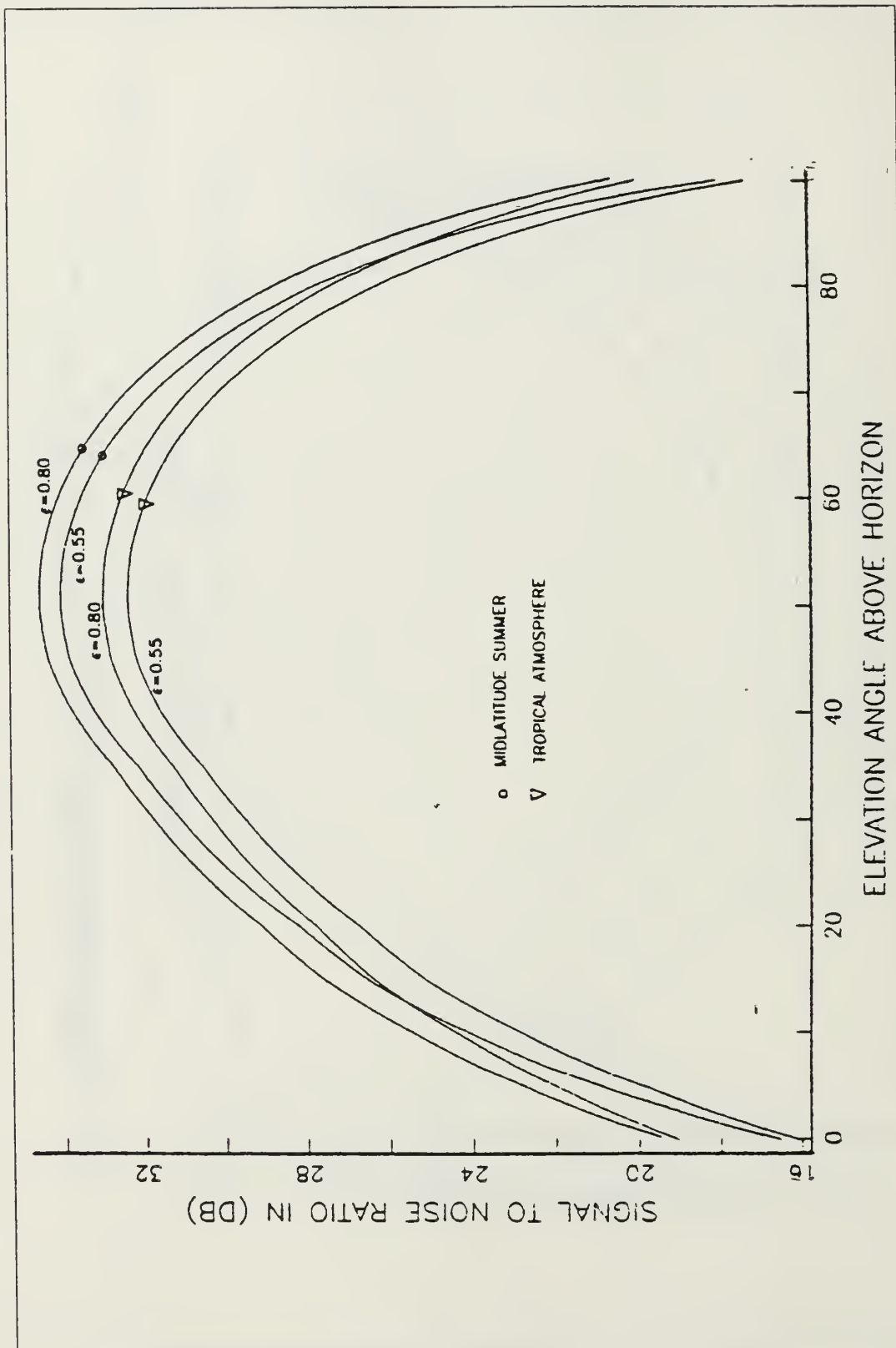


Figure 5.17 Influence of Emissivity and Atmospheric Profile for Flight Altitude 50m and Unscured Sun

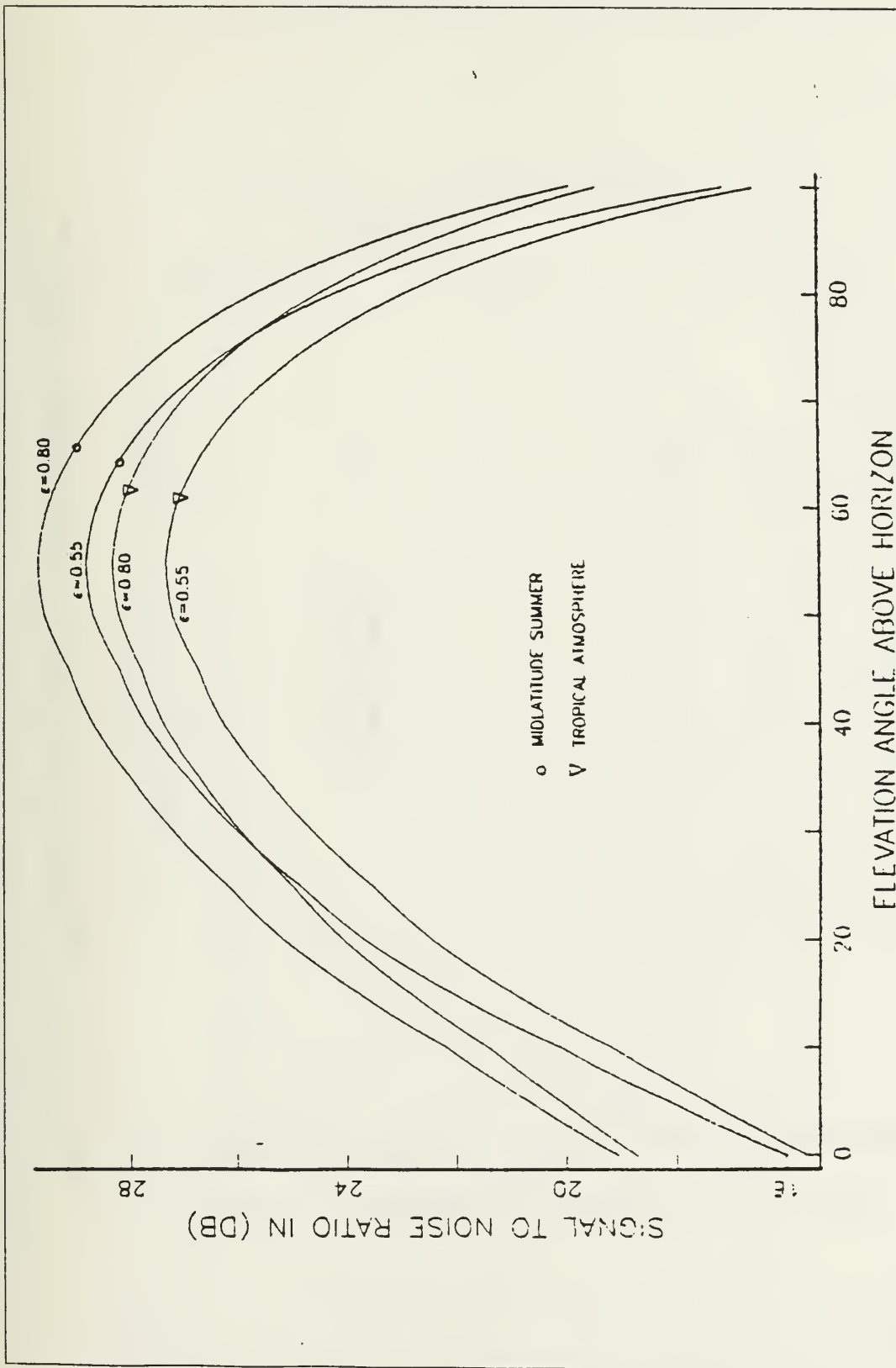


Figure 5.18 Influence of Emissivity and Atmospheric Profile for Flight Altitude 50m and Sun with Light Clouds

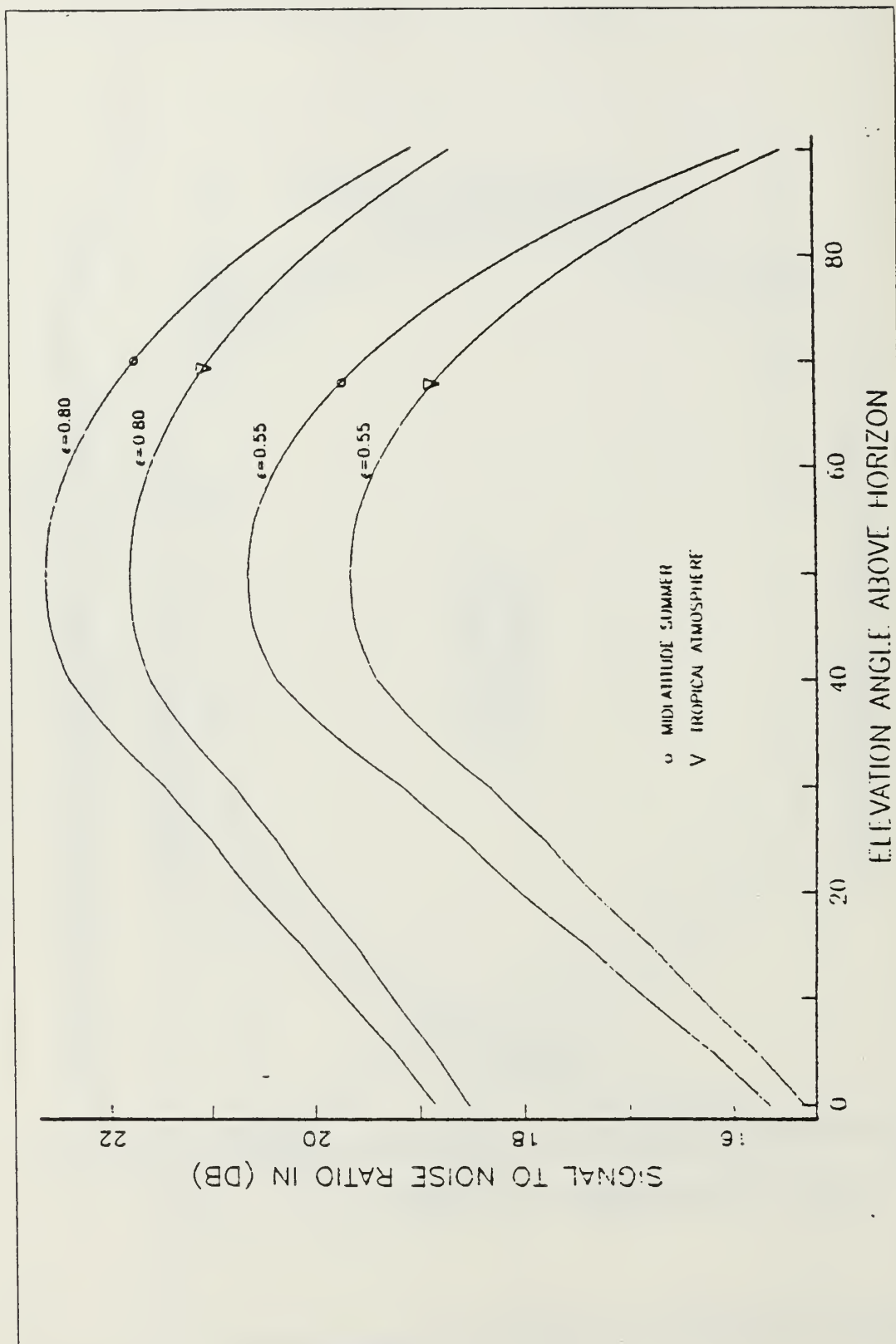


Figure 5.19 Influence of Emissivity and Atmospheric Profile for Flight Altitude 50m and Sun with Heavy Storm Clouds

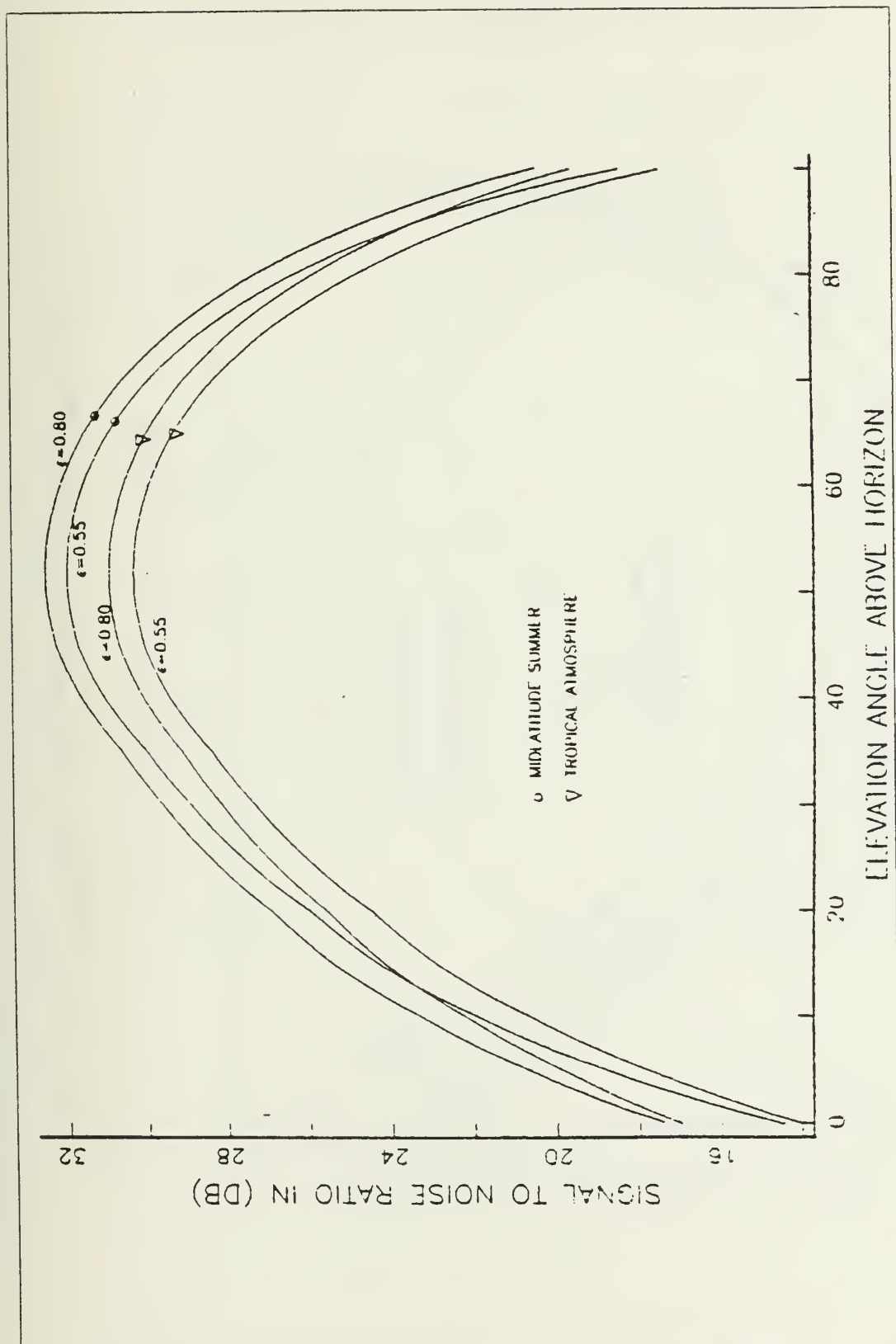


Figure 5.20 Influence of Emissivity and Atmospheric Profile for Flight Altitude 100m and Unscured Sun

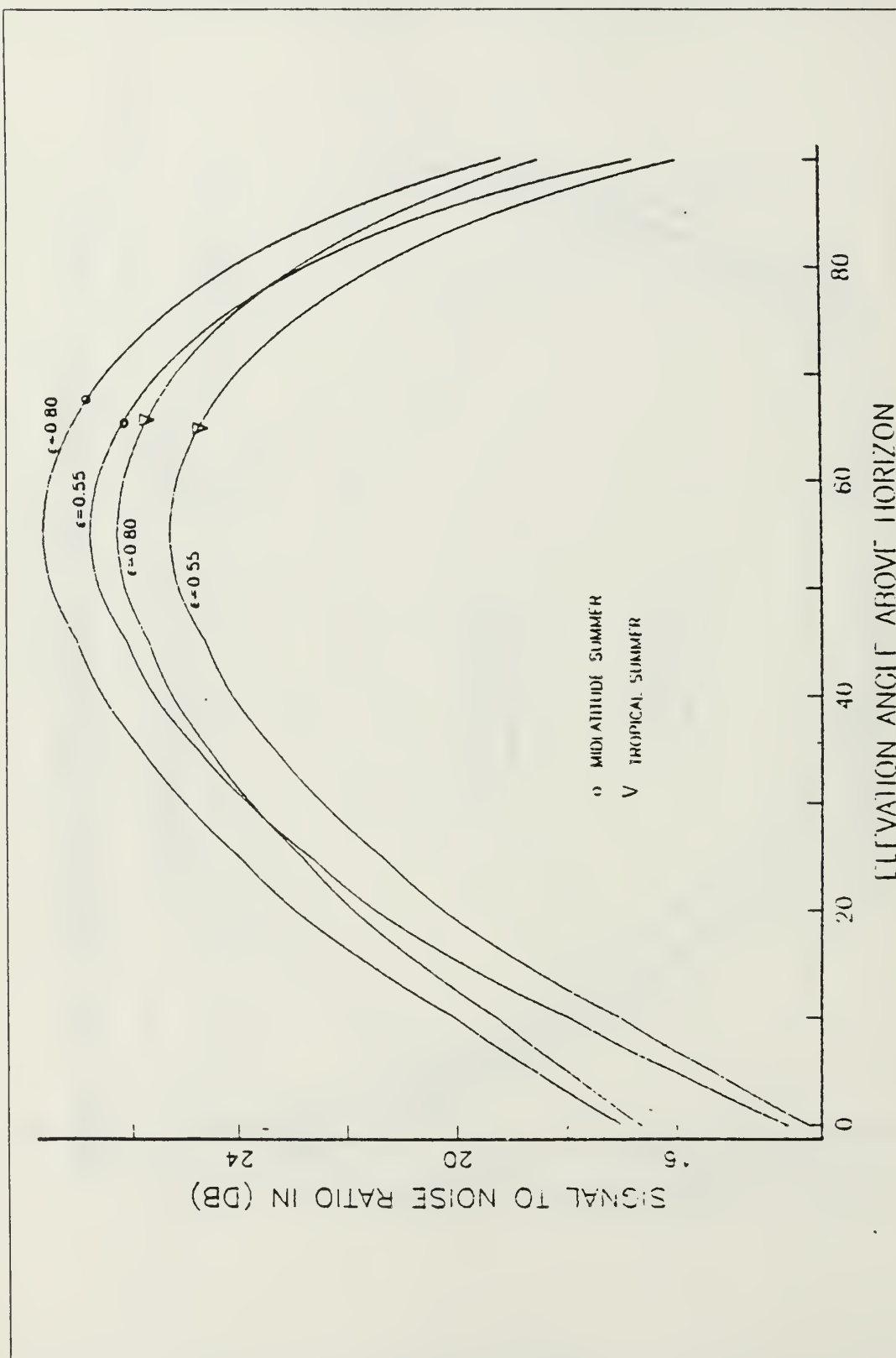


Figure 5.21. Influence of Emissivity and Atmospheric Profile for Flight Altitude 100m and Sun with Light Clouds

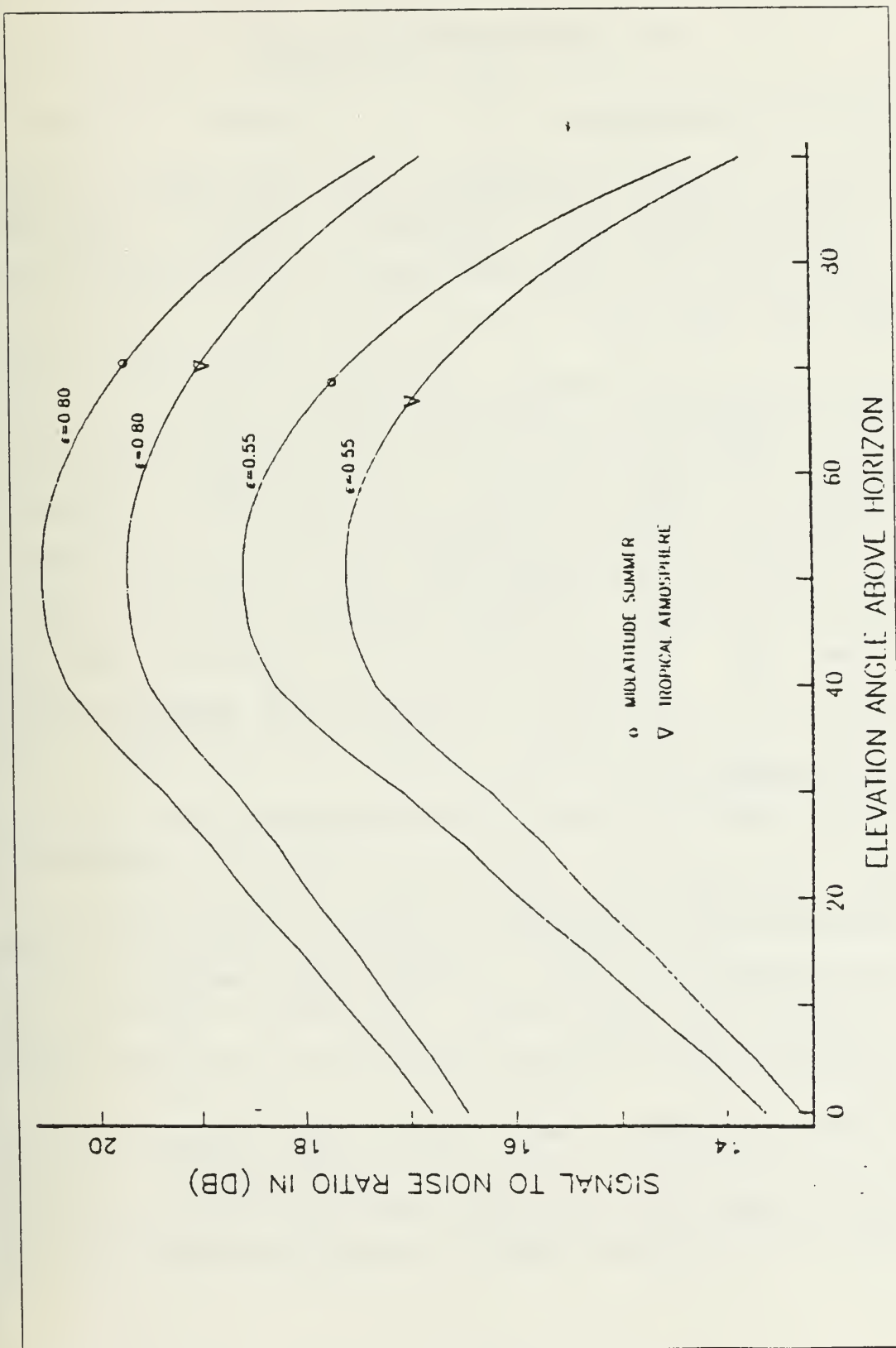


Figure 5.22 Influence of Emissivity and Atmospheric Profile for Flight Altitude 100m and Sun with Heavy Storm Clouds.

VI. RESULTS AND DISCUSSION

A. SHIP BODY TEMPERATURE

Tables 5 to 18 of Appendix A show the effects of the ship internal temperature, atmospheric profile, ship body paint emissivity, sun elevation angle and sky condition on the ship body temperature.

For both horizontal and vertical faces higher paint emissivity and ship internal temperature result in higher ship body temperature. Higher internal temperature corresponds to less ship body heat losses towards the internal compartments. Moreover higher paint emissivity (absorptivity for gray paint) corresponds in higher solar energy absorption and, for the 300K ship body temperature level, the dominant mechanism of heat transfer is that of convection. Hence the increase of the paint emissivity does not correspond to a significant increase of the energy radiated by the ship body, and the net result is an increase of the ship body temperature.

The sky condition appears to be significant as well. The more clear it is the more solar energy there is incident on the ship, resulting in an increase of its body temperature.

As far as the atmospheric profile is concerned, the Tropical Atmosphere results in higher body temperature than that of Midlatitude Summer since the ambient temperature is higher and the ship body heat losses towards the environment are less.

The sun elevation angle above the horizon affects vertical and horizontal faces in different ways. We know that the incident solar energy at sea level is an increasing function of the elevation angle. For an horizontal face the

temperature appears to be an increasing function of the elevation angle, the sine of which is used for the calculation of the incident angle effect. For vertical faces the cosine of the elevation angle is used and the temperature appears a maximum in the vicinity of 50° . The explanation is that, up to this value, the increasing effect of the solar energy dominates the decreasing one of the cosine function. After the value of about 50° the first derivative of the solar energy function becomes small and the cosine behavior dominates so that the net result is a decreasing temperature function from 50° to 90° .

As we see in the ship tracked area geometric analysis is constituted from both vertical and horizontal faces, but the vertical ones have much larger projected surface areas. Therefore the radiant energy from the tracked area is due mainly to that of the vertical faces and as we will see from the S/N ratio results they appear maximum at a value of elevation angle close to 50° .

B. DETECTOR S/N RATIO

Figures 5.5 to 5.22 show the effects of the sky condition, sun elevation angle and missile flight altitude on the detector S/N ratio.

In general we observe that the variation of the S/N ratio is similar to that of the ship body temperature. That means that the radiant energy from the ship body due to its temperature is the main thermal source for the detector. At this point, it is useful to discuss the influence of the stack exit plane thermal radiation. From our calculation we know that the radiant intensity of the CO in the stack exit plane has a magnitude of the order of 10^4 (W/cm²Sr) and that of the ship body of the order of 10^3 to 10^2 . Moreover the stack exit plane area is much smaller than the total tracked

area and the stack exit radiant flux is significantly smaller than this of the ship body tracked surface.

Sky condition and the paint emissivity affect S/N ratio similarly to the ship body temperature. The more clear is the sky and the higher is the paint emissivity the higher is the S/N ratio.

The atmospheric profile affects S/N in a different way. While the Tropical Atmosphere gives higher ship body temperature, it results in lower S/N ratios comparing with the Midlatitude Summer. The explanation for that is that the increase of the ship body radiance, due to its temperature increase, is less than the background noise increase (higher sea temperature). Moreover the atmospheric transmittance in the 5um window for the Tropical Atmosphere is about 10% less than this for Midlatitude Summer.

The missile flight altitude appears to be important as a parameter. The higher it is the lower is the S/N ratio and this decrease is higher between 50 to 70 (m) than between 70 to 100 (m). The explanation is that although higher missile flight altitude corresponds to lower background area (sea), the path between missile head and ship becomes larger and its square appears in the denominator of the signal voltage formula. Therefore the net result is to give lower values of S/N ratio.

The influence of the sun elevation angle above the horizon is similar to that on the ship body temperature and it has been discussed earlier.

C. RECOMMENDATIONS

Based on the relative influence of each parameter which has been varied in our analysis we recommend:

From the ship design point of view, lower internal temperature or, when it is not feasible, better wall

insulation, especially in the area where significant heat generation exist. In addition to that, paint of low emissivity and absorptivity is desirable.

From the missile point of view we recommend lower flight altitude. At this point we must notice that, lowering the flight altitude, we will reach a point where the background area (sea) will be very large, resulting in higher background noise and the coast or even the sun itself could constitute background noise for the detector. Therefore the flight altitude must be determined, in a certain design, accounting for all these conflicting parameters. Another solution could be the use of higher flight altitude, that assures us low background area, and to improve the detector optics design that will balance the loss of the signal voltage due to the greater path length.

APPENDIX A
TABLES FOR SHIP BODY TEMPERATURE

TABLE 5

Ship Body Temperature for Midlatitude Summer
 $T = 293.15\text{K}$ and $= 0.80$

ELEVATION ANGLE	UNOBSURED SUN		SUN WITH WITH LIGHT CLOUDS		SUN WITH HEAVY STORM CLOUDS	
	HORIZONTAL FACE	VERTICAL FACE	HORIZONTAL FACE	VERTICAL FACE	HORIZONTAL FACE	VERTICAL FACE
0.0	294.16	294.21	294.16	294.18	294.16	294.17
1.0	294.16	294.28	294.16	294.20	294.16	294.17
2.0	294.17	294.33	294.16	294.23	294.16	294.17
3.0	294.17	294.39	294.17	294.26	294.16	294.18
4.0	294.18	294.45	294.17	294.29	294.16	294.18
5.0	294.19	294.52	294.17	294.33	294.16	294.19
6.0	294.20	294.59	294.18	294.36	294.17	294.20
7.0	294.22	294.67	294.18	294.39	294.17	294.20
8.0	294.24	294.75	294.19	294.41	294.17	294.21
9.0	294.27	294.85	294.20	294.44	294.17	294.22
10.0	294.30	294.92	294.21	294.48	294.17	294.22
11.0	294.34	295.00	294.22	294.52	294.18	294.23
12.0	294.37	295.07	294.24	294.55	294.18	294.24
13.0	294.40	295.15	294.25	294.59	294.18	294.25
14.0	294.44	295.22	294.27	294.63	294.18	294.26
15.0	294.48	295.30	294.30	294.67	294.19	294.27
16.0	294.52	295.37	294.33	294.71	294.19	294.28
17.0	294.57	295.45	294.36	294.76	294.20	294.30
18.0	294.61	295.51	294.39	294.79	294.20	294.31
19.0	294.67	295.59	294.41	294.85	294.21	294.32
20.0	294.74	295.66	294.44	294.88	294.22	294.33
21.0	294.83	295.74	294.47	294.91	294.23	294.34
22.0	294.89	295.82	294.50	294.94	294.23	294.35
23.0	294.96	295.90	294.53	294.98	294.24	294.36
24.0	295.03	295.94	294.56	294.98	294.25	294.37
25.0	295.11	296.01	294.60	295.01	294.26	294.38
26.0	295.19	296.07	294.64	295.05	294.27	294.39
27.0	295.28	296.14	294.69	295.08	294.28	294.40
28.0	295.38	296.20	294.73	295.11	294.30	294.41
29.0	295.43	296.27	294.79	295.14	294.31	294.42
30.0	295.52	296.35	294.79	295.18	294.33	294.43
31.0	295.61	296.41	294.83	295.21	294.35	294.44

ELEVATION ANGLE	HORIZONTAL FACE	VERTICAL FACE	HORIZONTAL FACE	VERTICAL FACE	HORIZONTAL FACE	VERTICAL FACE
35.0	295.83	296.59	294.93	295.27	294.34	294.42
36.0	295.83	296.67	294.98	295.31	294.35	294.43
37.0	296.05	296.74	295.03	295.35	294.37	294.44
38.0	296.17	296.81	295.09	295.37	294.38	294.44
39.0	296.31	296.89	295.15	295.39	294.40	294.45
40.0	296.46	296.96	295.21	295.42	294.41	294.46
41.0	296.56	296.97	295.27	295.44	294.42	294.46
42.0	296.69	297.01	295.34	295.45	294.44	294.47
43.0	296.83	297.05	295.37	295.47	294.45	294.47
44.0	296.95	297.09	295.43	295.49	294.46	294.48
45.0	297.09	297.12	295.49	295.51	294.48	294.48
46.0	297.23	297.14	295.56	295.53	294.48	294.48
47.0	297.38	297.15	295.63	295.55	294.50	294.48
48.0	297.48	297.16	295.71	295.57	294.52	294.48
49.0	297.62	297.17	295.79	295.58	294.53	294.48
50.0	297.75	297.17	295.88	295.59	294.54	294.48
51.0	297.87	297.17	295.93	295.60	294.56	294.48
52.0	298.01	297.16	296.00	295.60	294.57	294.48
53.0	298.13	297.14	296.07	295.60	294.59	294.48
54.0	298.26	297.13	296.15	295.60	294.60	294.47
55.0	298.41	297.10	296.23	295.60	294.62	294.47
56.0	298.51	297.10	296.30	295.59	294.63	294.47
57.0	298.60	297.03	296.38	295.58	294.64	294.46
58.0	298.80	297.00	296.47	295.57	294.66	294.46
59.0	298.88	296.96	296.50	295.56	294.67	294.45
60.0	299.00	296.95	296.58	295.55	294.69	294.45
61.0	299.09	296.88	296.64	295.54	294.70	294.44
62.0	299.12	296.82	296.71	295.52	294.72	294.44
63.0	299.24	296.79	296.79	295.49	294.73	294.43
64.0	299.34	296.75	296.86	295.47	294.75	294.42
65.0	299.49	296.69	296.95	295.44	294.76	294.42
66.0	299.57	296.62	296.98	295.41	294.77	294.41
67.0	299.67	296.54	297.04	295.38	294.79	294.40
68.0	299.77	296.47	297.10	295.35	294.77	294.39
69.0	299.89	296.41	297.17	295.33	294.76	294.38
70.0	300.00	296.32	297.24	295.30	294.78	294.38

TABLE 6
Ship Body Temperature for Midlatitude Summer
 $T = 303.15\text{K}$ and $= 0.80$

ELEVATION ANGLE	UNOBSERVED SUN		SUN WITH LIGHT CLOUDS		SUN WITH HEAVY STORM CLOUDS	
	HORIZONTAL FACE	VERTICAL FACE	HORIZONTAL FACE	VERTICAL FACE	HORIZONTAL FACE	VERTICAL FACE
0.0	294.58	294.62	294.58	294.60	294.58	294.59
1.0	294.58	294.67	294.58	294.62	294.58	294.59
2.0	294.59	294.72	294.59	294.63	294.58	294.59
3.0	294.59	294.77	294.59	294.65	294.58	294.60
4.0	294.60	294.77	294.59	294.67	294.58	294.60
5.0	294.61	294.81	294.60	294.69	294.59	294.61
6.0	294.62	294.86	294.60	294.72	294.59	294.61
7.0	294.63	294.90	294.61	294.74	294.59	294.62
8.0	294.64	294.95	294.61	294.76	294.59	294.62
9.0	294.66	294.99	294.62	294.79	294.59	294.63
10.0	294.68	295.04	294.63	294.76	294.59	294.63
11.0	294.70	295.09	294.64	294.79	294.59	294.64
12.0	294.72	295.14	294.65	294.81	294.60	294.64
13.0	294.75	295.19	294.66	294.84	294.60	294.65
14.0	294.78	295.25	294.68	294.86	294.60	294.65
15.0	294.76	295.30	294.69	294.88	294.60	294.66
16.0	294.79	295.35	294.71	294.91	294.61	294.66
17.0	294.82	295.36	294.72	294.93	294.61	294.67
18.0	294.84	295.40	294.74	294.95	294.62	294.68
19.0	294.87	295.44	294.76	294.98	294.62	294.68
20.0	294.90	295.48	294.77	295.00	294.62	294.69
21.0	294.94	295.53	294.79	295.02	294.63	294.69
22.0	294.98	295.58	294.78	295.04	294.63	294.70
23.0	295.02	295.63	294.80	295.06	294.64	294.70
24.0	295.07	295.68	294.82	295.08	294.64	294.71
25.0	295.11	295.72	294.84	295.10	294.65	294.71
26.0	295.16	295.77	294.87	295.13	294.65	294.72
27.0	295.22	295.82	294.89	295.15	294.65	294.73
28.0	295.28	295.88	294.91	295.17	294.66	294.73
29.0	295.34	295.93	294.94	295.20	294.67	294.74
30.0	295.36	295.98	294.97	295.22	294.68	294.75
31.0	295.42	296.03	295.00	295.25	294.69	294.76
32.0	295.48	296.08	295.03	295.27	294.69	294.76

ELEVATION ANGLE	HORIZONTAL FACE	VERTICAL FACE	HORIZONTAL FACE	VERTICAL FACE	HORIZONTAL FACE	VERTICAL FACE
33.00	295.561	296.07	295.03	295.32	294.71	294.77
34.00	295.568	296.11	295.06	295.34	294.71	294.78
35.00	295.576	296.15	295.09	295.36	294.72	294.79
36.00	295.586	296.20	295.13	295.37	294.73	294.75
37.00	295.596	296.25	295.17	295.38	294.75	294.76
38.00	295.609	296.30	295.20	295.39	294.76	294.77
39.00	295.618	296.35	295.25	295.40	294.77	294.77
40.00	295.627	296.40	295.29	295.41	294.78	294.78
41.00	295.637	296.45	295.34	295.43	294.78	294.78
42.00	295.648	296.49	295.38	295.44	294.78	294.78
43.00	295.658	296.51	295.42	295.45	294.78	294.79
44.00	295.667	296.53	295.46	295.46	294.79	294.79
45.00	295.677	296.55	295.51	295.48	294.79	294.79
46.00	295.687	296.56	295.56	295.49	294.80	294.79
47.00	295.696	296.57	295.61	295.50	294.81	294.79
48.00	295.706	296.58	295.66	295.52	294.82	294.79
49.00	295.717	296.58	295.71	295.53	294.83	294.79
50.00	295.727	296.57	295.76	295.54	294.84	294.79
51.00	295.737	296.56	295.82	295.54	294.85	294.79
52.00	295.747	296.55	295.87	295.54	294.86	294.79
53.00	295.757	296.54	295.94	295.54	294.87	294.79
54.00	295.766	296.53	295.99	295.54	294.87	294.78
55.00	295.776	296.52	296.05	295.53	294.88	294.78
56.00	295.786	296.51	296.09	295.53	294.89	294.78
57.00	295.796	296.49	296.14	295.52	294.90	294.77
58.00	295.806	296.48	296.19	295.52	294.91	294.77
59.00	295.816	296.47	296.24	295.51	294.92	294.77
60.00	295.826	296.46	296.28	295.49	294.93	294.77
61.00	295.836	296.45	296.33	295.48	294.94	294.76
62.00	295.846	296.44	296.39	295.47	294.95	294.76
63.00	295.856	296.43	296.44	295.45	294.96	294.75
64.00	295.866	296.42	296.45	295.43	294.96	294.75
65.00	295.876	296.41	296.50	295.41	294.97	294.78
66.00	295.886	296.40	296.54	295.39	294.98	294.77

ELEVATION ANGLE	HORIZONTAL FACE	VERTICAL FACE	HORIZONTAL FACE	VERTICAL FACE	HORIZONTAL FACE	VERTICAL FACE
69.0	298.45	296.06	296.58	295.35	294.98	294.77
70.0	298.51	296.01	296.66	295.36	294.99	294.76
71.0	298.56	295.95	296.70	295.32	295.00	294.75
72.0	298.61	295.92	296.74	295.29	295.00	294.74
73.0	298.66	295.84	296.77	295.25	295.01	294.73
74.0	298.71	295.77	296.81	295.22	295.02	294.72
75.0	298.77	295.70	296.85	295.18	295.03	294.71
76.0	298.80	295.63	296.89	295.15	295.04	294.70
77.0	298.83	295.55	296.93	295.11	295.04	294.70
78.0	298.86	295.48	296.96	295.07	295.05	294.69
79.0	298.89	295.41	296.98	295.04	295.05	294.68
80.0	298.90	295.38	296.99	295.00	295.06	294.67
81.0	298.92	295.28	297.01	294.96	295.06	294.66
82.0	298.94	295.20	297.04	294.92	295.07	294.65
83.0	298.95	295.12	297.06	294.88	295.07	294.64
84.0	298.97	294.96	297.08	294.84	295.08	294.63
85.0	298.97	294.88	297.11	294.80	295.08	294.62
86.0	298.98	294.81	297.13	294.75	295.09	294.61
87.0	298.98	294.76	297.15	294.74	295.09	294.60
88.0	298.99	294.67	297.17	294.69	295.10	294.59
89.0	299.00	294.58	297.19	294.63	295.10	294.58

TABLE 7
Ship Body Temperature for Midlatitude Summer
 $T = 293.15\text{K}$ and $\epsilon = 0.55$

ELEVATION ANGLE	UNOBSURED SUN		SUN WITH LIGHT CLOUDS		SUN WITH HEAVY STORM CLOUDS	
	HORIZONTAL FACE	VERTICAL FACE	HORIZONTAL FACE	VERTICAL FACE	HORIZONTAL FACE	VERTICAL FACE
0.0	294.16	294.20	294.16	294.18	294.16	294.16
1.0	294.16	294.25	294.16	294.19	294.16	294.17
2.0	294.17	294.32	294.17	294.21	294.16	294.17
3.0	294.17	294.34	294.17	294.24	294.16	294.18
4.0	294.18	294.39	294.17	294.26	294.16	294.18
5.0	294.19	294.44	294.17	294.29	294.16	294.18
6.0	294.21	294.50	294.17	294.32	294.16	294.19
7.0	294.22	294.56	294.18	294.34	294.17	294.19
8.0	294.24	294.62	294.19	294.36	294.17	294.20
9.0	294.26	294.68	294.20	294.38	294.17	294.21
10.0	294.29	294.77	294.21	294.41	294.17	294.22
11.0	294.33	294.83	294.22	294.44	294.17	294.22
12.0	294.35	294.88	294.23	294.47	294.18	294.23
13.0	294.38	294.94	294.25	294.50	294.18	294.24
14.0	294.41	295.00	294.26	294.53	294.18	294.25
15.0	294.45	295.05	294.29	294.56	294.19	294.25
16.0	294.48	295.10	294.31	294.59	294.19	294.26
17.0	294.52	295.15	294.34	294.62	294.19	294.27
18.0	294.56	295.21	294.36	294.65	294.20	294.28
19.0	294.61	295.27	294.38	294.69	294.20	294.29
20.0	294.66	295.35	294.40	294.72	294.21	294.30
21.0	294.72	295.41	294.43	294.74	294.22	294.31
22.0	294.77	295.47	294.45	294.76	294.22	294.31
23.0	294.85	295.52	294.48	294.78	294.23	294.33
24.0	294.91	295.58	294.51	294.81	294.24	294.33
25.0	294.97	295.64	294.54	294.84	294.25	294.34
26.0	295.04	295.69	294.57	294.86	294.26	294.35
27.0	295.10	295.75	294.60	294.89	294.28	294.35
28.0	295.18	295.81	294.64	294.91	294.29	294.35
29.0	295.27	295.89	294.68	294.96	294.30	294.35
30.0	295.32	295.94	294.73	294.99	294.33	294.35

ELEVATION ANGLE	HORIZONTAL FACE	VERTICAL FACE	HORIZONTAL FACE	VERTICAL FACE	HORIZONTAL FACE	VERTICAL FACE
34.0	295.39	295.99	294.73	295.01	294.32	294.36
35.0	295.47	296.04	294.77	295.03	294.34	294.36
36.0	295.57	296.16	294.81	295.06	294.31	294.37
37.0	295.67	296.29	294.85	295.09	294.32	294.38
38.0	295.79	296.42	294.90	295.11	294.33	294.39
39.0	295.86	296.53	294.94	295.13	294.35	294.39
40.0	295.97	296.63	294.99	295.15	294.36	294.40
41.0	296.07	296.74	295.03	295.17	294.37	294.40
42.0	296.18	296.84	295.08	295.19	294.38	294.41
43.0	296.31	296.96	295.13	295.21	294.39	294.41
44.0	296.39	296.6.47	295.18	295.22	294.40	294.41
45.0	296.50	296.52	295.24	295.24	294.41	294.41
46.0	296.60	296.53	295.27	295.26	294.42	294.41
47.0	296.72	296.53	295.33	295.28	294.43	294.41
48.0	296.89	296.55	295.45	295.28	294.44	294.41
49.0	296.91	296.56	295.51	295.29	294.45	294.41
50.0	297.02	296.56	295.57	295.30	294.46	294.41
51.0	297.14	296.55	295.63	295.31	294.47	294.41
52.0	297.23	296.55	295.69	295.31	294.50	294.41
53.0	297.34	296.54	295.76	295.31	294.51	294.41
54.0	297.43	296.52	295.84	295.31	294.52	294.41
55.0	297.53	296.52	295.86	295.30	294.53	294.41
56.0	297.63	296.48	295.91	295.30	294.54	294.40
57.0	297.78	296.45	295.97	295.28	294.55	294.40
58.0	297.92	296.42	296.03	295.27	294.56	294.40
59.0	298.02	296.33	296.09	295.27	294.57	294.39
60.0	298.12	296.33	296.14	295.27	294.58	294.39
61.0	298.22	296.31	296.20	295.25	294.60	294.38
62.0	298.32	296.24	296.26	295.22	294.61	294.38
63.0	298.39	296.21	296.33	295.22	294.62	294.37
64.0	298.45	296.12	296.35	295.20	294.63	294.36
65.0	298.53	296.06	296.40	295.17	294.64	294.36
66.0	298.63	296.00	296.45	295.14	294.65	294.35
67.0	298.72	296.00	296.51	295.11	294.66	294.34
68.0	298.88	295.94	296.66	295.05	294.67	294.34
69.0	299.00	295.87	296.66	295.05	294.67	294.34

ELEVATION ANGLE	HORIZONTAL FACE	VERTICAL FACE	HORIZONTAL FACE	VERTICAL FACE	HORIZONTAL FACE	VERTICAL FACE
71.0	298.99	295.84	296.66	295.02	294.69	294.33
72.0	299.03	295.66	296.71	294.98	294.69	294.32
73.0	299.08	295.57	296.76	294.95	294.70	294.32
74.0	299.14	295.49	296.78	294.91	294.71	294.31
75.0	299.18	295.41	296.82	294.83	294.73	294.33
76.0	299.22	295.33	296.86	294.79	294.70	294.32
77.0	299.26	295.27	296.93	294.75	294.71	294.31
78.0	299.31	295.17	296.97	294.70	294.72	294.29
79.0	299.33	295.07	297.01	294.68	294.73	294.28
80.0	299.35	294.98	297.05	294.63	294.73	294.27
81.0	299.37	294.89	297.08	294.58	294.74	294.26
82.0	299.38	294.80	297.12	294.52	294.74	294.24
83.0	299.40	294.71	297.15	294.47	294.75	294.23
84.0	299.41	294.63	297.15	294.42	294.75	294.22
85.0	299.42	294.53	297.18	294.37	294.76	294.21
86.0	299.44	294.43	297.21	294.32	294.76	294.20
87.0	299.45	294.34	297.23	294.28	294.77	294.19
88.0	299.47	294.26	297.25	294.21	294.77	294.18
89.0	299.49	294.16	297.28	294.16	294.78	294.17
90.0	299.50	294.16	297.28	294.16	294.78	294.16

TABLE 8
Ship Body Temperature for Midlatitude Summer
T = 303.15K and = 0.55

ELEVATION ANGLE	UNOBSERVED SUN		SUN WITH LIGHT CLOUDS		SUN WITH HEAVY STORM CLOUDS	
	HORIZONTAL FACE	VERTICAL FACE	HORIZONTAL FACE	VERTICAL FACE	HORIZONTAL FACE	VERTICAL FACE
0.0	294.59	294.62	294.59	294.60	294.59	294.59
1.0	294.59	294.66	294.59	294.62	294.59	294.60
2.0	294.59	294.70	294.59	294.63	294.59	294.60
3.0	294.60	294.71	294.59	294.65	294.59	294.60
4.0	294.60	294.74	294.60	294.66	294.59	294.61
5.0	294.61	294.77	294.60	294.68	294.59	294.61
6.0	294.62	294.81	294.60	294.70	294.59	294.61
7.0	294.63	294.84	294.61	294.72	294.59	294.62
8.0	294.64	294.88	294.61	294.74	294.60	294.62
9.0	294.65	294.91	294.62	294.77	294.60	294.63
10.0	294.67	294.95	294.62	294.73	294.60	294.63
11.0	294.68	294.99	294.63	294.75	294.60	294.63
12.0	294.70	295.03	294.64	294.77	294.60	294.64
13.0	294.73	295.07	294.65	294.79	294.60	294.64
14.0	294.71	295.11	294.66	294.81	294.60	294.65
15.0	294.73	295.15	294.67	294.82	294.61	294.65
16.0	294.75	295.19	294.68	294.84	294.61	294.66
17.0	294.77	295.23	294.69	294.86	294.61	294.66
18.0	294.79	295.27	294.71	294.88	294.61	294.67
19.0	294.82	295.30	294.72	294.90	294.62	294.67
20.0	294.84	295.34	294.70	294.92	294.62	294.68
21.0	294.87	295.38	294.72	294.94	294.62	294.68
22.0	294.90	295.42	294.73	294.95	294.63	294.69
23.0	294.94	295.45	294.74	294.97	294.63	294.69
24.0	294.97	295.49	294.76	294.98	294.64	294.70
25.0	295.01	295.53	294.77	295.00	294.64	294.70
26.0	295.05	295.57	294.79	295.02	294.65	294.71
27.0	295.09	295.60	294.81	295.04	294.65	294.71
28.0	295.13	295.64	294.83	295.06	294.66	294.72
29.0	295.18	295.67	294.85	295.09	294.67	294.73
30.0	295.23	295.71	294.87	295.11	294.67	294.73
31.0	295.29	295.75	294.89	295.13	294.68	294.74
32.0	295.35	295.80	294.92	295.14	294.69	294.74
33.0	295.35	295.80	294.92	295.14	294.69	294.74

ELEVATION ANGLE	HORIZONTAL FACE	VERTICAL FACE	HORIZONTAL FACE	VERTICAL FACE	HORIZONTAL FACE	VERTICAL FACE
34.0	295.41	295.84	294.99	295.16	294.70	294.71
35.0	295.52	295.87	295.02	295.18	294.71	294.72
36.0	295.59	295.91	295.05	295.20	294.71	294.72
37.0	295.66	295.95	295.08	295.23	294.72	294.73
38.0	295.73	295.99	295.11	295.25	294.73	294.74
39.0	295.82	296.02	295.14	295.27	294.71	294.74
40.0	295.85	296.05	295.18	295.28	294.72	294.74
41.0	295.92	296.07	295.21	295.29	294.73	294.74
42.0	296.00	296.10	295.25	295.27	294.74	294.75
43.0	296.07	296.12	295.29	295.28	294.75	294.75
44.0	296.01	296.15	295.32	295.30	294.75	294.75
45.0	296.15	296.16	295.36	295.31	294.76	294.75
46.0	296.20	296.17	295.40	295.33	294.77	294.75
47.0	296.35	296.18	295.44	295.33	294.78	294.75
48.0	296.42	296.19	295.48	295.34	294.79	294.75
49.0	296.49	296.19	295.52	295.35	294.80	294.75
50.0	296.56	296.19	295.56	295.35	294.80	294.75
51.0	296.67	296.18	295.60	295.35	294.81	294.75
52.0	296.71	296.17	295.64	295.35	294.82	294.75
53.0	296.83	296.16	295.69	295.35	294.83	294.75
54.0	296.96	296.15	295.73	295.35	294.83	294.75
55.0	296.96	296.13	295.77	295.34	294.84	294.74
56.0	297.03	296.11	295.83	295.33	294.85	294.74
57.0	297.15	296.10	295.86	295.33	294.85	294.74
58.0	297.15	296.07	295.90	295.32	294.85	294.74
59.0	297.28	296.04	295.94	295.31	294.86	294.73
60.0	297.34	296.02	295.97	295.30	294.87	294.73
61.0	297.41	296.00	296.01	295.28	294.88	294.73
62.0	297.48	296.00	296.05	295.28	294.88	294.72
63.0	297.55	296.00	296.08	295.26	294.89	294.72
64.0	297.62	296.00	296.15	295.26	294.89	294.71
65.0	297.67	296.00	296.19	295.24	294.90	294.71
66.0	297.77	296.00	296.22	295.21	294.91	294.71
67.0	297.77	296.00	296.22	295.19	294.91	294.71
68.0	297.77	296.00	296.22	295.19	294.91	294.71
69.0	297.77	296.00	296.22	295.19	294.91	294.71
70.0	297.77	296.00	296.22	295.19	294.91	294.71

ELEVATION ANGLE	HORIZONTAL FACE	VERTICAL FACE	HORIZONTAL FACE	VERTICAL FACE	HORIZONTAL FACE	VERTICAL FACE
71.0	297.76	295.68	296.26	295.17	294.92	294.73
72.0	297.81	295.63	296.30	295.14	294.92	294.72
73.0	297.85	295.58	296.33	295.11	294.93	294.72
74.0	297.86	295.53	296.33	295.09	294.93	294.71
75.0	297.90	295.47	296.35	295.06	294.94	294.70
76.0	297.93	295.42	296.38	295.03	294.94	294.70
77.0	297.95	295.36	296.41	295.01	294.95	294.69
78.0	297.97	295.30	296.43	294.98	294.95	294.68
79.0	298.00	295.28	296.46	294.95	294.96	294.67
80.0	298.02	295.21	296.48	294.92	294.97	294.66
81.0	298.03	295.14	296.50	294.89	294.97	294.65
82.0	298.05	295.10	296.52	294.85	294.97	294.65
83.0	298.06	295.01	296.54	294.82	294.98	294.64
84.0	298.07	294.95	296.56	294.79	294.98	294.63
85.0	298.08	294.89	296.58	294.76	294.98	294.62
86.0	298.09	294.83	296.60	294.72	294.99	294.61
87.0	298.10	294.76	296.62	294.67	294.99	294.61
88.0	298.10	294.66	296.66	294.63	294.99	294.60
89.0	298.11	294.59	296.67	294.59	295.00	294.59

TABLE 9

Ship Body Temperature for Tropical
T = 293.15K and = 0.80

ELEVATION ANGLE	UNOBSERVED SUN		SUN WITH LIGHT CLOUDS		SUN WITH HEAVY STORM CLOUDS	
	HORIZONTAL FACE	VERTICAL FACE	HORIZONTAL FACE	VERTICAL FACE	HORIZONTAL FACE	VERTICAL FACE
0.0	299.44	299.49	299.44	299.46	299.44	299.44
1.0	299.44	299.56	299.44	299.49	299.44	299.45
2.0	299.44	299.64	299.44	299.51	299.44	299.45
3.0	299.45	299.70	299.44	299.54	299.44	299.46
4.0	299.46	299.78	299.45	299.57	299.44	299.47
5.0	299.47	299.88	299.46	299.62	299.44	299.48
6.0	299.49	299.91	299.46	299.64	299.44	299.49
7.0	299.50	299.99	299.46	299.66	299.44	299.49
8.0	299.52	300.07	299.47	299.69	299.45	299.50
9.0	299.55	300.15	299.48	299.72	299.45	299.51
10.0	299.60	300.24	299.49	299.76	299.45	299.52
11.0	299.62	300.34	299.51	299.82	299.45	299.53
12.0	299.64	300.38	299.52	299.87	299.46	299.54
13.0	299.67	300.46	299.54	299.91	299.46	299.54
14.0	299.71	300.54	299.55	299.95	299.47	299.55
15.0	299.76	300.62	299.60	299.99	299.47	299.56
16.0	299.82	300.70	299.63	300.04	299.48	299.57
17.0	299.89	300.77	299.65	300.08	299.49	299.61
18.0	299.94	300.85	299.67	300.12	299.49	299.61
19.0	299.99	300.93	299.70	300.16	299.50	299.62
20.0	299.06	300.96	299.72	300.20	299.50	299.63
21.0	300.13	301.04	299.76	300.24	299.51	299.63
22.0	300.21	301.13	299.80	300.28	299.52	299.64
23.0	300.29	301.22	299.84	300.33	299.53	299.64
24.0	300.33	301.31	299.88	300.37	299.54	299.65
25.0	300.41	301.46	299.92	300.43	299.55	299.66
26.0	300.50	301.55	299.97	300.47	299.56	299.67
27.0	300.58	301.66	300.01	300.50	299.57	299.68
28.0	300.67	301.73	300.05	300.54	299.61	299.69
29.0	300.77	301.81	300.10	300.57	299.62	299.71
30.0	300.89	301.89	300.16	300.61	299.63	
31.0	301.07	301.96	300.21		299.63	

ELEVATION ANGLE	HORIZONTAL FACE	VERTICAL FACE	HORIZONTAL FACE	VERTICAL FACE	HORIZONTAL FACE	VERTICAL FACE
34.0	301.130	302.14	300.28	300.674	299.64	299.723
35.0	301.30	302.18	300.34	300.671	299.65	299.73
36.0	301.44	302.26	300.36	300.715	299.66	299.745
37.0	301.61	302.34	300.42	300.781	299.69	299.776
38.0	301.70	302.41	300.48	300.815	299.70	299.779
39.0	301.85	302.49	300.54	300.87	299.72	299.79
40.0	302.00	302.55	300.61	300.890	299.74	299.80
41.0	302.18	302.62	300.67	300.935	299.75	299.80
42.0	302.24	302.69	300.74	300.97	299.77	299.81
43.0	302.26	302.74	300.81	300.996	299.79	299.81
44.0	302.27	302.76	300.89	300.98	299.81	299.82
45.0	302.28	302.78	300.97	300.96	299.83	299.82
46.0	302.30	302.80	301.01	300.98	299.86	299.82
47.0	302.31	302.82	301.09	301.002	299.85	299.82
48.0	302.33	302.82	301.12	301.024	299.87	299.82
49.0	302.34	302.82	301.16	301.05	299.88	299.81
50.0	302.36	302.81	301.17	301.055	299.91	299.81
51.0	302.37	302.81	301.19	301.06	299.93	299.81
52.0	302.39	302.81	301.24	301.066	299.94	299.80
53.0	302.41	302.81	301.26	301.066	299.95	299.80
54.0	302.45	302.81	301.29	301.065	299.97	299.80
55.0	302.47	302.77	301.33	301.04	299.98	299.79
56.0	302.47	302.74	301.37	301.01	299.99	299.78
57.0	302.47	302.67	301.42	301.00	299.99	299.77
58.0	302.47	302.61	301.46	300.99	299.99	299.76
59.0	302.47	302.55	301.49	300.96	299.99	299.75
60.0	302.47	302.48	301.51	300.95	299.99	299.74
61.0	302.47	302.43	301.54	300.91	299.99	299.73
62.0	302.47	302.37	301.57	300.87	299.99	299.72
63.0	302.47	302.31	301.61	300.83	299.99	299.71
64.0	302.47	302.25	301.64	300.79	299.99	299.70
65.0	302.47	302.20	301.68	300.75	299.99	299.69
66.0	302.47	302.15	301.72	300.71	299.99	299.68
67.0	302.47	302.10	301.75	300.67	299.99	299.67
68.0	302.47	302.05	301.79	300.63	299.99	299.66
69.0	302.47	302.01	301.83	300.59	299.99	299.65
70.0	302.47	302.00	301.86	300.55	299.99	299.64

ELEVATION ANGLE	HORIZONTAL FACE	VERTICAL FACE	HORIZONTAL FACE	VERTICAL FACE
71.0	306.19	301.75	302.96	300.65
72.0	306.23	301.65	303.03	300.60
73.0	306.31	301.58	303.10	300.55
74.0	306.41	301.45	303.13	300.50
75.0	306.46	301.33	303.19	300.44
76.0	306.51	301.21	303.25	300.39
77.0	306.56	301.09	303.30	300.33
78.0	306.62	300.96	303.36	300.27
79.0	306.69	300.87	303.41	300.22
80.0	306.70	300.73	303.47	300.16
81.0	306.73	300.60	303.53	300.09
82.0	306.76	300.47	303.58	300.02
83.0	306.78	300.34	303.63	299.95
84.0	306.81	300.23	303.67	299.88
85.0	306.83	300.09	303.70	299.74
86.0	306.85	299.96	303.74	299.66
87.0	306.86	299.70	303.78	299.61
88.0	306.87	299.57	303.82	299.54
89.0	306.88	299.44	303.85	299.44
90.0	306.89	299.31	303.88	299.31

TABLE 10
Ship Body Temperature for Tropical
 $T = 303.15K$ and $\epsilon = 0.80$

ELEVATION ANGLE	UNOBSERVED SUN		SUN WITH LIGHT CLOUDS		SUN WITH HEAVY STORM CLOUDS	
	HORIZONTAL FACE	VERTICAL FACE	HORIZONTAL FACE	VERTICAL FACE	HORIZONTAL FACE	VERTICAL FACE
0.0	299.85	299.88	299.85	299.86	299.85	299.85
1.0	299.85	299.93	299.85	299.90	299.85	299.85
2.0	299.85	299.98	299.85	299.92	299.85	299.86
3.0	299.86	300.02	299.85	299.94	299.85	299.87
4.0	299.86	300.07	299.85	299.96	299.85	299.87
5.0	299.87	300.12	299.86	299.98	299.85	299.88
6.0	299.88	300.18	299.86	300.00	299.85	299.88
7.0	299.89	300.24	299.87	300.02	299.85	299.89
8.0	299.91	300.30	299.88	300.04	299.85	299.89
9.0	299.92	300.37	299.88	300.06	299.86	299.90
10.0	299.94	300.42	299.89	300.09	299.86	299.90
11.0	299.96	300.48	299.90	300.12	299.86	299.91
12.0	299.98	300.53	299.91	300.15	299.86	299.91
13.0	300.01	300.58	299.93	300.18	299.86	299.92
14.0	300.03	300.64	299.94	300.21	299.87	299.92
15.0	300.06	300.69	299.95	300.24	299.87	299.93
16.0	300.09	300.74	299.97	300.27	299.87	299.93
17.0	300.13	300.79	299.99	300.31	299.88	299.94
18.0	300.16	300.84	300.00	300.34	299.88	299.94
19.0	300.20	300.89	300.02	300.37	299.88	299.95
20.0	300.24	300.96	300.04	300.35	299.89	299.95
21.0	300.29	300.97	300.06	300.37	299.89	299.96
22.0	300.35	300.97	300.08	300.39	299.90	299.97
23.0	300.40	301.03	300.11	300.41	299.90	299.97
24.0	300.45	301.08	300.13	300.43	299.91	299.98
25.0	300.50	301.13	300.16	300.46	299.91	299.98
26.0	300.56	301.18	300.19	300.49	299.92	299.99
27.0	300.61	301.24	300.22	300.51	299.92	299.99
28.0	300.67	301.29	300.25	300.54	299.93	299.99
29.0	300.74	301.34	300.29	300.56	299.94	300.00
30.0	300.81	301.39	300.33	300.58	299.95	300.01
31.0	300.89	301.44	300.32	300.61	299.96	300.01
32.0	300.98	301.50	300.35	300.63	299.96	300.02
33.0	300.98	301.56	300.35	300.63	299.96	300.03

ELEVATION ANGLE	HORIZONTAL FACE	VERTICAL FACE	HORIZONTAL FACE	VERTICAL FACE	HORIZONTAL FACE	VERTICAL FACE
34.0	301.01	301.57	300.39	300.65	299.97	300.04
35.0	301.09	301.62	300.42	300.67	299.98	300.04
36.0	301.18	301.67	300.46	300.70	299.99	300.05
37.0	301.27	301.73	300.50	300.72	300.01	300.06
38.0	301.37	301.78	300.54	300.74	300.02	300.07
39.0	301.47	301.83	300.58	300.77	300.03	300.08
40.0	301.59	301.88	300.63	300.79	300.04	300.08
41.0	301.65	301.92	300.67	300.80	300.05	300.09
42.0	301.74	301.96	300.72	300.82	300.06	300.09
43.0	301.85	302.00	300.76	300.84	300.07	300.09
44.0	301.95	302.04	300.81	300.85	300.08	300.09
45.0	302.07	302.09	300.86	300.86	300.09	300.09
46.0	302.14	302.11	300.93	300.89	300.10	300.09
47.0	302.24	302.12	300.95	300.90	300.11	300.09
48.0	302.34	302.13	301.01	300.92	300.12	300.09
49.0	302.44	302.14	301.06	300.94	300.13	300.09
50.0	302.57	302.14	301.12	300.95	300.14	300.09
51.0	302.67	302.14	301.17	300.96	300.15	300.09
52.0	302.73	302.13	301.23	300.97	300.17	300.09
53.0	302.83	302.11	301.29	300.97	300.18	300.09
54.0	302.93	302.10	301.35	300.97	300.19	300.09
55.0	303.03	302.07	301.41	300.97	300.20	300.09
56.0	303.16	302.05	301.46	300.96	300.22	300.08
57.0	303.21	302.02	301.53	300.95	300.23	300.08
58.0	303.30	302.02	301.59	300.94	300.24	300.08
59.0	303.40	301.99	301.61	300.93	300.25	300.07
60.0	303.50	301.92	301.66	300.91	300.26	300.07
61.0	303.57	301.88	301.71	300.89	300.28	300.06
62.0	303.65	301.83	301.76	300.87	300.29	300.06
63.0	303.74	301.79	301.81	300.85	300.30	300.05
64.0	303.84	301.75	301.87	300.83	300.31	300.05
65.0	303.95	301.69	301.92	300.80	300.32	300.04
66.0	304.06	301.64	302.00	300.78	300.33	300.04
67.0	304.13	301.58	302.08	300.75	300.34	300.03
68.0	304.21	301.55	302.14	300.72	300.35	300.03
69.0	304.30	301.48	302.15	300.69	300.36	300.02

ELEVATION ANGLE	HORIZONTAL FACE	VERTICAL FACE	HORIZONTAL FACE	VERTICAL FACE	HORIZONTAL FACE	VERTICAL FACE
71.0	304.32	301.40	302.19	300.66	300.33	300.01
72.0	304.38	301.33	302.13	300.63	300.33	300.00
73.0	304.43	301.25	302.27	300.59	300.33	300.00
74.0	304.48	301.18	302.31	300.56	300.34	299.99
75.0	304.54	301.10	302.35	300.52	300.35	299.98
76.0	304.58	301.03	302.43	300.48	300.36	299.97
77.0	304.63	300.95	302.47	300.44	300.37	299.96
78.0	304.67	300.89	302.50	300.40	300.38	299.95
79.0	304.69	300.80	302.54	300.36	300.38	299.94
80.0	304.71	300.71	302.58	300.32	300.39	299.93
81.0	304.73	300.62	302.61	300.31	300.39	299.92
82.0	304.75	300.54	302.65	300.26	300.40	299.91
83.0	304.76	300.45	302.68	300.21	300.40	299.91
84.0	304.78	300.36	302.67	300.15	300.41	299.90
85.0	304.79	300.32	302.69	300.10	300.41	299.89
86.0	304.80	300.21	302.72	300.05	300.42	299.88
87.0	304.80	300.11	302.74	300.00	300.42	299.87
88.0	304.81	300.02	302.76	299.95	300.43	299.86
89.0	304.81	299.93	302.78	299.90	300.43	299.85
90.0	304.81	299.85	302.78	299.85	300.43	299.85

TABLE 11

Ship Body Temperature for Tropical
 $T = 293.15\text{K}$ and $\epsilon = 0.55$

ELEVATION ANGLE	UNOBSCURED SUN		SUN WITH LIGHT CLOUDS		SUN WITH HEAVY STORM CLOUDS	
	HORIZONTAL FACE	VERTICAL FACE	HORIZONTAL FACE	VERTICAL FACE	HORIZONTAL FACE	VERTICAL FACE
0.0	299.43	299.47	299.43	299.45	299.43	299.43
1.0	299.43	299.52	299.43	299.46	299.43	299.44
2.0	299.44	299.57	299.43	299.48	299.43	299.44
3.0	299.44	299.63	299.44	299.50	299.43	299.45
4.0	299.45	299.67	299.44	299.52	299.43	299.45
5.0	299.45	299.71	299.44	299.54	299.43	299.45
6.0	299.46	299.78	299.44	299.57	299.43	299.46
7.0	299.48	299.82	299.45	299.59	299.43	299.46
8.0	299.49	299.87	299.45	299.63	299.44	299.47
9.0	299.49	299.93	299.46	299.64	299.44	299.47
10.0	299.53	299.98	299.47	299.66	299.44	299.48
11.0	299.55	300.04	299.48	299.68	299.44	299.49
12.0	299.57	300.10	299.49	299.71	299.44	299.49
13.0	299.60	300.17	299.50	299.74	299.44	299.50
14.0	299.64	300.24	299.51	299.78	299.45	299.51
15.0	299.66	300.31	299.53	299.82	299.45	299.51
16.0	299.68	300.36	299.54	299.85	299.46	299.52
17.0	299.71	300.41	299.56	299.88	299.46	299.53
18.0	299.75	300.46	299.57	299.91	299.47	299.54
19.0	299.80	300.50	299.59	299.93	299.47	299.54
20.0	299.82	300.57	299.63	299.96	299.48	299.55
21.0	299.86	300.63	299.66	299.98	299.49	299.55
22.0	299.91	300.69	299.68	300.01	299.49	299.56
23.0	299.96	300.75	299.70	300.03	299.50	299.56
24.0	300.01	300.82	299.72	300.06	299.50	299.57
25.0	300.07	300.88	299.75	300.09	299.51	299.58
26.0	300.13	300.94	299.79	300.12	299.51	299.58
27.0	300.20	300.95	299.83	300.15	299.52	299.59
28.0	300.24	301.00	299.86	300.17	299.52	299.59
29.0	300.30	301.05	299.90	300.20	299.53	299.63
30.0	300.36	301.10	299.93	300.23	299.54	299.63
31.0	300.43	301.16	299.97	300.25	299.55	299.64
32.0	300.51	301.21	299.99	300.26	299.55	299.64
33.0	300.59					

ELEVATION ANGLE	HORIZONTAL FACE	VERTICAL FACE	HORIZONTAL FACE	VERTICAL FACE	HORIZONTAL FACE	VERTICAL FACE
34.0	300.67	301.26	300.00	300.28	299.56	299.64
35.0	300.76	301.32	300.04	300.30	299.57	299.65
36.0	300.83	301.39	300.09	300.32	299.58	299.65
37.0	300.93	301.42	300.13	300.35	299.59	299.66
38.0	301.03	301.47	300.18	300.37	299.63	299.66
39.0	301.12	301.52	300.24	300.39	299.64	299.67
40.0	301.24	301.57	300.25	300.41	299.65	299.67
41.0	301.35	301.62	300.30	300.43	299.66	299.68
42.0	301.45	301.66	300.34	300.44	299.66	299.68
43.0	301.54	301.70	300.39	300.46	299.67	299.68
44.0	301.65	301.73	300.43	300.47	299.68	299.68
45.0	301.76	301.76	300.48	300.48	299.68	299.68
46.0	301.88	301.78	300.54	300.50	299.69	299.68
47.0	301.96	301.80	300.60	300.52	299.70	299.68
48.0	302.06	301.83	300.66	300.53	299.71	299.68
49.0	302.17	301.83	300.73	300.55	299.72	299.68
50.0	302.29	301.83	300.80	300.55	299.73	299.68
51.0	302.37	301.83	300.83	300.56	299.75	299.68
52.0	302.45	301.82	300.89	300.57	299.76	299.68
53.0	302.56	301.81	300.95	300.58	299.77	299.68
54.0	302.69	301.79	301.01	300.58	299.79	299.68
55.0	302.78	301.77	301.07	300.57	299.80	299.68
56.0	302.88	301.74	301.12	300.57	299.82	299.67
57.0	302.99	301.71	301.18	300.57	299.84	299.67
58.0	303.09	301.68	301.24	300.56	299.88	299.67
59.0	303.17	301.65	301.31	300.55	299.88	299.67
60.0	303.23	301.61	301.37	300.54	299.84	299.66
61.0	303.27	301.57	301.40	300.52	299.85	299.66
62.0	303.34	301.53	301.45	300.51	299.86	299.65
63.0	303.39	301.48	301.51	300.49	299.87	299.65
64.0	303.47	301.44	301.56	300.47	299.88	299.64
65.0	303.56	301.38	301.61	300.45	299.89	299.64
66.0	303.73	301.34	301.67	300.42	299.90	299.64
67.0	303.88	301.27	301.72	300.37	299.91	299.63
68.0	303.99	301.20	301.77	300.33	299.92	299.63
69.0	304.11	301.14	301.83	300.30	299.92	299.63
70.0	304.20	301.11	301.89	300.30	299.92	299.63

ELEVATION ANGLE	HORIZONTAL FACE	VERTICAL FACE	HORIZONTAL FACE	VERTICAL FACE	HORIZONTAL FACE	VERTICAL FACE
71.0	304.16	301.06	301.91	300.28	299.93	299.63
72.0	304.22	300.91	301.95	300.25	299.94	299.59
73.0	304.28	300.84	301.99	300.20	299.95	299.59
74.0	304.33	300.78	302.03	300.15	299.96	299.58
75.0	304.39	300.69	302.08	300.11	299.97	299.56
76.0	304.44	300.60	302.12	300.06	299.98	299.55
77.0	304.49	300.51	302.15	300.02	299.98	299.55
78.0	304.52	300.42	302.19	299.93	299.99	299.54
79.0	304.55	300.33	302.23	299.88	300.00	299.53
80.0	304.57	300.25	302.26	299.84	300.00	299.52
81.0	304.59	300.18	302.29	299.81	300.01	299.51
82.0	304.61	300.07	302.31	299.74	300.02	299.50
83.0	304.63	299.88	302.33	299.69	300.03	299.48
84.0	304.65	299.82	302.38	299.65	300.04	299.47
85.0	304.66	299.70	302.44	299.61	300.04	299.46
86.0	304.67	299.63	302.49	299.59	300.05	299.45
87.0	304.67	299.52	302.51	299.54	300.05	299.44
88.0	304.68	299.43	302.53	299.48	300.05	299.43
89.0	304.68					
90.0	304.68					

TABLE 12
Ship Body Temperature for Tropical
 $T = 303.15\text{K}$ and ≈ 0.55

ELEVATION ANGLE	UNOBSERVED SUN		SUN WITH LIGHT CLOUDS		SUN WITH HEAVY STORM CLOUDS	
	HORIZONTAL FACE	VERTICAL FACE	HORIZONTAL FACE	VERTICAL FACE	HORIZONTAL FACE	VERTICAL FACE
0.0	299.85	299.88	299.85	299.86	299.85	299.85
1.0	299.85	299.91	299.85	299.87	299.85	299.85
2.0	299.85	299.94	299.85	299.89	299.85	299.86
3.0	299.86	299.98	299.85	299.90	299.85	299.86
4.0	299.86	300.01	299.86	299.91	299.85	299.86
5.0	299.87	300.04	299.86	299.93	299.85	299.87
6.0	299.87	300.08	299.86	299.94	299.85	299.87
7.0	299.88	300.12	299.87	299.96	299.85	299.88
8.0	299.89	300.16	299.87	299.97	299.85	299.88
9.0	299.90	300.21	299.88	299.99	299.85	299.88
10.0	299.92	300.25	299.88	300.00	299.86	299.88
11.0	299.93	300.29	299.89	300.02	299.86	299.89
12.0	299.95	300.33	299.90	300.04	299.86	299.90
13.0	299.96	300.37	299.91	300.06	299.86	299.90
14.0	299.98	300.41	299.92	300.08	299.86	299.90
15.0	299.00	300.47	299.93	300.10	299.87	299.91
16.0	299.02	300.51	299.94	300.12	299.87	299.91
17.0	299.05	300.57	299.95	300.15	299.87	299.91
18.0	299.07	300.54	299.96	300.17	299.87	299.92
19.0	299.09	300.57	299.97	300.19	299.88	299.93
20.0	299.12	300.61	299.99	300.21	299.88	299.93
21.0	299.16	300.65	300.00	300.23	299.88	299.93
22.0	299.19	300.69	300.02	300.25	299.89	299.94
23.0	299.23	300.74	300.03	300.25	299.89	299.94
24.0	299.27	300.78	300.05	300.26	299.89	299.95
25.0	299.31	300.82	300.07	300.28	299.90	299.95
26.0	299.35	300.86	300.09	300.30	299.90	299.95
27.0	299.39	300.90	300.11	300.32	299.91	299.96
28.0	299.43	300.93	300.13	300.33	299.91	299.96
29.0	299.47	300.96	300.16	300.35	299.91	299.97
30.0	299.52	300.96	300.18	300.37	299.92	299.97
31.0	299.57	301.00	300.21	300.38	299.93	299.98
32.0	299.63	301.03	300.24	300.40	299.93	299.98
33.0						

ELEVATION ANGLE	HORIZONTAL FACE	VERTICAL FACE	HORIZONTAL FACE	VERTICAL FACE	HORIZONTAL FACE	VERTICAL FACE
34.0	300.68	301.07	300.26	300.42	299.94	299.98
35.0	300.74	301.10	300.28	300.43	299.95	299.99
36.0	300.82	301.14	300.31	300.45	299.95	299.99
37.0	300.85	301.18	300.34	300.46	299.96	300.00
38.0	300.98	301.22	300.37	300.48	299.97	300.00
39.0	301.18	301.26	300.40	300.49	299.98	300.01
40.0	301.05	301.30	300.43	300.51	299.99	300.01
41.0	301.12	301.33	300.46	300.52	299.99	300.02
42.0	301.19	301.36	300.49	300.53	299.99	300.02
43.0	301.27	301.39	300.52	300.54	300.00	300.02
44.0	301.35	301.40	300.55	300.55	300.01	300.02
45.0	301.40	301.42	300.59	300.57	300.02	300.02
46.0	301.47	301.44	300.64	300.58	300.03	300.02
47.0	301.54	301.44	300.68	300.59	300.04	300.02
48.0	301.61	301.44	300.72	300.60	300.04	300.02
49.0	301.68	301.44	300.77	300.61	300.05	300.02
50.0	301.75	301.44	300.82	300.61	300.06	300.02
51.0	301.83	301.44	300.86	300.62	300.07	300.02
52.0	301.92	301.43	300.90	300.62	300.08	300.02
53.0	302.00	301.43	300.94	300.62	300.09	300.02
54.0	302.09	301.42	300.98	300.62	300.10	300.02
55.0	302.16	301.40	301.02	300.61	300.11	300.02
56.0	302.22	301.39	301.05	300.61	300.11	300.01
57.0	302.28	301.38	301.09	300.60	300.12	300.01
58.0	302.34	301.35	301.13	300.59	300.13	300.01
59.0	302.41	301.32	301.17	300.58	300.14	300.01
60.0	302.47	301.29	301.21	300.57	300.15	300.00
61.0	302.53	301.26	301.24	300.56	300.15	300.00
62.0	302.60	301.23	301.28	300.55	300.16	300.00
63.0	302.67	301.19	301.33	300.53	300.17	299.99
64.0	302.73	301.15	301.37	300.52	300.18	299.99
65.0	302.80	301.11	301.41	300.50	300.19	299.98
66.0	302.87	301.10	301.44	300.48	300.20	299.98
67.0	302.92	301.09	301.47	300.46	300.20	299.97
68.0	302.99	301.07	301.51	300.44	300.20	299.97
69.0	303.02	301.06	301.54	300.43	300.20	299.97
70.0	303.05	301.05	301.57	300.42	300.20	299.97

ELEVATION ANGLE	HORIZONTAL FACE	VERTICAL FACE	HORIZONTAL FACE	VERTICAL FACE
71.0	303.01	300.94	301.50	300.42
72.0	303.05	300.89	301.53	300.40
73.0	303.09	300.84	301.56	300.37
74.0	303.14	300.82	301.59	300.35
75.0	303.19	300.76	301.62	300.32
76.0	303.18	300.69	301.64	300.30
77.0	303.20	300.63	301.67	300.27
78.0	303.22	300.57	301.69	300.24
79.0	303.25	300.51	301.72	300.25
80.0	303.27	300.45	301.75	300.21
81.0	303.28	300.39	301.77	300.17
82.0	303.31	300.33	301.79	300.14
83.0	303.32	300.28	301.81	300.10
84.0	303.33	300.25	301.84	300.06
85.0	303.33	300.17	301.86	300.03
86.0	303.33	300.10	301.88	299.99
87.0	303.34	300.04	301.90	299.96
88.0	303.35	299.97	301.92	299.92
89.0	303.35	299.91	301.90	299.89
90.0	303.35	299.85	301.92	299.85

APPENDIX B
TABLES FOR DETERMINATION OF I.F.V.

TABLE 13

Side of Instantaneous Field of View in Meters
for Flight Altitude= 50 m

DELTA	PHI=2.00	PHI=2.50	PHI=3.00	PHI=3.50	PHI=4.00	PHI=4.50	PHI=5.00
0.20	9.091	7.409	6.25	5.41	4.77	4.26	3.82
0.22	9.912	8.076	6.84	5.92	5.22	4.67	4.22
0.24	10.721	8.942	7.498	6.42	5.67	5.07	4.59
0.26	11.511	9.762	8.154	7.00	6.11	5.47	4.95
0.28	12.285	10.508	8.840	7.74	6.55	5.86	5.31
0.30	13.05	11.235	9.510	8.49	7.14	6.42	5.82
0.32	13.803	11.989	10.164	9.23	7.84	7.05	6.42
0.34	14.526	12.759	10.819	9.98	8.51	7.65	7.02
0.36	15.237	13.520	11.472	10.73	9.18	8.33	7.63
0.38	15.937	14.280	12.125	11.48	9.86	9.03	8.23
0.40	16.636	15.039	12.777	12.22	10.51	9.70	8.87
0.42	17.304	15.797	13.429	12.97	11.15	10.37	9.47
0.44	17.960	16.555	14.080	13.71	11.80	11.01	10.10
0.46	18.703	17.311	14.730	14.45	12.44	11.65	10.74
0.48	19.436	18.067	15.380	15.19	13.08	12.29	11.40
0.50	20.161	18.823	16.029	15.93	13.72	12.95	12.03
0.52	20.878	19.577	16.678	16.67	14.36	13.61	12.69
0.54	21.588	20.331	17.324	17.40	15.00	14.27	13.36
0.56	22.291	21.084	17.969	18.13	15.64	14.93	14.01
0.58	22.988	21.836	18.614	18.86	16.28	15.59	14.67
0.60	23.679	22.588	19.259	19.59	16.92	16.25	15.33

TABLE 14
Path in Meters for Flight Altitude= 50 m

DELTA	PHI=2.00	PHI=2.50	PHI=3.00	PHI=3.50	PHI=4.00	PHI=4.50	PHI=5.00
0	1302.43	1061.37	895.68	774.78	682.68	610.19	551.66
0	1290.70	1053.59	890.12	770.61	679.45	607.61	549.56
0	1279.21	1045.90	884.65	766.51	676.25	605.06	547.46
0	1267.86	1038.31	879.21	762.43	673.08	602.52	545.38
0	1256.75	1030.86	873.58	758.41	669.94	600.00	543.28
0	1245.09	1023.51	868.33	754.42	666.83	597.51	541.24
0	1233.96	1016.23	863.17	750.57	663.70	595.08	539.25
0	1221.96	1009.10	858.02	746.71	660.67	592.15	537.25
0	1214.19	1002.05	853.04	742.87	657.67	590.73	535.28
0	1203.33	995.23	848.10	738.10	654.67	587.73	533.31
0	1193.04	988.25	843.24	735.34	651.75	585.96	531.39
0	1184.37	981.78	838.43	731.64	648.84	582.61	529.46
0	1174.81	974.21	833.66	727.97	645.95	580.27	527.54
0	1165.41	966.70	828.97	720.33	642.07	578.95	525.64
0	1155.20	959.29	824.32	716.73	637.42	575.65	523.76
0	1146.10	951.99	819.71	713.18	634.63	573.38	521.88
0	1137.13	944.73	815.18	709.64	631.87	571.16	519.03
0	1129.34	936.51	809.68	706.15	628.12	569.86	517.16
0	1119.67	930.49	805.23	702.70	626.42	566.64	515.35
0	1110.12	924.49	799.68	699.27	623.33	562.42	512.35

TABLE 15

Side of Instantaneous Field of View in Meters
for Flight Altitude= 60 m

DELTA	PHI=2.00	PHI=2.50	PHI=3.00	PHI=3.50	PHI=4.00	PHI=4.50	PHI=5.00
0	10.91	8.89	7.50	6.49	5.72	5.11	4.62
0	11.89	9.71	8.29	7.10	6.26	5.60	5.06
0	12.86	10.51	8.89	7.30	6.33	5.68	5.14
0	13.74	11.31	9.58	8.00	6.86	6.04	5.37
0	14.66	12.09	10.25	8.48	7.39	6.51	5.80
0	15.56	12.86	11.01	9.06	7.90	7.08	6.23
0	16.44	13.62	11.77	10.06	8.41	7.44	6.57
0	17.31	14.37	12.50	11.20	8.92	7.90	7.07
0	18.16	15.14	13.23	11.76	9.42	8.36	7.49
0	19.00	15.86	14.00	12.32	9.92	8.81	7.90
0	20.03	16.56	14.74	12.87	10.41	9.26	8.32
0	20.64	17.27	15.36	13.49	10.90	9.70	8.72
0	21.64	17.96	15.96	14.01	11.39	10.14	9.12
0	22.34	18.64	16.56	14.58	11.87	10.58	9.53
0	23.23	19.30	17.15	15.01	12.35	11.01	9.93
0	24.01	20.01	17.74	15.50	12.82	11.45	10.32
0	24.77	20.63	18.32	16.05	13.29	11.87	10.71
0	25.52	21.32	18.89	16.56	14.75	12.30	11.10
0	26.26	21.97	19.45	17.07	15.21	12.72	11.49
0	26.98	22.61	20.01	17.58	15.67	13.14	11.88
0	27.70	23.24					

TABLE 16

Path in Meters for Flight Altitude= 60 m

DELTA	PHI=2.00	PHI=2.50	PHI=3.00	PHI=3.50	PHI=4.00	PHI=4.50	PHI=5.00
00	1562.91	1273.64	1074.81	929.73	819.21	732.23	661.99
00	1548.84	1264.31	1068.14	924.74	815.34	729.14	659.47
00	1535.05	1255.09	1061.57	919.81	811.50	726.07	656.96
00	1521.44	1245.97	1055.05	914.91	807.69	723.02	654.46
00	1508.10	1237.04	1048.62	910.09	803.93	720.00	651.99
00	1495.02	1228.21	1042.29	905.31	800.20	717.02	649.54
00	1482.44	1219.48	1036.00	900.56	796.49	714.04	647.10
00	1469.03	1210.92	1029.80	895.25	792.84	711.09	644.68
00	1457.06	1202.46	1023.69	891.25	789.20	708.18	642.28
00	1444.76	1194.09	1017.64	886.61	785.61	705.24	639.90
00	1432.85	1185.88	1011.72	882.12	782.04	702.40	637.54
00	1420.24	1177.73	1005.89	877.16	778.50	699.55	635.18
00	1409.27	1169.73	999.12	873.77	775.01	696.73	632.86
00	1397.49	1161.86	994.39	868.40	771.54	693.92	630.55
00	1386.43	1154.35	988.76	864.08	768.09	691.14	628.27
00	1375.52	1146.79	982.78	860.55	764.63	688.38	625.97
00	1364.71	1138.28	977.18	855.78	761.31	685.65	623.71
00	1353.21	1131.89	971.65	851.38	757.95	682.93	621.46
00	1343.80	1123.89	966.82	847.38	754.64	680.24	619.23
00	1332.55	1116.39	960.82	843.12	751.35	677.57	617.02
00	1322.55	1110.39	955.47	839.12	748.08	674.91	614.81

TABLE 17
Side of Instantaneous Field of View in Meters
for Flight Altitude= 70 m

DELTA	PHI=2.00	PHI=2.50	PHI=3.00	PHI=3.50	PHI=4.00	PHI=4.50	PHI=5.00
0	12.73	10.37	8.75	7.57	6.67	5.96	5.39
0	13.88	11.33	9.57	8.29	7.31	6.53	5.91
0	15.00	12.27	10.38	8.99	7.93	7.10	6.42
0	16.11	13.19	11.17	9.69	8.55	7.66	6.93
0	17.20	14.11	11.96	10.38	9.17	8.21	7.43
0	18.27	15.01	12.73	11.06	9.78	8.76	7.94
0	19.31	15.89	13.50	11.74	10.38	9.31	8.43
0	20.33	16.77	14.26	12.40	10.98	9.85	8.93
0	21.33	17.63	15.01	13.07	11.57	10.39	9.40
0	22.33	18.48	15.75	13.72	12.16	10.91	9.86
0	23.33	19.32	16.48	14.37	12.74	11.44	10.31
0	24.25	20.14	17.20	15.01	13.32	11.97	10.76
0	25.19	20.96	17.92	15.65	13.89	12.48	11.21
0	26.11	21.77	18.62	16.28	14.41	13.00	11.65
0	27.10	22.56	19.32	16.90	14.95	13.51	12.09
0	28.09	23.34	20.01	17.51	15.47	14.02	12.51
0	28.97	24.12	20.69	18.12	16.01	14.52	12.92
0	29.73	24.88	21.37	18.73	16.57	15.02	13.33
0	30.48	25.63	22.04	19.33	17.11	15.51	13.72
0	31.23	26.38	22.70	19.92	17.62	16.00	14.11
0	32.32	27.11	23.35	20.50	18.28	16.49	14.50

TABLE 18

Path in Meters for Flight Altitude=70 m

DELTA	PHI=2.00	PHI=2.50	PHI=3.00	PHI=3.50	PHI=4.00	PHI=4.50	PHI=5.00
0.20	1823.40	1485.92	1253.95	1084.69	955.75	854.27	772.38
0.22	1806.98	1475.03	1246.17	1078.86	951.24	850.66	769.45
0.24	1790.89	1464.27	1238.50	1073.11	946.31	847.09	766.53
0.26	1775.04	1453.63	1230.89	1067.40	942.31	843.53	763.66
0.28	1759.44	1443.21	1223.39	1061.77	937.92	840.00	760.79
0.30	1744.20	1432.91	1216.01	1056.19	933.57	836.52	757.95
0.32	1729.12	1422.77	1208.67	1050.65	929.24	833.05	754.13
0.34	1714.38	1412.86	1201.44	1045.20	924.98	829.61	752.33
0.36	1699.55	1402.10	1194.31	1039.72	920.74	826.22	749.55
0.38	1685.51	1393.53	1187.23	1034.42	916.54	822.9.47	746.79
0.40	1671.66	1383.03	1180.25	1029.14	912.38	819.16	743.05
0.42	1657.12	1374.09	1173.34	1023.89	908.17	816.18	741.33
0.44	1644.76	1364.50	1166.80	1018.56	904.13	812.58	738.64
0.46	1630.57	1355.38	1159.80	1013.46	900.10	809.33	735.95
0.48	1617.57	1346.41	1153.12	1008.43	896.14	806.19	732.30
0.50	1604.94	1337.58	1146.05	1003.45	892.19	803.93	730.66
0.52	1591.38	1328.82	1139.59	998.50	888.18	799.75	727.03
0.54	1579.08	1319.20	1133.25	993.61	884.41	796.61	725.44
0.56	1567.03	1311.72	1127.96	988.79	880.57	793.50	722.86
0.58	1554.98	1302.29	1120.77	983.98	876.76	790.39	719.17
0.60	1542.98	1294.29	1114.74	978.98	872.76	787.71	717.28

TABLE 19
Side of Instantaneous Field of View in Meters
for Flight Altitude= 80 m

DELTA	PHI=2.00	PHI=2.50	PHI=3.00	PHI=3.50	PHI=4.00	PHI=4.50	PHI=5.00
0	14.55	11.86	10.00	8.65	7.63	6.82	6.16
0	15.86	12.95	10.94	9.47	8.35	7.47	6.75
0	17.15	14.02	11.86	10.27	9.06	8.11	7.34
0	18.41	15.08	12.77	11.07	9.77	8.75	7.92
0	19.65	16.12	13.67	11.86	10.48	9.38	8.50
0	20.87	17.15	14.55	12.64	11.18	10.01	9.07
0	22.07	18.16	15.43	13.41	11.86	10.63	9.64
0	23.25	19.16	16.30	14.18	12.55	11.25	10.20
0	24.41	20.15	17.15	14.93	13.22	11.87	10.76
0	25.55	21.12	18.00	15.68	13.89	12.47	11.32
0	26.67	22.08	18.83	16.42	14.56	13.07	11.87
0	27.77	23.02	19.66	17.16	15.22	13.67	12.42
0	28.86	23.95	20.48	17.88	15.87	14.26	12.96
0	29.93	24.88	21.28	18.60	16.51	14.84	13.50
0	30.98	25.78	22.08	19.31	17.16	15.41	14.04
0	32.01	26.68	22.87	20.02	17.80	16.00	14.57
0	33.02	27.56	23.65	20.71	18.43	16.59	15.10
0	34.01	28.43	24.42	21.40	19.05	17.16	15.62
0	35.01	29.29	25.18	22.09	19.67	17.73	16.14
0	35.98	30.14	25.94	22.76	20.28	18.29	16.66
0	36.93	30.98	26.68	23.43	20.89	18.85	17.17

TABLE 20
Path in Meters for Flight Altitude= 80 m

DELTA	PHI=2.00	PHI=2.50	PHI=3.00	PHI=3.50	PHI=4.00	PHI=4.50	PHI=5.00
0.20	2083.88	1698.19	1433.09	1239.64	1092.28	976.31	882.66
0.22	2065.12	1685.74	1424.19	1232.42	1087.13	972.18	879.29
0.24	2046.58	1667.45	1415.43	1226.42	1082.01	968.10	875.94
0.26	2028.37	1649.38	1406.16	1219.88	1076.91	964.03	872.61
0.28	2010.31	1637.97	1398.72	1213.45	1071.93	960.00	869.05
0.30	1997.14	1625.56	1381.33	1207.07	1066.99	956.02	866.05
0.32	1976.27	1614.32	1364.92	1200.52	1061.11	952.05	862.58
0.34	1959.71	1603.22	1348.86	1194.33	1057.27	948.13	859.38
0.36	1942.30	1592.18	1335.68	1188.20	1052.47	944.24	856.30
0.38	1926.37	1581.32	1324.09	1182.21	1047.72	940.37	853.20
0.40	1910.47	1570.65	1313.48	1176.16	1042.00	936.54	850.05
0.42	1894.99	1559.94	1303.33	1170.42	1038.37	932.74	846.81
0.44	1878.72	1549.17	1293.55	1164.36	1033.71	928.97	843.73
0.46	1864.91	1538.88	1284.31	1158.52	1028.11	925.22	840.76
0.48	1848.36	1528.37	1275.91	1152.57	1024.58	921.52	837.62
0.50	1833.91	1518.38	1268.35	1147.09	1019.50	917.84	834.61
0.52	1805.00	1508.52	1259.54	1141.43	1015.60	914.25	831.66
0.54	1790.94	1498.88	1251.28	1135.84	1010.69	910.69	828.55
0.56	1777.07	1488.81	1243.96	1129.83	1006.19	906.43	825.69
0.58	1763.40	1479.19	1237.33	1124.83	1001.44	903.88	822.75
0.60				1118.83	997.44		819.75

TABLE 21
Side of Instantaneous Field of View in Meters
for Flight Altitude= 90 m

DELTA	PHI=2.00	PHI=2.50	PHI=3.00	PHI=3.50	PHI=4.00	PHI=4.50	PHI=5.00
0.0	16.37	13.34	11.26	9.74	8.58	7.67	6.93
0.2	17.84	14.56	12.34	10.56	9.39	8.40	7.66
0.2	19.29	15.77	13.36	11.46	10.20	9.12	8.29
0.2	20.71	16.96	14.37	12.32	11.00	9.84	8.91
0.2	22.48	18.29	15.37	13.22	11.89	10.66	9.56
0.3	23.48	19.43	16.36	14.09	12.53	11.26	10.24
0.3	24.67	20.56	17.33	15.09	13.35	12.06	10.84
0.3	26.16	22.67	18.30	16.08	14.18	12.85	11.33
0.3	27.77	23.76	19.25	17.04	15.03	13.65	11.73
0.4	28.01	24.84	20.12	17.83	15.63	14.37	12.35
0.4	30.42	26.95	21.12	18.64	16.38	15.05	12.97
0.4	31.47	27.98	22.04	19.30	17.08	15.67	13.58
0.4	32.68	29.00	22.94	20.12	17.85	16.37	14.19
0.4	34.01	30.01	23.84	21.15	18.58	17.02	14.79
0.5	36.80	31.01	24.73	22.30	19.30	17.73	15.38
0.5	37.18	31.99	25.61	23.08	20.02	18.40	15.96
0.5	38.59	32.96	26.47	24.05	20.73	19.09	16.51
0.5	39.39	33.84	27.33	24.85	21.43	19.73	17.04
0.4	40.55	33.74	28.18	25.61	22.12	20.39	17.42
0.0	0.56	0.33	0.10	0.03	0.00	0.00	0.00

TABLE 22

Path in Meters for Flight Altitude=90 m

DELTA	PHI=2.00	PHI=2.50	PHI=3.00	PHI=3.50	PHI=4.00	PHI=4.50	PHI=5.00
0	2344.37	1910.46	1612.22	1394.60	1228.82	1098.35	992.99
0	2323.25	1896.46	1602.22	1387.11	1223.02	1093.71	989.20
0	2302.15	1882.63	1592.36	1379.72	1217.26	1089.11	985.49
0	2282.14	1868.56	1582.58	1372.37	1211.54	1084.53	981.69
0	2262.54	1855.31	1572.93	1365.19	1205.90	1080.00	977.31
0	2242.16	1842.22	1563.44	1357.84	1200.30	1075.53	974.03
0	2223.17	1829.38	1554.70	1350.83	1194.74	1071.06	970.64
0	2204.54	1816.38	1544.70	1343.87	1189.25	1066.27	967.43
0	2185.13	1803.13	1535.44	1336.97	1183.41	1062.92	963.84
0	2167.08	1791.82	1526.47	1329.97	1178.04	1057.93	959.31
0	2149.28	1778.66	1517.58	1323.14	1173.73	1053.33	955.62
0	2131.68	1766.40	1508.84	1316.74	1167.51	1049.08	952.78
0	2113.86	1754.70	1499.17	1309.15	1162.30	1045.09	949.33
0	2096.74	1742.53	1489.59	1303.60	1157.10	1040.71	945.82
0	2079.15	1731.06	1482.17	1296.12	1152.33	1036.54	942.35
0	2063.78	1719.58	1474.78	1289.72	1147.96	1032.48	938.57
0	2046.63	1708.18	1465.48	1283.36	1141.93	1028.39	935.19
0	2030.81	1696.92	1457.32	1277.07	1136.96	1024.35	932.85
0	2014.81	1685.92	1449.32	1271.87	1131.02	1020.35	929.53
0	1999.28	1674.09	1441.21	1264.69	1127.12	1016.36	925.22
0	1983.83	1664.09	1433.21	1258.69	1122.12	1012.36	922.52

TABLE 23
Side of Instantaneous Field of View in Meters
for Flight Altitude=100 m

DELTA	PHI=2.00	PHI=2.50	PHI=3.00	PHI=3.50	PHI=4.00	PHI=4.50	PHI=5.00
0	18.18	14.82	12.51	10.82	9.53	8.52	7.70
0	19.43	16.18	13.68	11.84	10.44	9.33	8.44
0	21.01	17.52	14.96	12.84	11.33	10.14	9.17
0	23.57	18.15	15.08	13.80	12.22	10.94	9.90
0	26.09	20.44	17.19	15.80	13.97	11.73	10.62
0	29.59	22.70	19.37	17.72	15.83	13.51	12.34
0	30.52	23.18	20.44	18.60	16.68	14.29	13.05
0	33.72	25.40	21.50	19.63	17.53	15.03	13.75
0	33.72	26.78	22.54	20.53	18.20	15.83	14.45
0	36.07	27.94	23.57	21.44	19.02	16.59	15.20
0	37.41	29.09	24.60	22.35	19.84	17.37	16.52
0	38.72	31.23	25.60	23.42	20.65	18.57	17.41
0	40.01	32.35	26.60	24.14	21.45	19.30	18.27
0	41.28	33.45	27.59	25.02	22.03	20.74	18.83
0	43.76	34.54	28.56	25.89	23.08	21.46	19.51
0	44.97	35.62	29.53	26.75	24.53	22.16	20.17
0	46.17	36.77	30.48	27.61	25.35	22.86	20.82
0			31.33	28.92	26.11	23.56	21.46
0			32.33	29.92			
0			33.33				

TABLE 24

Path in Meters for Flight Altitude=100 m

DELTA	PHI=2.00	PHI=2.50	PHI=3.00	PHI=3.50	PHI=4.00	PHI=4.50	PHI=5.00
0	2604.85	2122.74	1791.36	1549.55	1365.35	1220.39	1103.32
0	2581.39	2107.18	1780.24	1541.23	1358.91	1215.23	1099.11
0	2558.42	2091.81	1769.29	1533.02	1352.51	1210.12	1094.93
0	2535.73	2076.62	1758.42	1524.85	1346.15	1205.04	1090.76
0	2513.49	2061.73	1747.70	1516.82	1339.89	1200.00	1086.56
0	2491.71	2047.01	1737.15	1508.84	1333.67	1195.07	1082.47
0	2470.18	2032.47	1726.67	1500.93	1327.48	1190.16	1078.47
0	2449.03	2018.20	1716.34	1493.15	1321.33	1185.30	1074.47
0	2428.38	2004.09	1706.16	1485.42	1315.34	1180.46	1070.49
0	2407.93	1990.15	1696.04	1477.75	1309.40	1175.67	1066.56
0	2387.87	1976.47	1686.07	1470.20	1303.50	1170.92	1062.76
0	2368.09	1962.90	1676.28	1462.69	1297.68	1166.21	1058.91
0	2348.74	1949.56	1666.48	1455.95	1291.89	1161.54	1055.08
0	2329.82	1936.40	1656.86	1448.66	1285.14	1156.90	1051.28
0	2310.39	1923.59	1647.32	1440.47	1278.48	1151.30	1047.52
0	2291.44	1910.98	1637.94	1433.36	1271.85	1147.75	1043.82
0	2272.25	1897.46	1628.64	1426.30	1265.27	1143.22	1039.57
0	2253.68	1885.15	1619.35	1419.30	1258.73	1138.75	1035.06
0	2235.33	1873.02	1610.37	1412.41	1252.28	1133.39	1032.36
0	2217.44	1861.99	1601.45	1405.54	1246.80	1128.85	1028.69

APPENDIX C
TABLES WITH DATA USED FOR LOWTRAN 6

TABLE 25

Data Used for Month October

CARD 1

MODEL	:	2	:	Midlatitude Summer
ITYPE	:	2	:	Slant Path Between Two Altitudes
IEMSCT	:	0	:	Program Execution in Transmittance Mode
M1	:	2	:	Midlatitude Summer T and P Profile
M2	:	2	:	Midlatitude Summer Water Vapor Profile
M3	:	2	:	Midlatitude Summer Ozone Profile
IM	:	0	:	Normal Operation of Program
NOPRT	:	0	:	Normal Operation of Program
TBOUND	:	0	:	Normal Operation of Program
SALB	:	0	:	Normal Operation of Program

CARD 2

IHAZE	:	3	:	Navy Maritime Extinction
ISEASN	:	2	:	Fall - Winter
IVULCN	:	0	:	No Stratospheric Background
ICSTL	:	5	:	Medium Continental Influence
ICIR	:	0	:	No Cirrus
IVSA	:	0	:	Not Used
VIS	:	10	:	Meteorological Range(Km)
WSS	:	2.09	:	Current Wind Speed (m/s)
WHH	:	2.09	:	24 hours Average Wind Speed (m/s)
RAINRT	:	0	:	Rain Rate (mm/h)

CARD 3

H1	:	From Section G of Chapter II : Initial Altitude		
H2	:	From Table 22 : Final Altitude		
ANGLE	:	--	:	Not Necessary to Define
RANGE	:	From Table 22 : Path Length		
BETA	:	--	:	Not Necessary to Define
RO	:	--	:	Not Necessary to Define
LEN	:	0	:	Normal Operation

CARD 4

V1	:	2255	:	Initial Frequency
V2	:	2000	:	Final Frequency
DV	:	10	:	Frequency Increment

TABLE 26

Average Transmittances for Month October

FINAL ALTITUDE INITIAL ALTITUDE	0.050 (Km)	0.060 (Km)	0.070 (Km)	0.080 (Km)	0.090 (Km)	0.100 (Km)
0.004 (Km)	0.4718	0.4715	0.4712	0.4712	0.4711	0.4711
0.007 (Km)	0.4719	0.4716	0.4713	0.4713	0.4712	0.4712
0.012 (Km)	0.4720	0.4717	0.4715	0.4715	0.4714	0.4714
0.016 (Km)	0.4722	0.4719	0.4716	0.4716	0.4715	0.4715
0.018 (Km)	0.4722	0.4719	0.4717	0.4717	0.4716	0.4716
0.021 (Km)	0.4723	0.4720	0.4718	0.4718	0.4717	0.4717
0.022 (Km)	0.4723	0.4720	0.4718	0.4718	0.4717	0.4717
Average per Altitude	0.4721	0.4718	0.4716	0.4716	0.4715	0.4715

Total Average of the Month = 0.4717

TABLE 27
Data Used for Month November

CARD 1

MODEL	:	2	:	Midlatitude Summer
ITYPE	:	2	:	Slant Path Between Two Altitudes
IEMSCT	:	0	:	Program Execution in Transmittance Mode
M1	:	2	:	Midlatitude Summer T and P Profile
M2	:	2	:	Midlatitude Summer Water Vapor Profile
M3	:	2	:	Midlatitude Summer Ozone Profile
IM	:	0	:	Normal Operation of Program
NOPRT	:	0	:	Normal Operation of Program
TBOUND	:	0	:	Normal Operation of Program
SALB	:	0	:	Normal Operation of Program

CARD 2

IHAZE	:	3	:	Navy Maritime Extinction
ISEASN	:	2	:	Fall - Winter
IVULCN	:	0	:	No Stratospheric Background
ICSTL	:	5	:	Medium Continental Influence
ICIR	:	0	:	No Cirrus
IVSA	:	0	:	Not Used
VIS	:	10	:	Meteorological Range (Km)
WSS	:	2.09	:	Current Wind Speed (m/s)
WHH	:	2.09	:	24 hours Average Wind Speed (m/s)
RAINRT	:	0	:	Rain Rate (mm/h)

CARD 3

H1	:	From Section G of Chapetr II : Initial Altitude		
H2	:	Form Table 22 : Final Altitude		
ANGLE	:	--	:	Not Necessary to Define
RANGE	:	From Table 22 : Path Length		
BETA	:	--	:	Not Necessary to Define
RO	:	--	:	Not Necessary to Define
LEN	:	0	:	Normal Operation

CARD 4

V1	:	2255	:	Initial Frequency
V2	:	2000	:	Final Frequency
DV	:	10	:	Frequency Increment

TABLE 28
Average Transmittances for Month November

FINAL ALTITUDE INITIAL. ALTITUDE	0.050 (Km)	0.060 (Km)	0.070 (Km)	0.080 (Km)	0.090 (Km)	0.100 (Km)
0.004 (Km)	0.4705	0.4702	0.4699	0.4699	0.4698	0.4698
0.007 (Km)	0.4706	0.4703	0.4700	0.4700	0.4699	0.4699
0.012 (Km)	0.4708	0.4705	0.4702	0.4702	0.4701	0.4701
0.016 (Km)	0.4709	0.4706	0.4703	0.4703	0.4702	0.4702
0.018 (Km)	0.4710	0.4707	0.4704	0.4704	0.4703	0.4703
0.021 (Km)	0.4711	0.4708	0.4705	0.4705	0.4704	0.4704
0.022 (Km)	0.4711	0.4708	0.4705	0.4705	0.4704	0.4704
Average per Altitude	0.4709	0.4706	0.4703	0.4703	0.4702	0.4702

Total Average of the Month = 0.4704

TABLE 29
Data Used for Month December

CARD 1

MODEL	:	2	:	Midlatitude Summer
ITYPE	:	2	:	Slant Path Between Two Altitudes
IEMSCT	:	0	:	Program Execution in Transmittance Mode
M1	:	2	:	Midlatitude Summer T and P Profile
M2	:	2	:	Midlatitude Summer Water Vapor Profile
M3	:	2	:	Midlatitude Summer Ozone Profile
IM	:	0	:	Normal Operation of Program
NOPT	:	0	:	Normal Operation of Program
TBOUND	:	0	:	Normal Operation of Program
SALB	:	0	:	Normal Operation of Program

CARD 2

IHAZE	:	3	:	Navy Maritime Extinction
ISEASN	:	2	:	Fall - Winter
IVULCN	:	0	:	No Stratospheric Background
ICSTL	:	5	:	Medium Continental Influence
ICIR	:	0	:	No Cirrus
IVSA	:	0	:	Not Used
VIS	:	10	:	Meteorological Range
WSS	:	2.05	:	Current Wind Speed
WHH	:	2.05	:	24 hours Average Wind Speed (m/s)
RAINRT	:	0	:	Rain Rate (mm/h)

CARD 3

H1	:	From Section G of Chapter II : Initial Altitude		
H2	:	From Table 22 : Final Altitude		
ANGLE	:	--	:	Not Necessary to Define
RANGE	:	From Table 22 : Path Length		
BETA	:	--	:	Not Necessary to Define
RO	:	--	:	Not Necessary to Define
LEN	:	0	:	Normal Operation

CARD 4

V1	:	2255	:	Initial Frequency
V2	:	2000	:	Final Frequency
DV	:	10	:	Frequency Increment

TABLE 30
Average Transmittances for Month December

FINAL ALTITUDE INITIAL ALTITUDE	0.050 (Km)	0.060 (Km)	0.070 (Km)	0.080 (Km)	0.090 (Km)	0.100 (Km)
0.004 (Km)	0.4705	0.4702	0.4699	0.4699	0.4698	0.4698
0.007 (Km)	0.4706	0.4703	0.4700	0.4700	0.4699	0.4699
0.012 (Km)	0.4708	0.4705	0.4702	0.4702	0.4701	0.4701
0.016 (Km)	0.4709	0.4706	0.4703	0.4703	0.4702	0.4702
0.018 (Km)	0.4710	0.4707	0.4704	0.4704	0.4703	0.4703
0.021 (Km)	0.4711	0.4708	0.4705	0.4705	0.4704	0.4704
0.022 (Km)	0.4711	0.4708	0.4705	0.4705	0.4704	0.4704
Average per Altitude	0.4709	0.4706	0.4703	0.4703	0.4702	0.4702

Total Average of the Month = 0.4704

TABLE 31
Data Used for Month January

CARD 1

MODEL	:	2	:	Midlatitude Summer
ITYPE	:	2	:	Slant Path Between Two Altitudes
IEMSCT	:	0	:	Program Execution in Transmittance Mode
M1	:	2	:	Midlatitude Summer T and P Profile
M2	:	2	:	Midlatitude Summer Water Vapor Profile
M3	:	2	:	Midlatitude Summer Ozone Profile
IM	:	0	:	Normal Operation of Program
NOPRT	:	0	:	Normal Operation of Program
TBOUND	:	0	:	Normal Operation of Program
SALB	:	0	:	Normal Operation of Program

CARD 2

IHAZE	:	3	:	Navy Maritime Extinction
ISEASN	:	2	:	Fall - Winter
IVULCN	:	0	:	No Stratospheric Background
ICSTL	:	5	:	Medium Continental Influence
ICIR	:	0	:	No Cirrus
IVSA	:	0	:	Not Used
VIS	:	15	:	Meteorological Range
WSS	:	2.06	:	Current Wind Speed
WHH	:	2.06	:	24 hours Average Wind Speed (m/s)
RAINRT	:	0	:	Rain Rate (mm/h)

CARD 3

H1	:	From Section G of Chapter II : Initial Altitude		
H2	:	From Table 22 : Final Altitude		
ANGLE	:	--	:	Not Necessary to Define
RANGE	:	From Table 22 : Path Length		
BETA	:	--	:	Not Necessary to Define
RO	:	--	:	Not Necessary to Define
LEN	:	0	:	Normal Operation

CARD 4

V1	:	2255	:	Initial Frequency
V2	:	2000	:	Final Frequency
DV	:	10	:	Frequency Increment

TABLE 32

Average Transmittances for Month January

FINAL ALTITUDE INITIAL ALTITUDE	0.050 (Km)	0.060 (Km)	0.070 (Km)	0.080 (Km)	0.090 (Km)	0.100 (Km)
0.004 (Km)	0.4705	0.4702	0.4699	0.4699	0.4698	0.4698
0.007 (Km)	0.4706	0.4703	0.4700	0.4700	0.4699	0.4699
0.012 (Km)	0.4708	0.4705	0.4702	0.4702	0.4701	0.4701
0.016 (Km)	0.4709	0.4706	0.4703	0.4703	0.4702	0.4702
0.018 (Km)	0.4710	0.4707	0.4704	0.4704	0.4703	0.4703
0.021 (Km)	0.4711	0.4708	0.4705	0.4705	0.4704	0.4704
0.022 (Km)	0.4711	0.4708	0.4705	0.4705	0.4704	0.4704
Average per Altitude	0.4709	0.4706	0.4703	0.4703	0.4702	0.4702

Total Average of the Month = 0.4704

TABLE 33
Data Used for Month February

CARD 1

MODEL	:	2	:	Midlatitiitude Summer
ITYPE	:	2	:	Slant Path Between Two Altitudes
IEMSCT	:	0	:	Program Execution in Transmittance Mode
M1	:	2	:	Midlatitude Summer T and P Profile
M2	:	2	:	Midlatitude Summer Water Vapor Profile
M3	:	2	:	Midlatitude Summer Ozone Profile
IM	:	0	:	Normal Operation of Program
NOPRT	:	0	:	Normal Operation of Program
TBOUND	:	0	:	Normal Operation of Program
SALB	:	0	:	Normal Operation of Program

CARD 2

IHAZE	:	3	:	Navy Maritime Extinction
ISEASN	:	2	:	Fall - Winter
IVULCN	:	0	:	No Stratospheric Background
ICSTL	:	5	:	Medium Continental Influence
ICIR	:	0	:	No Cirrus
IVSA	:	0	:	Not Used
VIS	:	15	:	Meteorological Range (Km)
WSS	:	2.22	:	Current Wind Speed (m/s)
WHH	:	2.22	:	24 hours Average Wind Speed (m/s)
RAINRT	:	0	:	Rain Rate (mm/h)

CARD 3

H1	:	From Section G of Chapter II : Initial Altitude		
H2	:	From Table 22 : Final Altitude		
ANGLE	:	--	:	Not Necessary to Define
RANGE	:	From Table 22 : Path Length		
BETA	:	--	:	Not Necessary to Define
RO	:	--	:	Not Necessary to Define
LEN	:	0	:	Normal Operation

CARD 4

V1	:	2255	:	Initial Frequency
V2	:	2000	:	Final Frequency
DV	:	10	:	Frequency Increment

TABLE 34

Average Transmittances for Month February

FINAL ALTITUDE INITIAL ALTITUDE	0.050 (Km)	0.060 (Km)	0.070 (Km)	0.080 (Km)	0.090 (Km)	0.100 (Km)
0.004 (Km)	0.4711	0.4708	0.4705	0.4704	0.4704	0.4704
0.007 (Km)	0.4712	0.4709	0.4706	0.4705	0.4705	0.4705
0.012 (Km)	0.4714	0.4711	0.4708	0.4707	0.4707	0.4707
0.016 (Km)	0.4715	0.4712	0.4709	0.4708	0.4708	0.4708
0.018 (Km)	0.4716	0.4713	0.4710	0.4709	0.4709	0.4709
0.021 (Km)	0.4717	0.4714	0.4712	0.4710	0.4710	0.4710
0.022 (Km)	0.4717	0.4714	0.4711	0.4710	0.4710	0.4710
Average per Altitude	0.4715	0.4712	0.4709	0.4708	0.4708	0.4708

Total Average of the Month = 0.4710

TABLE 35

Data Used for Month March

CARD 1

MODEL	:	2	:	Midlatitude Summer
ITYPE	:	2	:	Slant Path Between Two Altitudes
IEMSCT	:	0	:	Program Execution in Transmittance Mode
M1	:	2	:	Midlatitude Summer T and P Profile
M2	:	2	:	Midlatitude Summer Water Vapor Profile
M3	:	2	:	Midlatitude Summer Ozone Profile
IM	:	0	:	Normal Operation of Program
NOPRT	:	0	:	Normal Operation of Program
TBOUND	:	0	:	Normal Operation of Program
SALB	:	0	:	Normal Operation of Program

CARD 2

IHAZE	:	3	:	Navy Maritime Extinction
ISEASN	:	2	:	Fall - Winter
IVULCN	:	0	:	No Stratospheric Background
ICSTL	:	5	:	Medium Continental Influence
ICIR	:	0	:	No Cirrus
IVSA	:	0	:	Not Used
VIS	:	15	:	Meteorological Range (Km)
WSS	:	2.13	:	Current Wind Speed (m/s)
WHH	:	2.13	:	24 hours Average Wind Speed (m/s)
RAINRT	:	0	:	Rain Rate (mm/h)

CARD 3

H1	:	From Section G of Chapter II : Initial Altitude		
H2	:	From Table 22 : Final Altitude		
ANGLE	:	--	:	Not Necessary to Define
RANGE	:	From Table 22 : Path Length		
BETA	:	--	:	Not Necessary to Define
RO	:	--	:	Not Necessary to Define
LEN	:	0	:	Normal Operation

CARD 4

V1	:	2255	:	Initial Frequency
V2	:	2000	:	Final Frequency
DV	:	10	:	Frequency Increment

TABLE 36
Average Transmittances for Month March

FINAL ALTITUDE / INITIAL ALTITUDE	0.050 (Km)	0.060 (Km)	0.070 (Km)	0.080 (Km)	0.090 (Km)	0.100 (Km)
0.004 (Km)	0.4718	0.4713	0.4712	0.4711	0.4711	0.4711
0.007 (Km)	0.4719	0.4714	0.4713	0.4712	0.4712	0.4712
0.012 (Km)	0.4720	0.4716	0.4715	0.4714	0.4714	0.4714
0.016 (Km)	0.4722	0.4717	0.4716	0.4715	0.4715	0.4715
0.018 (Km)	0.4722	0.4718	0.4717	0.4716	0.4716	0.4716
0.021 (Km)	0.4723	0.4719	0.4718	0.4717	0.4717	0.4717
0.022 (Km)	0.4723	0.4719	0.4718	0.4717	0.4717	0.4717
Average per Altitude	0.4721	0.4717	0.4716	0.4715	0.4715	0.4715

Total Average of the Month = 0.4713

TABLE 37

Data Used for Month April

CARD 1

MODEL	:	2	:	Midlatitude Summer
ITYPE	:	2	:	Slant Path Between Two Altitudes
IEMSCT	:	0	:	Program Execution in Transmittance Mode
M1	:	2	:	Midlatitude Summer T and P Profile
M2	:	2	:	Midlatitude Summer Water Vapor Profile
M3	:	2	:	Midlatitude Summer Ozone Profile
IM	:	0	:	Normal Operation of Program
NOPRT	:	0	:	Normal Operation of Program
TBOUND	:	0	:	Normal Operation of Program
SALB	:	0	:	Normal Operation of Program

CARD 2

IHAZE	:	3	:	Navy Maritime Extinction
ISEASN	:	2	:	Fall - Winter
IVULCN	:	0	:	No Stratospheric Background
ICSTL	:	5	:	Medium Continental Influence
ICIR	:	0	:	No Cirrus
IVSA	:	0	:	Not Used
VIS	:	15	:	Meteorological Range (Km)
WSS	:	2.12	:	Current Wind Speed (m/s)
WHH	:	2.12	:	24 hours Average Wind Speed (m/s)
RAINRT	:	0	:	Rain Rate (mm/h)

CARD 3

H1	:	From Section G of Chapter II	:	Initial Altitude
H2	:	From Table 22	:	Final Altitude
ANGLE	:	--	:	Not Necessary to Define
RANGE	:	From Table 22	:	Path Length
BETA	:	--	:	Not Necessary to Define
RO	:	--	:	Not Necessary to Define
LEN	:	0	:	Normal Operation

CARD 4

V1	:	2255	:	Initial Frequency
V2	:	2000	:	Final Frequency
DV	:	10	:	Frequency Increment

TABLE 38
Average Transmittances for Month April

FINAL ALTITUDE INITIAL ALTITUDE	0.050 (Km)	0.060 (Km)	0.070 (Km)	0.080 (Km)	0.090 (Km)	0.100 (Km)
0.004 (Km)	0.4718	0.4713	0.4712	0.4711	0.4711	0.4711
0.007 (Km)	0.4719	0.4714	0.4713	0.4712	0.4712	0.4712
0.012 (Km)	0.4720	0.4716	0.4715	0.4714	0.4714	0.4714
0.016 (Km)	0.4722	0.4717	0.4716	0.4715	0.4715	0.4715
0.018 (Km)	0.4722	0.4718	0.4717	0.4716	0.4716	0.4716
0.021 (Km)	0.4723	0.4719	0.4718	0.4717	0.4717	0.4717
0.022 (Km)	0.4723	0.4719	0.4718	0.4717	0.4717	0.4717
Average per Altitude	0.4721	0.4717	0.4716	0.4715	0.4715	0.4715

Total Average of the Month = 0.4713

TABLE 39
Data Used for Month May

CARD 1

MODEL	:	1	:	Tropical Atmosphere
ITYPE	:	2	:	Slant Path Between Two Altitudes
IEMSC	:	0	:	Program Execution in Transmittance Mode
M1	:	1	:	Tropical Temperature and Pressure Profile
M2	:	1	:	Tropical Water Vapor Profile
M3	:	1	:	Tropical Ozone Profile
IM	:	0	:	Normal Operation of Program
NOPRT	:	0	:	Normal Operation of Program
TBOUND	:	0	:	Normal Operation of Program
SALB	:	0	:	Normal Operation of Program

CARD 2

IHAZE	:	3	:	Navy Maritime Extinction
ISEASN	:	1	:	Spring - Summer
IVULCN	:	0	:	No Stratospheric Background
ICSTL	:	5	:	Medium Continental Influence
ICIR	:	0	:	No Cirrus
IVSA	:	0	:	Not Used
VIS	:	15	:	Meteorological Range (Km)
WSS	:	2.02	:	Current Wind Speed (m/s)
WHH	:	2.02	:	24 hours Average Wind Speed (m/s)
RAINRT	:	0	:	Rain Rate (mm/h)

CARD 3

H1	:	From Section G of Chapter II : Initial Altitude		
H2	:	From Table 22 : Final Altitude		
ANGLE	:	--	:	Not Necessary to Define
RANGE	:	From Table 22 : Path Length		
BETA	:	--	:	Not Necessary to Define
RO	:	--	:	Not Necessary to Define
LEN	:	0	:	Normal Operation

CARD 4

V1	:	2255	:	Initial Frequency
V2	:	2000	:	Final Frequency
DV	:	10	:	Frequency Increment

TABLE 40
Average Transmittances for Month May

FINAL ALTITUDE INITIAL ALTITUDE	0.050 (Km)	0.060 (Km)	0.070 (Km)	0.080 (Km)	0.090 (Km)	0.100 (Km)
0.004 (Km)	0.4270	0.4267	0.4264	0.4262	0.4263	0.4263
0.007 (Km)	0.4271	0.4268	0.4265	0.4263	0.4264	0.4264
0.012 (Km)	0.4273	0.4270	0.4267	0.4265	0.4266	0.4266
0.016 (Km)	0.4274	0.4271	0.4268	0.4267	0.4268	0.4268
0.018 (Km)	0.4275	0.4272	0.4269	0.4268	0.4269	0.4269
0.021 (Km)	0.4276	0.4273	0.4270	0.4269	0.4270	0.4270
0.022 (Km)	0.4276	0.4273	0.4270	0.4269	0.4270	0.4270
Average per Altitude	0.4273	0.4271	0.4268	0.4266	0.4267	0.4267

Total Average of the Month = 0.4269

TABLE 41
Data Used for Month June

CARD 1

MODEL	:	1	:	Tropical Atmosphere
ITYPE	:	2	:	Slant Path Between Two Altitudes
IEMSCT	:	0	:	Program Execution in Transmittance Mode
M1	:	1	:	Tropical Temperature and Pressure Profile
M2	:	1	:	Tropical Water Vapor Profile
M3	:	1	:	Tropical Ozone Profile
IM	:	0	:	Normal Operation of Program
NOPRT	:	0	:	Normal Operation of Program
TBOUND	:	0	:	Normal Operation of Program
SALB	:	0	:	Normal Operation of Program

CARD 2

IHAZE	:	3	:	Navy Maritime Extinction
ISEASN	:	1	:	Spring - Summer
IVULCN	:	0	:	No Stratospheric Background
ICSTL	:	5	:	Medium Continental Influence
ICIR	:	0	:	No Cirrus
IVSA	:	0	:	Not Used
VIS	:	12	:	Meteorological Range (Km)
WSS	:	2.15	:	Current Wind Speed (m/s)
WHH	:	2.15	:	24 hours Average Wind Speed (m/s)
RAINRT	:	0	:	Rain Rate (mm/h)

CARD 3

H1	:	From Section G of Chapter II : Initial Altitude		
H2	:	From Table 22 : Final Altitude		
ANGLE	:	--	:	Not Necessary to Define
RANGE	:	From Table 22 : Path Length		
BETA	:	--	:	Not Necessary to Define
RO	:	--	:	Not Necessary to Define
LEN	:	0	:	Normal Operation

CARD 4

V1	:	2255	:	Initial Frequency
V2	:	2000	:	Final Frequency
DV	:	10	:	Frequency Increment

TABLE 42
Average Transmittances for Month June

FINAL ALTITUDE INITIAL ALTITUDE	0.050 (Km)	0.060 (Km)	0.070 (Km)	0.080 (Km)	0.090 (Km)	0.100 (Km)
0.004 (Km)	0.4264	0.4261	0.4258	0.4257	0.4257	0.4257
0.007 (Km)	0.4265	0.4262	0.4259	0.4258	0.4258	0.4258
0.012 (Km)	0.4267	0.4264	0.4261	0.4260	0.4260	0.4260
0.016 (Km)	0.4268	0.4265	0.4262	0.4262	0.4262	0.4262
0.018 (Km)	0.4269	0.4266	0.4263	0.4262	0.4262	0.4262
0.021 (Km)	0.4270	0.4267	0.4264	0.4263	0.4263	0.4263
0.022 (Km)	0.4270	0.4267	0.4264	0.4263	0.4263	0.4263
Average per Altitude	0.4267	0.4264	0.4261	0.4260	0.4260	0.4260

Total Average of the Month = 0.4262

TABLE 43
Data Used for Month July

CARD 1

MODEL	:	1	:	Tropical Atmosphere
ITYPE	:	2	:	Slant Path Between Two Altitudes
IEMSCT	:	0	:	Program Execution in Transmittance Mode
M1	:	1	:	Tropical Temperature and Pressure Profile
M2	:	1	:	Tropical Water Vapor Profile
M3	:	1	:	Tropical Ozone Profile
IM	:	0	:	Normal Operation of Program
NOPRT	:	0	:	Normal Operation of Program
TBOUND	:	0	:	Normal Operation of Program
SALB	:	0	:	Normal Operation of Program

CARD 2

IHAZE	:	3	:	Navy Maritime Extinction
ISEASN	:	1	:	Spring - Summer
IVULCN	:	0	:	No Stratospheric Background
ICSTL	:	5	:	Medium Continental Influence
ICIR	:	0	:	No Cirrus
IVSA	:	0	:	Not Used
VIS	:	12	:	Meteorological Range (Km)
WSS	:	2.15	:	Current Wind Speed (m/s)
WHH	:	2.15	:	24 hours Average Wind Speed (m/s)
RAINRT	:	0	:	Rain Rate (mm/h)

CARD 3

H1	:	From Section G of Chapter II : Initial Altitude		
H2	:	From Table 22 : Final Altitude		
ANGLE	:	--	:	Not Necessary to Define
RANGE	:	From Table 22 : Path Length		
BETA	:	--	:	Not Necessary to Define
RO	:	--	:	Not Necessary to Define
LEN	:	0	:	Normal Operation

CARD 4

V1	:	2255	:	Initial Frequency
V2	:	2000	:	Final Frequency
DV	:	10	:	Frequency Increment

TABLE 44
Average Transmittances for Month July

FINAL ALTITUDE INITIAL ALTITUDE	0.050 (Km)	0.060 (Km)	0.070 (Km)	0.080 (Km)	0.090 (Km)	0.100 (Km)
0.004 (Km)	0.4264	0.4261	0.4258	0.4257	0.4257	0.4257
0.007 (Km)	0.4265	0.4262	0.4259	0.4258	0.4258	0.4258
0.012 (Km)	0.4267	0.4264	0.4261	0.4260	0.4260	0.4260
0.016 (Km)	0.4268	0.4265	0.4262	0.4262	0.4262	0.4262
0.018 (Km)	0.4269	0.4266	0.4263	0.4262	0.4262	0.4262
0.021 (Km)	0.4270	0.4267	0.4264	0.4263	0.4263	0.4263
0.022 (Km)	0.4270	0.4267	0.4264	0.4263	0.4263	0.4263
Average per Altitude	0.4267	0.4264	0.4261	0.4260	0.4260	0.4260

Total Average of the Month = 0.4262

TABLE 45

Data Used for Month August

CARD 1

MODEL	:	1	:	Tropical Atmosphere
ITYPE	:	2	:	Slant Path Between Two Altitudes
IEMSCT	:	0	:	Program Execution in Transmittance Mode
M1	:	1	:	Tropical Temperature and Pressure Profile
M2	:	1	:	Tropical Water Vapor Profile
M3	:	1	:	Tropical Ozone Profile
IM	:	0	:	Normal Operation of Program
NOPRT	:	0	:	Normal Operation of Program
TBOUND	:	0	:	Normal Operation of Program
SALB	:	0	:	Normal Operation of Program

CARD 2

IHAZE	:	3	:	Navy Maritime Extinction
ISEASN	:	1	:	Spring - Summer
IVULCN	:	0	:	No Stratospheric Background
ICSTL	:	5	:	Medium Continental Influence
ICIR	:	0	:	No Cirrus
IVSA	:	0	:	Not Used
VIS	:	10	:	Meteorological Range (Km)
WSS	:	2.20	:	Current Wind Speed (m/s)
WHH	:	2.20	:	24 hours Average Wind Speed (m/s)
RAINRT	:	0	:	Rain Rate (mm/h)

CARD 3

H1	:	From Section G of Chapter II : Initial Altitude		
H2	:	From Table 22 : Final Altitude		
ANGLE	:	--	:	Not Necessary to Define
RANGE	:	From Table 22 : Path Length		
BETA	:	--	:	Not Necessary to Define
RO	:	--	:	Not Necessary to Define
LEN	:	0	:	Normal Operation

CARD 4

V1	:	2255	:	Initial Frequency
V2	:	2000	:	Final Frequency
DV	:	10	:	Frequency Increment

TABLE 46
Average Transmittances for Month August

FINAL ALTITUDE INITIAL ALTITUDE	0.050 (Km)	0.060 (Km)	0.070 (Km)	0.080 (Km)	0.090 (Km)	0.100 (Km)
0.004 (Km)	0.4258	0.4255	0.4252	0.4251	0.4251	0.4251
0.007 (Km)	0.4259	0.4256	0.4253	0.4252	0.4252	0.4252
0.012 (Km)	0.4261	0.4258	0.4255	0.4253	0.4253	0.4253
0.016 (Km)	0.4262	0.4259	0.4256	0.4255	0.4255	0.4255
0.018 (Km)	0.4263	0.4260	0.4257	0.4256	0.4256	0.4256
0.021 (Km)	0.4264	0.4261	0.4258	0.4257	0.4257	0.4257
0.022 (Km)	0.4264	0.4261	0.4258	0.4257	0.4257	0.4257
Average per Altitude	0.4261	0.4258	0.4255	0.4254	0.4254	0.4254

Total Average of the Month = 0.4256

TABLE 47
Data Used for Month September

CARD 1

MODEL	:	1	:	Tropical Atmosphere
ITYPE	:	2	:	Slant Path Between Two Altitudes
IEMSCT	:	0	:	Program Execution in Transmittance Mode
M1	:	1	:	Tropical Temperature and Pressure Profile
M2	:	1	:	Tropical Water Vapor Profile
M3	:	1	:	Tropical Ozone Profile
IM	:	0	:	Normal Operation of Program
NOPRT	:	0	:	Normal Operation of Program
TBOUND	:	0	:	Normal Operation of Program
SALB	:	0	:	Normal Operation of Program

CARD 2

IHAZE	:	3	:	Navy Maritime Extinction
ISEASN	:	1	:	Spring - Summer
IVULCN	:	0	:	No Stratospheric Background
ICSTL	:	5	:	Medium Continental Influence
ICIR	:	0	:	No Cirrus
IVSA	:	0	:	Not Used
VIS	:	8	:	Meteorological Range (Km)
WSS	:	2.17	:	Current Wind Speed (m/s)
WHH	:	2.17	:	24 hours Average Wind Speed (m/s)
RAINRT	:	0	:	Rain Rate (mm/h)

CARD 3

H1	:	From Section G of Chapter II : Initial Altitude		
H2	:	From Table 22 : Final Altitude		
ANGLE	:	--	:	Not Necessary to Define
RANGE	:	From Table 22 : Path Length		
BETA	:	--	:	Not Necessary to Define
RO	:	--	:	Not Necessary to Define
LEN	:	0	:	Normal Operation

CARD 4

V1	:	2255	:	Initial Frequency
V2	:	2000	:	Final Frequency
DV	:	10	:	Frequency Increment

TABLE 48
Average Transmittances for Month September

FINAL ALTITUDE INITIAL ALTITUDE	0.050 (Km)	0.060 (Km)	0.070 (Km)	0.080 (Km)	0.090 (Km)	0.100 (Km)
0.004 (Km)	0.4249	0.4246	0.4243	0.4242	0.4242	0.4242
0.007 (Km)	0.4250	0.4247	0.4244	0.4243	0.4243	0.4243
0.012 (Km)	0.4252	0.4249	0.4246	0.4245	0.4245	0.4245
0.016 (Km)	0.4253	0.4250	0.4247	0.4246	0.4246	0.4246
0.018 (Km)	0.4254	0.4251	0.4248	0.4247	0.4247	0.4247
0.021 (Km)	0.4255	0.4252	0.4249	0.4248	0.4248	0.4248
0.022 (Km)	0.4255	0.4252	0.4249	0.4248	0.4248	0.4248
Average per Altitude	0.4252	0.4249	0.4246	0.4245	0.4245	0.4245

Total Average of the Month = 0.4247

APPENDIX D
PLOTS OF S/N RATIO

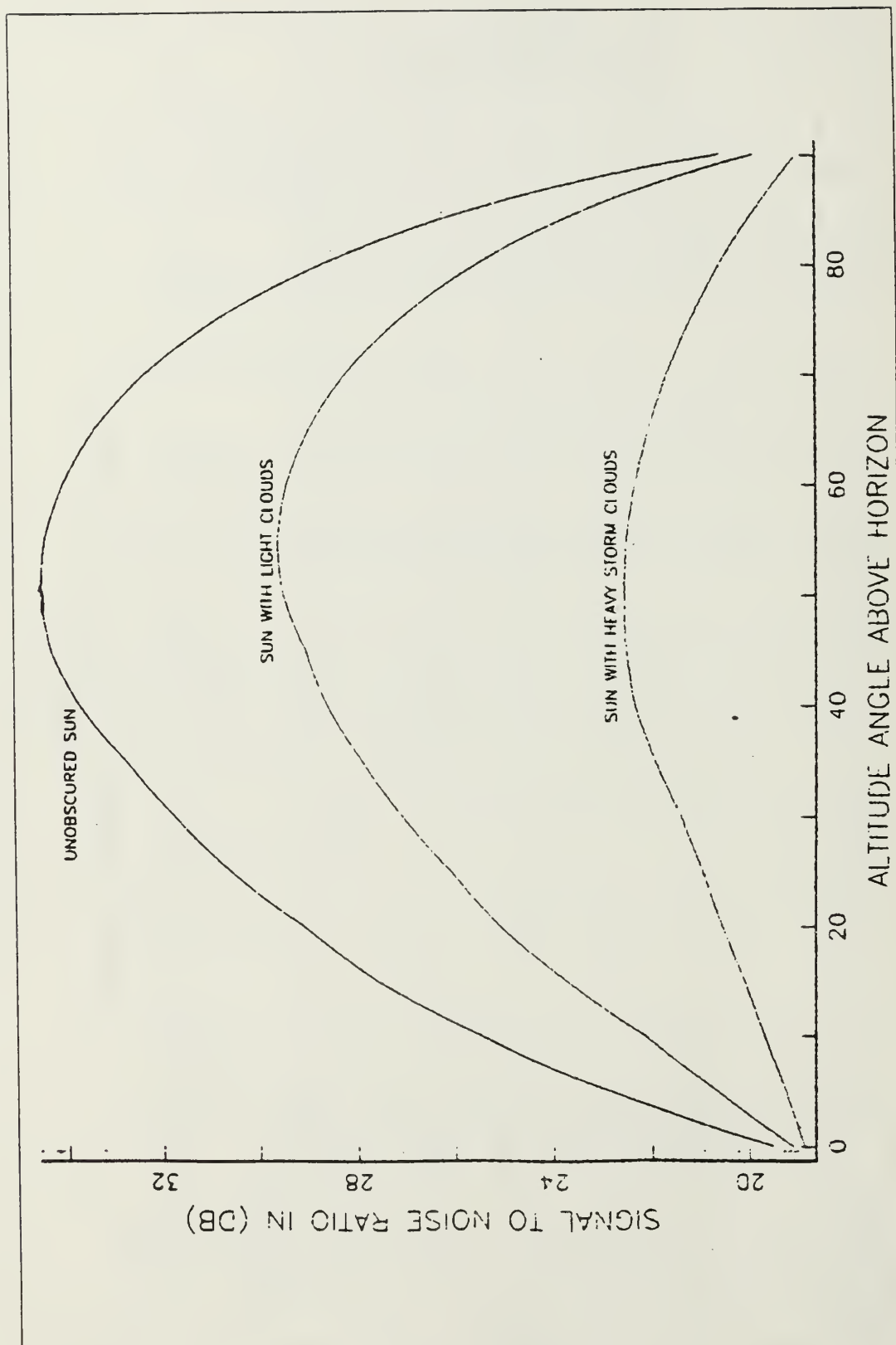


Figure D.1 S/N Ratio for Midlatitude Summer, $\xi_0=0.80$ and Flight Altitude 50m

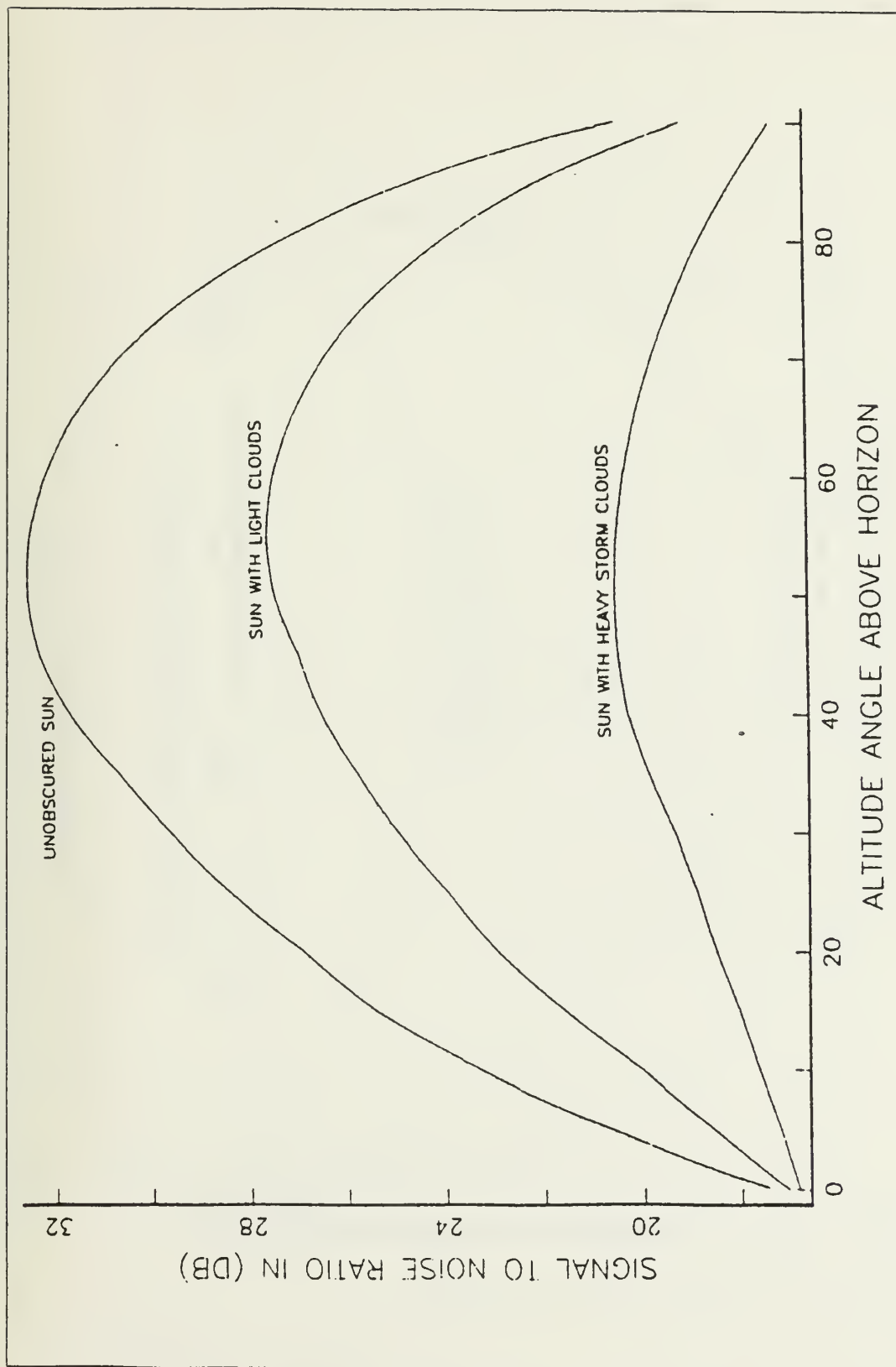


Figure D.2 S/N Ratio for Midlatitude Summer, $\xi_o=0.80$
and Flight Altitude 100m

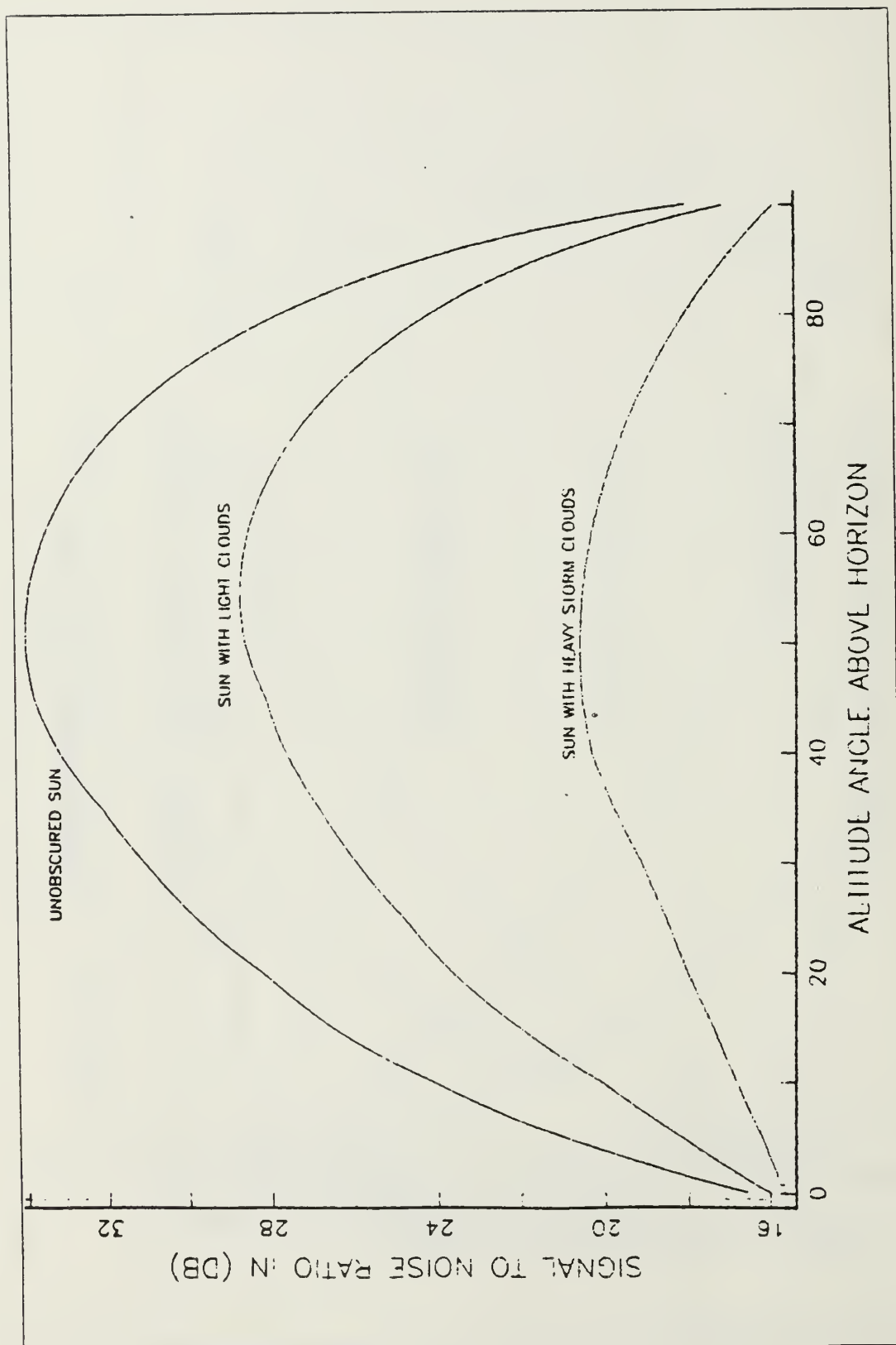


Figure D.3 S/N Ratio for Midlatitude Summer, $\epsilon_s=0.55$ and Flight Altitude 50m

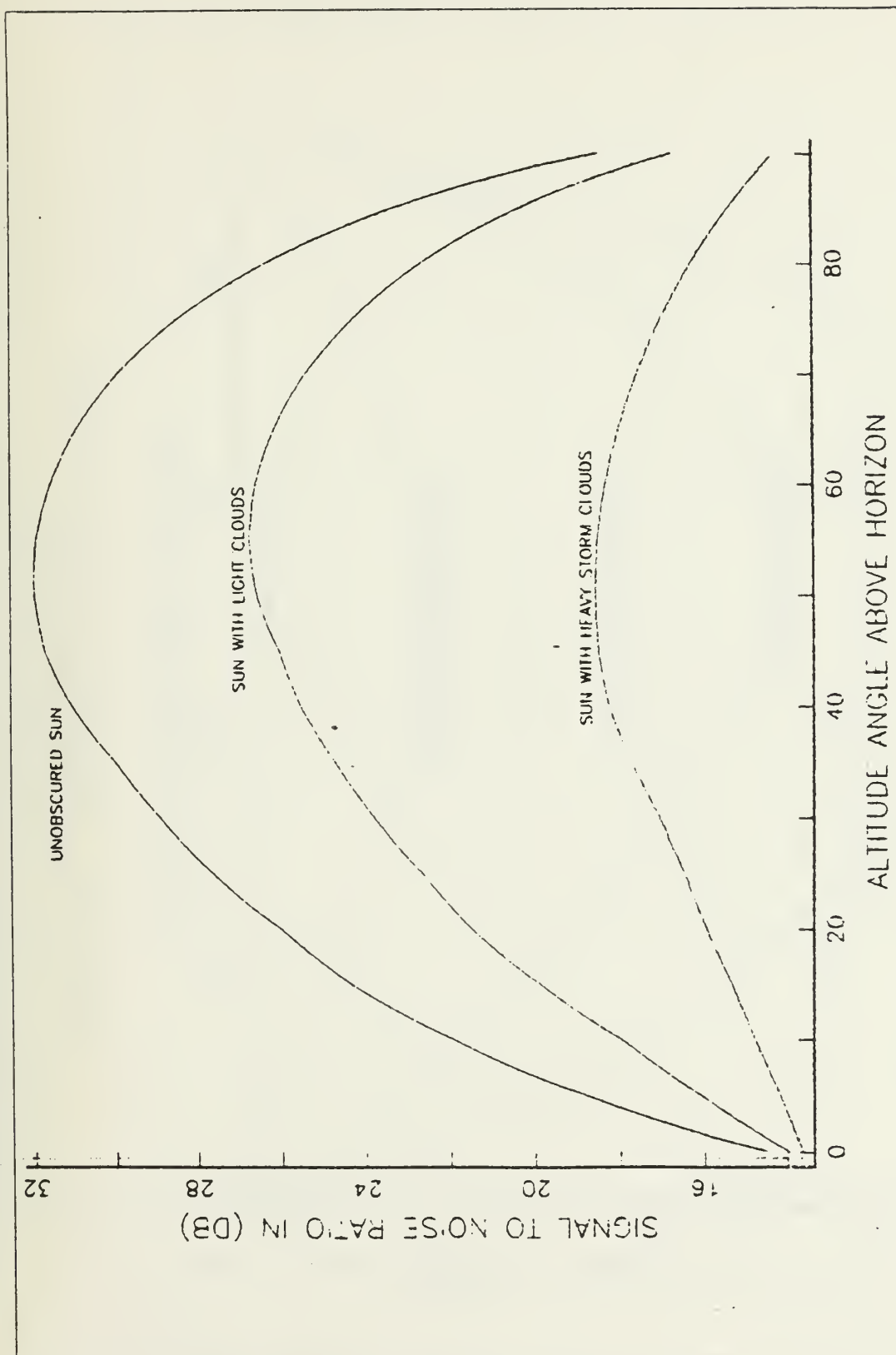


Figure D.4 S/N Ratio for Midlatitude Summer, ≈ 0.55
and Flight Altitude 100m

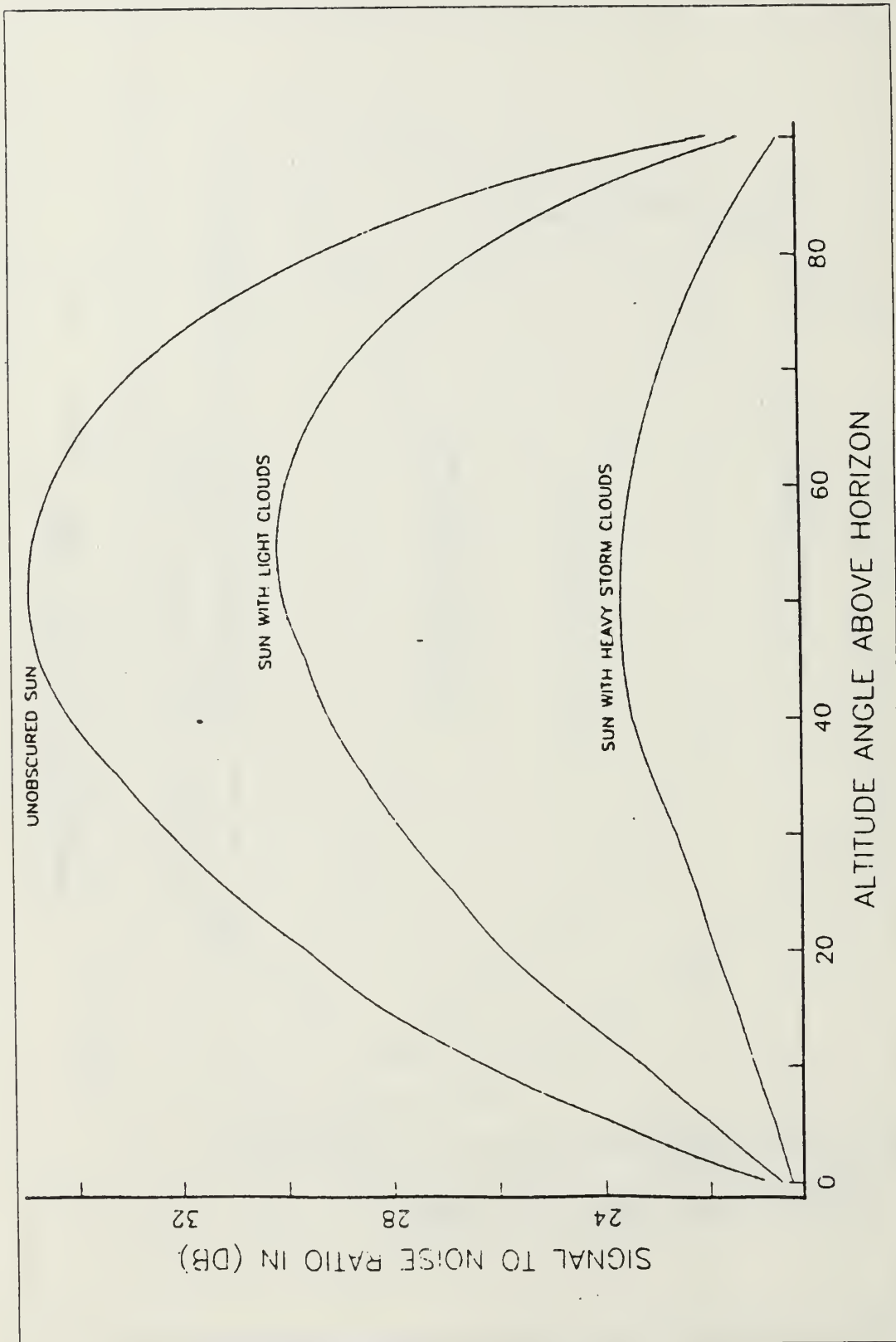


Figure D.5 S/N Ratio for Tropical, $\epsilon_s=0.80$ and Flight Altitude 50m

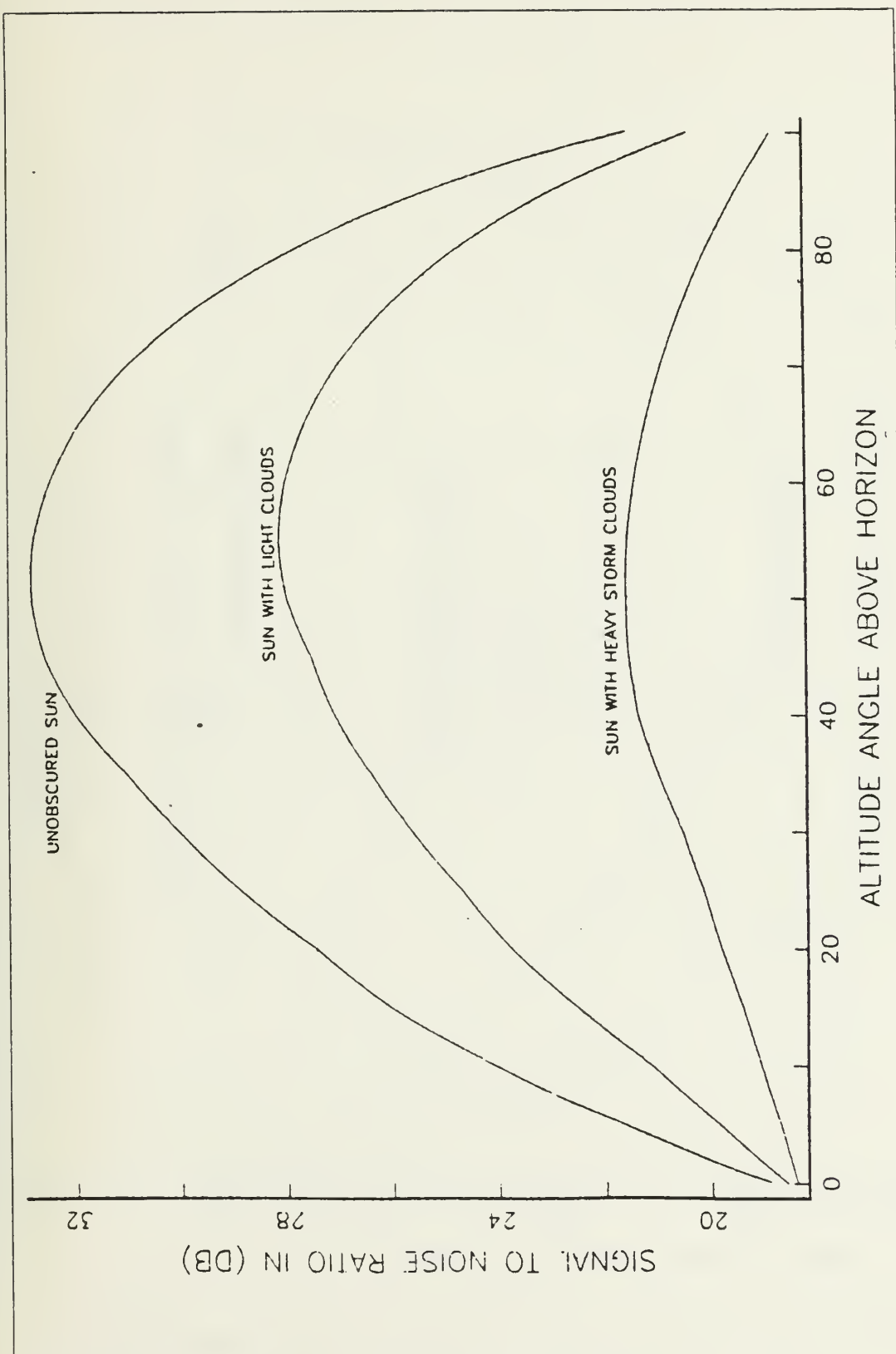


Figure D.6 S/N Ratio for Tropical, $\epsilon_0=0.80$ and Flight Altitude 100m

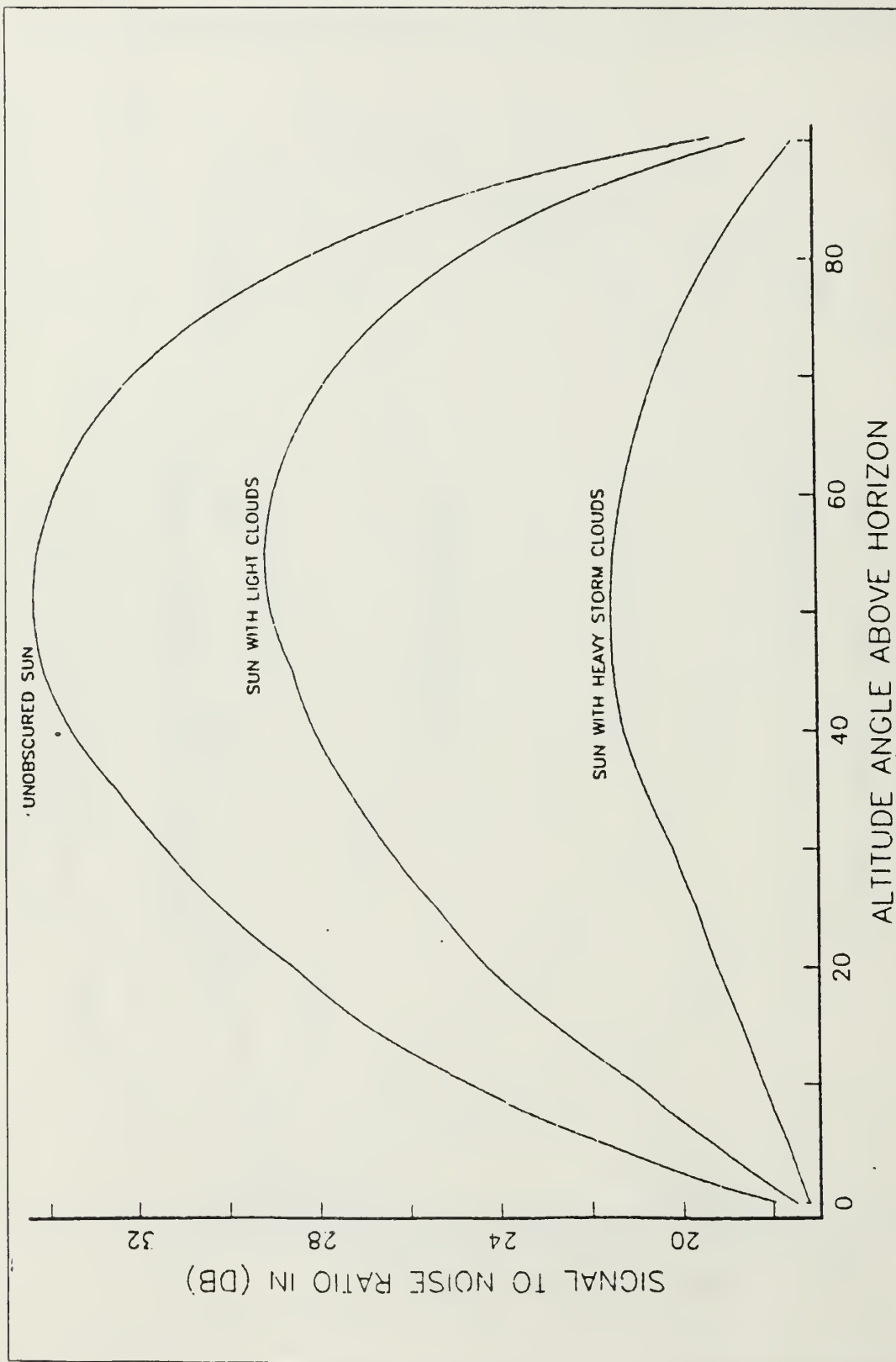


Figure D.7 S/N Ratio for Tropical, $\epsilon_0=0.55$ and Flight Altitude 50m

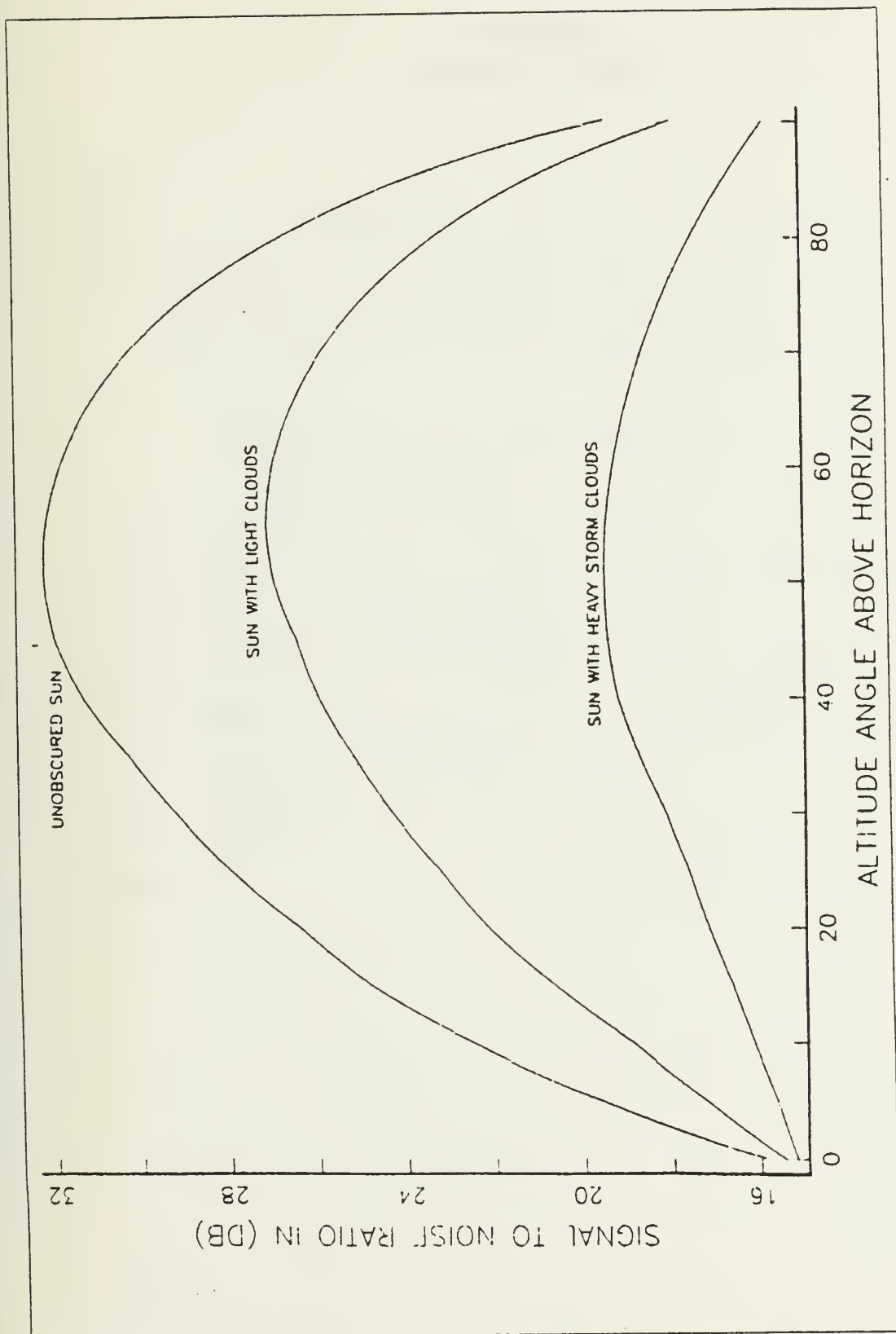


Figure D.8 S/N Ratio for Tropical, $\alpha = 0.55$
and Flight Altitude 100m

APPENDIX E
COMPUTER PROGRAMS

\$JOB

PROGRAM SHIP1

CALCULATION OF SIDE OF INSTANTANEOUS FIELD OF VIEW

DIMENSION H(6), PHI(7), DELTA(21), SIDE(6,7,21), PATH(6,7,21)

DATA (H(I), I=1,6)/50.,60.,70.,80.,90.,100./

DATA (PHI(K), K=1,7)/2.0,2.5,3.0,3.5,4.0,4.5,5.0/

DATA (DELTA(L), L=1,21)/.2,.22,.24,.26,.28,.3,.32,.34,.36,.38,
1 .4,.42,.44,.46,.48,.5,.52,.54,.56,.58,.6/

DO 50 I=1,6

DO 45 K=1,7

DO 40 L=1,21

TH=(90.-PHI(K)-DELTA(L))*3.141592/180.

B=I(I)*TAN(TH)

C=(H(I)*H(I)+B*B)**.5

D=DELTA(L)*3.141592/180.

SIDE(I,K,L)=2.*C*SIN(D)

PATH(I,K,L)=SIDE(I,K,L)/(2.*TAN(D))

40 CONTINUE

45 CONTINUE

WRITE(6,39) H(I)

39 15X, 'FOR FLIGHT HEIGHT=', F4.0, 1X, 'METERS'//

WRITE(6,38) (PHI(K), K=1,7)

38 FORMAT(2X, 'DELTA', 3X, 7('PHI=', F4.2, 2X)/)

DO 35 L=1,21

WRITE(6,34) DELTA(L), (SIDE(I,K,L), K=1,7)

34 FORMAT(10, 2X, F4.2, 1X, 7F10.2)

35 CONTINUE

WRITE(6,49) H(I)

49 1 'PATH IN METERS'//5X, 'FOR FLIGHT HEIGHT=', F4.0,

1X, 'METERS'//)

WRITE(6,48) (PHI(K), K=1,7)

48 FORMAT(2X, 'DELTA', 3X, 7('PHI=', F4.2, 2X)/)

DO 47 L=1,21

WRITE(6,46) DELTA(L), (PATH(I,K,L), K=1,7)

46 FORMAT(10, 2X, F4.2, 1X, 7F10.2)

47 CONTINUE

50 CONTINUE

STOP

END

\$ENTRY

5JOB

PROGRAM SHIP THERMAL SIGNATURE

DIMENSION T(2,2,3,91), TIN(2), TS(3,91), ESN(2,3,91), D(91)
 DIMENSION HDL(2,2,3,91), HDLR(2,3,91), HDLT(2,2,3,91)
 DIMENSION RI1(3,91), RI2(3,91), RI3(3,91), RI4(3,91)
 DIMENSION RIS(3,91), RIR(3,91)
 DIMENSION VS(3,91), SNR(3,91)

DATA (TIN(J), J=1,2)/293.15,303.15/
 DATA ESN,PI/.44,3.141592/
 DATA TO,TRANS/294.2,J.4711/
 DATA TO,TRANS/299.7,J.4259/
 DATA EO,AO/0.30,0.30/
 DATA EO,AO/0.35,0.35/
 DATA HEIGHT,SIDE,PATH/5000.0,2136.0,111934.0/
 DATA HEIGHT,SIDE,PATH/6000.0,2197.0,112389.0/
 DATA HEIGHT,SIDE,PATH/7000.0,2204.0,112725.0/
 DATA HEIGHT,SIDE,PATH/8000.0,2209.0,112984.0/
 DATA HEIGHT,SIDE,PATH/9000.0,2213.0,113196.0/
 DATA HEIGHT,SIDE,PATH/10000.0,2216.0,113372.0/
 DATA PATHS,AREAS/183698.,1149000./
 DATA PATHS,AREAS/164807.,1316800./
 DATA PATHS,AREAS/154747.,1277600./
 DATA PATHS,AREAS/148194.,1223000./
 DATA PATHS,AREAS/143350.,1144200./
 DATA PATHS,AREAS/139507.,1116000./
 DATA HCONV/56.750/
 DATA APERT,TROPI,RESPON/113.1,31.2E+04/
 DATA FOCL,XTOT,EN,TIMEF,DETECI/4.24,50000.,1.,.01,9E+10/
 DATA C1,C2,SE/3.7415E-12,1.4386,5.67E-08/
 DATA (C(L), L=1,91,5)/0.,5.,10.,15.,20.,25.,30.,35.,40.,45.,50.,
 55.,60.,65.,70.,75.,80.,85.,90.,95.
 DATA (ES(1,L), L=1,91,5)/6.7,48.5,95.5,147.8,195.7,256.7,319.9,
 391.3,473.9,564.0,636.7,703.1,760.7,813.6,854.0,899.9,933.1,
 993.1,990.0/
 DATA (ES(2,L), L=1,91,5)/2.7,19.7,39.1,64.4,91.7,117.4,143.5,
 181.7,219.1,254.8,300.3,342.2,379.3,413.0,444.1,469.6,493.4,
 511.2,532.2/
 DATA (ES(3,L), L=1,91,5)/0.5,4.3,9.0,13.7,19.6,25.4,32.3,43.0,
 53.2,61.0,67.7,74.3,79.9,85.1,89.8,94.5,98.3,102.1,105.7/
 1 53.2,61.0,67.7,74.3,79.9,85.1,89.8,94.5,98.3,102.1,105.7/

THE BELOW DATA ARE IN CM OR CM2

DATA #1,H1,H2,H3/1620.,720.,210.,900./
 DATA W4,H4,H5,H6/17/900.,360.,180.,180.,1260./
 DATA A4,RI6N/3.073E+05,35.475/
 DATA HEIGHT,SIDE,PATH/6000.0,2197.,112389./
 DATA PATHS,AREAS/164807.,1316800./
 DATA EO,TA/0.90,292.15/
 DATA TRANS/J.4259/
 DATA (WL(N), N=1,40)/5.000,4.983,4.975,4.963,4.950,4.938,4.926,
 14.914,4.902,4.890,4.878,4.866,4.854,4.843,4.831,4.819,4.808,4.796,
 14.785,4.773,4.762,4.751,4.739,4.728,4.717,4.706,4.695,4.684,4.673,
 14.662,4.651,4.640,4.630,4.619,4.608,4.598,4.587,4.577,4.566,4.556/
 DATA (WL(N), N=41,52)/4.545,4.535,4.525,4.515,4.505,4.494,4.484,
 14.474,4.464,4.454,4.444,4.433/
 DATA (TRL(N), N=1,33)/0.1577,0.1800,0.2165,0.2070,0.2070,0.2448,
 10.2917,0.3334,0.3619,0.3797,0.3869,0.3902,0.3952,0.3974,0.4242,
 10.4747,0.5732,0.6250,0.6427,0.6438,0.6224,0.6343,0.6625,0.6931,
 10.6886,0.6017,0.6565,0.6467,0.6365,0.6502,0.6643,0.6868,0.7053/
 DATA (TRL(N), N=34,52)/0.7339,0.7263,0.7131,0.6899,0.6277,0.5907,
 10.5342,0.4940,0.4653,0.4255,0.4174,0.3906,0.3589,0.3221,0.2620,
 10.2099,0.1466,0.1148,0.0938/
 DATA (TSL(N), N=1,33)/0.0990,0.1222,0.1457,0.1406,0.1421,0.1727,
 10.2165,0.2550,0.2810,0.3104,0.3034,0.3143,0.3126,0.3035,0.3511,
 10.3995,0.5017,0.5528,0.5733,0.5748,0.5527,0.5657,0.6217,
 10.6057,0.5974,0.5923,0.5835,0.5747,0.5384,0.6030,0.6293,0.6542,
 DATA (TSL(N), N=34,52)/0.6896,0.6857,0.6755,0.6362,0.5974,0.5641,
 10.5111,0.4735,0.4450,0.4075,0.4000,0.3760,0.3469,0.3123,0.2555,

```

C      10.2046,0.1438,0.1127,0.0024/
C      DC 3 K=1,3
C      DC 2 I=1,18
C      NN=5*I+1
C      N=5*(I-1)+1
C      DO 1 L=1,NN
C      ES(K,L)=ES(K,NN)-(ES(K,NN)-ES(K,N))*FLOAT(NN-L)/5.
C      D(L)=D(HH)-(D(HH)-D(N))*FLOAT(NN-L)/5.
1      CONTINUE
2      CONTINUE
3      CONTINUE

C      CALCULATION OF NORMAL COMPONENTS OF ES
C      DO 6 I=1,2
C      DC 5 K=1,3
C      DC 4 L=1,91
C      TH=D(L)*PI/180.
C      IF(L.EQ.1) A=3*IN(TH)
C      IF(L.EQ.2) A=CON(TH)
C      ESN(I,K,L)=ES(K,L)*A
C      HDLR(I,K,L)=(9.04E-07)*ESN(I,K,L)
4      CONTINUE
5      CONTINUE
6      CONTINUE

C      WRITE(6,7)
C      FORMAT(11,'SX,'SOLAR CONSTANT ES IN W/M2'///)
C      WRITE(6,9)
C      FORMAT(1X,'ALTA. ANGLE',3X,'UNCLOUDED SUN',2X,'SUN WITH LIGHT CLOUDS',
C      1DS',2X,'SUN WITH HEAVY STORM CLOUDS'/)
C      DO 10 L=1,91
C      WRITE(6,9) D(L), (ES(K,L),K=1,3)
C      FORMAT(1X,F6.0,3X,F10.2,3X,F10.2,14X,F10.2)
9      CONTINUE
10     CONTINUE
C      WRITE(6,11)
C      FORMAT(11,'NORMAL COMPONENT OF RADIANCE DUE TO REFLECTED SOLAR EN
C      1ERGY'//1X,'IN W/(C12*SQ) IN THE WINDOW OF 5 MICROMETER'///)
C      WRITE(6,12)
C      FORMAT(10,'SX,'UNCLOUDED SUN',3X,'SUN WITH LIGHT CLOUDS',2X,
C      1'SUN WITH HEAVY STORM CLOUDS'/)
11     CONTINUE
12     CONTINUE
C      WRITE(6,13)
C      FORMAT(1X,'ALTITUDE',1X,3('HORIZONTAL',2X,'VERTICAL',2X))
C      WRITE(6,14)
C      FORMAT(1X,'ANGLE',1X,3('FACE',8X,'FACE',6X)//)
13     CONTINUE
14     CONTINUE
C      DO 16 L=1,91
C      WRITE(6,15) D(L), (HDLR(I,1,L),I=1,2), (HDLR(I,2,L),I=1,2),
C      1(HDLR(I,3,L),I=1,2)
C      FORMAT(1X,F4.0,3X,3(E10.4,1X,E10.4,1X))
15     CONTINUE
16     CONTINUE
C      CALCULATION OF SHIP BODY TEMPERATURE
C      DO 20 I=1,2
C      DC 19 J=1,2
C      DO 18 K=1,3
C      DO 17 L=1,91
C      T04=TC**4.
C      TIN4=TIN(J)**4.
C      ESN(I,K,L)=(2./3.)*ESN(I,K,L)
C      A=ESN(I,K,L)*AC+EG*SB*TC+EIN*SB*TIN4
C      B=(20+EL4)*SB
C      XK=(A/B)**0.25
C      T4=XK**4.
C      F1=EO*SB*(T4-T04)+EIN*SB*(T4-TIN)+HCCNV*(XK-T0)-ESN(I,K,L)*AC
C      XA=XK+F1
C      X4=XA**4.
C      F2=EO*SB*(X4-T04)+EIN*SB*(X4-TIN)+HCCNV*(XA-T0)-ESN(I,K,L)*AC
C      XK1=XK-F1*(F2-F1)
C      DIF=ABS(XK1-XK)
C      XK=XK1
2000

```

```

      IF (DIF.GT.0.000001) GO TO 2000
      T(I,J,K,L)=XK
17      CONTINUE
18      CONTINUE
19      CONTINUE
20      CONTINUE

      DO 27 J=1,2
      WRITE(6,21) TIN(J)
21      FORMAT('1',3X,'SHIP BODY TEMPERATURE IN K FOR TIN=',F7.2,1X,
1      'K',//)
      WRITE(6,22)
22      FORMAT('0',9X,'UNOBSERVED SUN',3X,'SUN WITH LIGHT CLOUD',2X,
1      'SUN WITH HEAVY STORM CLOUDS'//)
      WRITE(6,23)
23      FORMAT('1X',2X,'ALTITUDE',1X,3('HORIZONTAL',2X,'VERTICAL',2X))
      WRITE(6,24)
24      FORMAT('1X',2X,'ANGLE',4X,3('FACE',3X,'FACE',3X)//)
      DO 26 L=1,31
      WRITE(6,25) J(L), (T(I,J,1,L), I=1,2), (T(I,J,2,L), I=1,2),
1      (T(I,J,3,L), I=1,2)
25      FORMAT('1X',F6.1,3(F10.2,1X,F10.2,1X))
26      CONTINUE
27      CONTINUE

      CALCULATION OF NORMAL COMPONENT OF SPECTRAL RADIANCE IN THE
      WINDOW OF 5 MICROMETER (I.E. 4.435-5.000)

      DO J2 I=1,2
      DO J1 J=1,2
      DO J0 K=1,3
      DO J3 L=1,31
      S1=0.0
      S2=0.0
      X1=C2/(T(I,J,K,L)*4.435E-04)
      X2=C2/(T(I,J,K,L)*5.000E-04)
      DO J4 J=1,3
      A1=FLOAT(J)*X1
      A2=FLOAT(J)*X2
      B=FLOAT(J)*4.
      S1=S1+EXP(-A1)*(A1**3.+3.*A1*A1+B.*A1+B.)/B
      S2=S2+EXP(-A2)*(A2**3.+3.*A2*A2+B.*A2+B.)/B
23      CONTINUE
      HDLT(I,J,K,L)=C1*EC*(T(I,J,K,L)**4.)*(S2-S1)/(PI*(C2**4.))
      HDL(I,J,K,L)=HDLT(I,J,K,L)+HDL(I,K,L)
29      CONTINUE
30      CONTINUE
31      CONTINUE
32      CONTINUE

      CALCULATION OF NORMAL COMPONENT OF SEA RADIANCE IN THE
      WINDOW OF 5 MICROMETER (I.E. 4.435-5.000)

      S1=0.0
      S2=0.0
      X1=C2/(TW*4.435E-04)
      X2=C2/(TW*5.000E-04)
      DO J5 M=1,8
      A1=FLOAT(M)*X1
      A2=FLOAT(M)*X2
      B=FLOAT(M)*4.
      S1=S1+EXP(-A1)*(A1**3.+3.*A1*A1+B.*A1+B.)/B
      S2=S2+EXP(-A2)*(A2**3.+3.*A2*A2+B.*A2+B.)/B
128      CONTINUE
      HDLW=C1*EW*(TW**4.)*(S2-S1)/(PI*(C2**4.))

      DO 40 J=1,2
      WRITE(6,33)
33      FORMAT('1',1X,'NORMAL COMPONENT OF RADIANCE IN W/(CM2*SB)'//1X,
1      'DUE TO THERMAL RADIATION'//)

```

```

C      WRITE(6,34) TIN(J)
C      FORMAT(2X,'THE WINDOW OF 5 MICROMETER FOR TIN=',F7.2,1X,'K'///)
C      WRITE(6,35)
C      FORMAT(10,'9X,'UNOBSCURED SUN',3X,'SUN WITH LIGHT CLCUD',2X,
C      1  'SUN WITH HEAVY STORM CLOUDS'//)
C      WRITE(6,36)
C      FORMAT(1X,'ALTITUDE',1X,3('HORIZONTAL',2X,'VERTICAL',2X))
C      WRITE(6,37)
C      FORMAT(1X,'ANGLE',4X,3('FACE',3X,'FACE',6X)///)
C      DO 39 L=1,91
C      1  WRITE(6,38) D(L),(HDL(I,J,1,L),I=1,2),(HDL(I,J,2,L),I=1,2),
C      38  FORMAT(1X,F6.1,2X,3(E10.4,1X,E10.4,1X))
C      39  CONTINUE
C      40  CONTINUE

C      WRITE(6,138) TW,HDLW
C      138  FORMAT(11',2X,'SEA RADIANCE FOR TW=',F6.2,2X,E15.4)

C      CALCULATION OF SHIP SURFACES AND THEIR CORRESPONDING MEAN ELEVATIONS
C      FROM THE SEA, INSIDE THE INSTANTANEOUS DETECTOR FIELD OF VIEW IN THE
C      REGION OF THE HIGHER RADIANT INTENSITY.

C      A1=W1*H1
C      A11=(SIDE-H1)*H1
C      HM1=H1/2.

C      A2=W1*H2
C      A22=(SIDE-W1)*H2
C      HM2=H1

C      A3=SIDE*H3
C      HM3=H1+H3/2.

C      HM4=H1+H3+H4/2.

C      A5=W5*H5
C      HM5=H1+H3+H4+H5/2.

C      HM6=H1+H3+H4+H5

C      A7=SIDE*H7-PI*W4*W4/4.
C      HM7=H1+H3

C      CALCULATION OF THE RADIANT INTENSITY IN (W/SR) OF THE
C      SURFACES (A1+A11),(A2+A22),A3,A4,A5,A7 IN THE WINDOW OF
C      5 MICROMETER, IN THE DIRECTION SHIP-MISSILE

C      DO 42 K=1,3
C      DO 41 L=1,91
C      RI1N=HDL(2,2,K,L)*A1+HDL(2,1,K,L)*A11
C      C11=(HEIGHT-HM1)/PAIH
C      C1=(1.-C11*C11)*0.5
C      RI1(K,L)=RI1N*C1
C      RI2N=HDL(1,2,K,L)*A2+HDL(1,1,K,L)*A22
C      C22=(HEIGHT-HM2)/PATH
C      RI2(K,L)=RI2N*C22
C      RI3N=HDL(2,1,K,L)*A3
C      C33=(HEIGHT-HM3)/PATH
C      C3=(1.-C33*C33)*0.5
C      RI3(K,L)=RI3N*C3
C      RI4N=HDL(2,2,K,L)*A4
C      C44=(HEIGHT-HM4)/PAIH
C      C4=(1.-C44*C44)*0.5
C      RI4(K,L)=RI4N*C4
C      RI5N=HDL(2,2,K,L)*A5
C      C55=(HEIGHT-HM5)/PAIH
C      C5=(1.-C55*C55)*0.5
C      RI5(K,L)=RI5N*C5
C      C66=(HEIGHT-HM6)/PATH
C      RI6=RI6N*C66
C      RI7N=HDL(1,1,K,L)*A7

```

```

      C77=(HEIGHT-H*7)/PAIH
      RI7(K,L)=RI7N*C77
41      CONTINUE
42      CONTINUE
C
C      CALCULATION OF SHIP SIGNAL VOLIAGE
C
      DO 50 K=1,3
      DO 49 L=1,91
      VS(K,L)=(RI1(K,L)+RI2(K,L)+RI3(K,L)+RI4(K,L)+RI5(K,L)+RI6+
49      1      RI7(K,L))*TRANS*RESPON*0.01*AP2R1/(PATH*PAIH)
50      CONTINUE
50      CONTINUE
C
C      CALCULATION OF NOISE VOLTAGE
C
      OMINST=SIDE*SIDE/(PATH*PAIH)
      AD=OMINST*FOCL*FOCL
      OMTOT=(SIDE/PATH)*ALOG((PATH+XTOT)/(PATH-XTOT))
      DFRF=OMTOT/(2.*OMINST*EN*TIMEF)
      VNOPI=RESPON*((AD*DFRF)**.5)/LETECT
      VB=HDL*AREAS*TRANS*RESPON*0.01*AP2R1/(PATHS*PATHS)
      VNTOT=VNOPI+VB
C
C      CALCULATION OF SIGNAL TO NOISE RATIO
C
      DO 60 K=1,3
      DO 59 L=1,91
      SNR(K,L)=20.*ALOG10(VS(K,L)/VNTOT)
59      CONTINUE
60      CONTINUE
C
C      TABULATION OF THE DETECTOR SIGNAL TO NOISE RATIO
C
      WRITE(6,70)
70      FORMAT(1,'0X','DETECTOR SIGNAL TO NOISE RATIO'
1/8X,'FOR FLIGHT HEIGHT=50 METERS AND SIDE=21.08 METERS'//)
      WRITE(6,71)
71      FORMAT(10,'ALT.ANGLE',3X,'UNOBSCURED SUN',3X,'SUN WITH LIGHT CLOUD
10',3X,'SUN WITH HEAVY STORM CLOUDS'//)
      DO 73 L=1,91
      WRITE(6,72) L, (SNR(K,L),K=1,3)
72      FORMAT(1X,F8.0,3X,F10.3,7X,F10.3,13X,F10.3)
73      CONTINUE
      STOP
      END
$ENTRY

```


LIST OF REFERENCES

1. International Defense Institute "Janes Warships 1983-1984", London, 1983
2. Ingalls Shipbuilding, "SPRUANCE (DD 963) Class Destroyers Compartmentation", Litton Co, Boston, 1974.
3. McCallum D.N., David Little, "DDG 47 Class Contract Design Phase Full Scale Stack Gas Testing on DD 964", NAVSEC Report No 6136-77-12, Annapolis MD, 1977.
4. Wolfe W.L., G.J. Zissis, "The Infrared Handbook", Infrared Information and Analysis (IRIA) Center, Environmental Research Institute of Michigan, Washington D.C., 1978.
5. R C A, "Electro-Optics Handbook", RCA Solid State Division Electro-Optics and Devices, Lancaster PA, 1978.
6. Meserve J.M., "US Marine Climatic Atlas of the World Volume 1", U.S. Department of Commerce, National Climatic Center, Washington D.C., 1974.
7. Peters W.N., A.D. Ritter, "Evaluation of ship Signature Modification techniques", General Research Corporation, McLean, Virginia, 1981.
8. U.S. NAVY, "NSTM for Class FRAM II" U.S. NAVY, Virginia, 1945.
9. Gilmer T.C., B. Johnson, "Introduction to Naval Architectures", Naval Institute Press, Annapolis MD. 1982.
10. Cooper A.W., "Electro-Optics", Course Notes, Department of Physics, Naval Postgraduate School, Monterey CA, 1983.
11. Kioustelidis J., "Numerical Analysis", Technical University of Athens, Athens Greece, 1977.
12. HUDSON Jr R.D., "Infrared System Engineering", Wiley Interscience, New York, 1969.

INITIAL DISTRIBUTION LIST

	No.	Copies
1. Defense Technical Information Center Cameron Station Alexandria, Virginia 22314	2	
2. Library, Code 0142 Naval Postgraduate School Monterey, California 93943	2	
3. Department Chairman, Code 61 Department of Physics Naval Postgraduate School Monterey, California 93943	1	
4. Prof. A.W. Cooper, Code 61Cr Department of Physics Naval Postgraduate School Monterey, California 93943	2	
5. Prof. E. C. Crittenden, Code 61Ct Department of Physics Naval Postgraduate School Monterey, California 93943	1	
6. Ioannis Egolfopoulos 33 Tepeleniou St. Papagos Athens - GREECE	3	
7. Hellenik Navy General Staff Grafeion Ekpaideusews Exwterikou Stratopedon Papagou Holargos Athens - GREECE	3	

13537 5

4.1 23

Thesis

E2673 Egoopoulos

c.1 Infrared of surface
vehicle, calculation
using atmospheric model
LOWTRAN 6.

thesE2673
Infrared detection of surface vehicle, c



3 2768 001 90366 9
DUDLEY KNOX LIBRARY